Ultrashort-pulse generation from quantum-dot semiconductor diode lasers

Thesis presented for the degree of Doctor of Philosophy
to the University of St Andrews

by

Maria Ana Cataluna

School of Physics and Astronomy
University of St Andrews

December 2007

DECLARATIONS

I, Maria Ana Cataluna, hereby certify that this thesis, which is approximately thirty three thousand words in length, has been written by me, that it is the record of work carried out by me and that it has not been submitted in any previous application for a higher degree.

Date Signature of candidate

I was admitted as a research student and as a candidate for the degree of Doctor of Philosophy in October, 2003; the higher study for which this is a record was carried out in the University of St Andrews between 2003 and 2007.

Date Signature of candidate

In submitting this thesis to the University of St Andrews I understand that I am giving permission for it to be made available for use in accordance with the regulations of the University Library for the time being in force, subject to any copyright vested in the work not being affected thereby. I also understand that the title and abstract will be published, and that a copy of the work may be made and supplied to any bona fide library or research worker, that my thesis will be electronically accessible for personal or research use, and that the library has the right to migrate my thesis into new electronic forms as required to ensure continued access to the thesis. I have obtained any third-party copyright permissions that may be required in order to allow such access and migration.

Date Signature of candidate

I hereby certify that the candidate has fulfilled the conditions of the Resolution and Regulations appropriate for the degree of Doctor of Philosophy in the University of St Andrews and that the candidate is qualified to submit this thesis in application for that degree.

Date Signature of supervisor

To my Mother

ABSTRACT

In this thesis, novel regimes of mode locking in quantum-dot semiconductor laser diodes have been investigated by exploiting the unique features offered by quantum dots. Using an unconventional approach, the role of excited-state transitions in the quantum dots was exploited as an additional degree of freedom for the mode locking of experimental quantum-dot lasers.

For the first time, passive mode locking via ground (1260nm) or excited state (1190nm) was demonstrated in a quantum-dot laser. Picosecond pulses were generated at a repetition rate of 21GHz and 20.5GHz, for the ground and excited states respectively, with average powers in excess of 25mW. Switching between these two states in the mode-locking regime was achieved by changing the electrical biasing conditions, thus providing full control of the operating spectral band.

A novel regime for mode locking in a quantum-dot laser was also investigated, where the simultaneous presence of cw emission in the excited-state band at high injection current levels, dramatically reduced the duration of the pulses generated via the ground state, whilst simultaneously boosting its peak power. This represents a radically different trend from the one typically observed in mode-locked lasers. From this investigation, it was concluded that the role of the excited state can not be neglected in the generation of ultrashort pulses from quantum-dot lasers.

Stable passive mode locking of a quantum-dot laser over an extended temperature range (from 20^{o}C to 80^{o}C) was also demonstrated at relatively high output average powers. It was observed that the pulse duration and the spectral width decreased significantly as the temperature was increased up to 70^{o}C. The process of carrier escape in the absorber was identified as the main contributing factor that led to a decrease in the absorber recovery time as a function of increasing temperature which facilitated a decrease in the pulse durations. These results are shown to open the way for the ultimate deployment of ultra-stable and uncooled mode-locked semiconductor diode lasers.

LIST OF PUBLICATIONS

CONTRIBUTIONS TO BOOKS

1. **Novel quantum-dot devices for ultrafast optoelectronics *(invited)***
   M. A. Cataluna, W. Sibbett, and E. U. Rafailov
   Encyclopedia of Nanoscience and Nanotechnology, 2nd edition (in press).

PUBLICATIONS IN PEER-REVIEWED JOURNALS

1. **Mode-locked quantum-dot lasers *(review)***
   E. U. Rafailov, M. A. Cataluna, and W. Sibbett
   Nature Photonics, 1, 395 (2007).

2. **High power all-quantum-dot-based external cavity mode-locked laser**
   A. D. Mcrobbie, M.A. Cataluna, S. A. Zolotovskaya, D. A. Livshits, W. Sibbett, and E. U. Rafailov
   Electronics Letters, 43, 812 (2007).

3. **Dynamics of a two-state quantum dot laser with saturable absorber**
   E. A. Viktorov, M. A. Cataluna, L. O'Faolain, T. F. Krauss, W. Sibbett, E.U.Rafailov, and P. Mandel
   Applied Physics Letters, 90, 121113 (2007).
   This paper was also selected to be published on:
   Virtual Journal of Nanoscale Science & Technology, 15, issue 13 (2007).

4. **Temperature dependence of pulse duration in a mode-locked quantum-dot laser**
   M. A. Cataluna, E. A. Viktorov, P. Mandel, W. Sibbett, D. A.Livshits, A.R.Kovsh, and E.U.Rafailov
   Applied Physics Letters, 90, 101102 (2007).
   This paper was also selected to be published on:
   Virtual Journal of Nanoscale Science & Technology, 15, issue 11 (2007).

5. **Anomalous dynamic characteristics of semiconductor quantum-dot lasers generating on two quantum states**
   G. S. Sokolovskii, M. A. Cataluna, A. G. Deryagin, V. I. Kuchinskii, I. I. Novikov, M. V. Maksimov, A. E. Zhukov, V. M. Ustinov, W. Sibbett, and E. U. Rafailov
   Technical Physics Letters, Vol. 33, No. 1, pp. 4–7 (2007).

6. **Stable mode locking via ground or excited-state transitions in a two-section quantum-dot laser**
   M. A. Cataluna, W. Sibbett, D. A. Livshits, J. Weimert, A. R. Kovsh, and E. U. Rafailov
   Applied Physics Letters, 89, 081124 (2006).
   This paper was also selected to be published on:
   Virtual Journal of Nanoscale Science & Technology, 14, issue 11 (2006) and
   Virtual Journal of Ultrafast Science, 5, issue 9 (2006).

7. **Stable mode-locked operation up to 80°C from an InGaAs quantum-dot laser**
   M. A. Cataluna, E. U. Rafailov, A. D. McRobbie, W. Sibbett, D. A. Livshits, and A. R. Kovsh
   IEEE Photonics Technology Letters, 18 (13-16), 1500 (2006).

8. **Reduced surface sidewall recombination and diffusion in quantum dot lasers**
   S. Moore, L. O'Faolain, M. A. Cataluna, M. B. Flynn, M. V. Kotlyar, and T. F. Krauss
   IEEE Photonics Technology Letters, 18 (17-20), 1861 (2006).

9. **Investigation of transition dynamics in a quantum-dot laser optically pumped by femtosecond pulses**
   E. U. Rafailov, A. D. McRobbie, M. A. Cataluna, L. O'Faolain, W. Sibbett, and D. A. Livshits
   Applied Physics Letters, 88, 041101 (2006). - ***Paper featured on the front cover***
   This paper was also selected to be published on:
   Virtual Journal of Nanoscale Science & Technology, 13, issue 5 (2006) and
   Virtual Journal of Ultrafast Science, 5, issue 2 (2006).

10. **High-power picosecond and femtosecond pulse generation from two-section modelocked quantum-dot laser**
    E. U. Rafailov, M. A. Cataluna, W. Sibbett, N. D. Il'inskaya, Y. M. Zadiranov, A. E. Zhukov, V.M.Ustinov, D. A. Livshits, A. R. Kovsh, and N. N. Ledentsov
    Applied Physics Letters, 87, 081107 (2005).
    This paper was also selected to be published on:
    Virtual Journal of Nanoscale Science & Technology, 12, issue 9 (2005) and
    Virtual Journal of Ultrafast Science, 4, issue 9 (2005).

11. **Compact laser-diode-based femtosecond sources *(invited review)***
    C. T. A. Brown, M. A. Cataluna, A. A. Lagatsky, E. U. Rafailov, M. B. Agate, C. G. Leburn, and W. Sibbett
    New Journal of Physics, special issue *Focus on Ultrafast Optics, 6, 175 (2004).*

CONTRIBUTIONS TO PEER-REVIEWED CONFERENCES

1. **Dynamics of a two-state quantum dot laser with saturable absorber**
   E. A. Viktorov, M. A. Cataluna, L. O'Faolain, T. F. Krauss, W. Sibbett, E.U.Rafailov, and P. Mandel
   CLEO/Europe-IQEC 2007, Munich, Germany, IG-2-MON (2007).

2. **Temperature dependence of electroabsorption dynamics in an InAs quantum dot saturable absorber at 1.3 μm**
   D. B. Malins, A. Gomez-Iglesias, M. A. Cataluna, E. U. Rafailov, W. Sibbett, and A. Miller
   CLEO/Europe-IQEC 2007, Munich, Germany, CF-6-MON (2007).

3. **Self-sustained pulsations and signal peaking in the oxide-confined VCSELs based on submonolayer InGaAs quantum dots**
   G. S. Sokolovskii, N. A. Maleev, A. G. Kuzmenkov, S. A. Blokhin, A. D. McRobbie, M. A. Cataluna, A. G. Deryagin, S. V. Chumak, A. S. Shulenkov, S. S. Mikhrin, A. R. Kovsh, V. I. Kuchinskii, V. M. Ustinov, W. Sibbett, and E. U. Rafailov
   CLEO/Europe-IQEC 2007, Munich, Germany, CB7-6-WED (2007).

4. **Temperature dependence of pulse duration in a mode-locked quantum-dot laser: experiment and theory**
   M. A. Cataluna, E. A. Viktorov, P. Mandel, W. Sibbett, D. A.Livshits, A.R.Kovsh, and E.U.Rafailov
   LEOS 2006, Montreal, Canada, ThJ5 (2006).

5. **High power all-quantum-dot based external cavity mode-locked laser**
   A. D. McRobbie, M. A. Cataluna, D. A. Livshits, W. Sibbett, and E. U. Rafailov
   LEOS 2006, Montreal, Canada, ThJ4 (2006).

6. **Anomalous dynamics of two-state lasing quantum-dot laser diodes**
   G. S. Sokolovskii, I. I. Novikov, M. V. Maximov, A. E. Zhukov, A. G. Deryagin, V. I. Kuchinskii, V.M.Ustinov, M. A. Cataluna, W. Sibbett, and E. U. Rafailov
   14th International Symposium NANOSTRUCTURES: Physics and Technology, St Petersburg, Russia (2006).

7. **New mode-locking regime in a quantum-dot laser: enhancement by simultaneous cw excited-state emission**
   M. A. Cataluna, A. D. McRobbie, W. Sibbett, D. A. Livshits, A. R. Kovsh, and E. U. Rafailov
   CLEO 2006, Paper CThH3, Long Beach, USA (2006).

8. **Compact and efficient femtosecond lasers**
   C. T. A Brown, A. Lagatsky, C. G. Leburn, A. McWilliam, A. Sarmani, M. A. Cataluna, B. Agate, K. Dholakia, D. Stevenson, W. Sibbett, Y. Chai, P. Jiang, K. Tan, R. Penty, I. White, E. U. Rafailov, and N. V. Kuleshov.
   Solid State Lasers and Amplifiers II, Proc. SPIE, Vol. 6190 (2006).

9. **Ground and excited-state modelocking in a two-section quantum-dot laser**
   M. A. Cataluna, E. U. Rafailov, A. D. McRobbie, W. Sibbett, D. A. Livshits, and A. R. Kovsh
   LEOS 2005, Sydney, Australia, ThS2 (2005).

10. **Investigation of transition dynamics in a quantum-dot laser optically pumped by femtosecond pulses**
    E. U. Rafailov, A. D. McRobbie, M. A. Cataluna, L. O'Faolain, W. Sibbett, and D. A. Livshits
    LEOS 2005, Sydney, Australia, ThN4 (2005).

11. **Quantum-dot based saturable absorber for mode locking of fibre lasers**
    R. Herda, G. Okhotnikov, E. U. Rafailov, M. A. Cataluna, W. Sibbett, P. Crittenden, and A. Starodumov
    LEOS 2005, Sydney, Australia, ThN5 (2005).

12. **Stable modelocked operation from a quantum-dot laser in a broad temperature range**
    E. U. Rafailov, M. A. Cataluna, W. Sibbett, D. A. Livshits, A. R. Kovsh, and N. N. Ledentsov
    CLEO 2005, Baltimore, U.S.A., CTuV4 (2005).

13. **Diode-based ultrafast lasers**
    A. A. Lagatsky, A. R. Sarmani, C. G. Leburn, E. U. Rafailov, M. A. Cataluna, B. Agate, C. T. A. Brown, and W. Sibbett
    Advanced Solid State Photonics 2005, Proceedings Vol. 98, pp640-645 (2005).

14. **High power ultrashort pulses output from a modelocked two section quantum dot laser**
    E. U. Rafailov, M. A. Cataluna, W. Sibbett, N. D. Il'inskaya, Y. M. Zadiranov, A. E. Zhukov, V. M. Ustinov, D. A. Livshits, A. R. Kovsh, and N. N. Ledentsov
    CLEO 2004, San Francisco, U.S.A., Post-deadline paper CPDB5 (2004).

ACKNOWLEDGEMENTS

The past four years of Ph. D. studies, for me, were not just a period of graduate study. It was more of an invaluable journey in my life full of new experiences and new learning. This journey would not have been successful without many people supporting, accompanying, and encouraging me.

First and foremost, I would like to thank my supervisor Professor Wilson Sibbett for the opportunity to work in St Andrews and for his incessant guidance, availability, advice and encouragement throughout these years. I have learnt so much from his vast knowledge and experience.

Many special thanks also go to Dr. Edik Rafailov, with whom I have worked in the lab almost since the day I arrived in St Andrews! His enthusiasm and knowledge about ultrafast quantum-dot optical devices have been a major driving force of this research, and it has been a privilege to work with him in a wide variety of research projects in this exciting field.

I'm also indebted to Prof. Thomas Krauss whose knowledge, help and encouragement were invaluable during my studies. I greatly appreciate the many thought-provoking discussions we have had throughout these years!

I would like to express my deep gratitude towards my former supervisors in Portugal: Professor Tito Mendonça and Dr. Helder Crespo, who introduced me to the fascinating world of ultrafast physics! Both played a crucial role in my initial training as a researcher and in my decision to pursue a Ph. D.. The stimulating discussions that we have still kept in the past years have been very refreshing, even being so far apart.

I also would like to thank my colleagues from the W-Squad, particularly: Dr. Alexander Lagatsky, who has always been willing to help with any problems arising in the lab; Dr. William Whelan-Curtin, for patiently teaching me about the fabrication of semiconductor lasers; and Dr. Ben Agate, for his good humour and constant availability to answer a wide range of questions that went from second harmonic generation to Scottish culture!

A special word of thanks goes to Dr. Viktorov and Prof. Mandel, who have kindly provided a theoretical framework for some of the phenomena investigated experimentally. I am grateful for the fruitful discussions we have had in the last year

and half, which allowed a much deeper understanding of the physics involved. I would like to thank Dr. Gregory Sokolovskii from the Ioffe Institute, for our insightful discussions and collaboration. I also would like to thank Innolume and the Ioffe Institute for providing the laser sources here studied.

At a personal level, I would like to thank my friends, in Portugal and in Scotland, and especially Filipa, Mei-Hua and Ruth. I thank them for their support, for their patience and for hearing me.

I would like to thank my mother and my brother, for their constant understanding, optimism and incredible humour!!

I am forever indebted to my boyfriend Henrique. His support throughout this thesis has been tremendous, and there will never be enough words to thank him.

I would like to acknowledge the essential financial support of FCT - *Fundação para a Ciência e Tecnologia,* Portugal, through a Ph. D. scholarship (reference SFRH/BD/10879/2002).

Finally, I also would like to acknowledge the IEEE Laser and Electro-Optics Society for the LEOS Graduate Student Fellowship 2007.

Table of contents

1. INTRODUCTION

This chapter introduces the aims of this research work and outlines some of the key aspects of this thesis. A comparison between the main aspects of pulse generation from vibronic and semiconductor lasers is explored as a basis for the motivation behind this research work. The basics on quantum-dot materials are also covered, allowing a better understanding of their unique properties and their suitability for ultrafast laser diodes. Some of the emerging applications that are driving the investigation of ultrafast quantum-dot lasers are described. Finally, the goals and structure of this thesis are outlined.

1.1. Motivation

1.1.1. Optical sources for the generation of ultrashort pulses

Over the past two decades, ultrashort pulses have been providing new insights of the most intricate mechanisms of light-matter interaction. Using ultrafast lasers as a tool, science has gained knowledge about microscopic and ultrafast events, even enabling real-time monitoring of chemical reactions – a feat unimaginable two decades ago. The enormous impact of ultrafast optical sources has already been recognised in the attribution of two Nobel prizes to A. Zewail (1999) and T. Hansch (2005), for applications in femtochemistry and laser-based precision spectroscopy [1,2], respectively.

The generation of femtosecond optical pulses has opened up a range of applications from real-time monitoring of chemical reactions [3], to ultra-high bit rate optical communications [4], enabling the realisation of new concepts in femtosecond optical networking, signal processing and transmission [5]. Compact lasers having multi-gigahertz repetition rates are becoming key components in photonic switching devices, optical interconnects and clock distribution in integrated circuits [6], ultrafast electro-optic sampling [7] and high-speed analog-to-digital converters [8,9].

The combination of high peak power with low average power has opened up a range of other applications such as micro-machining [10] and photo-ablation of biological tissues with minimal thermal effects [11]. On the other hand, the ultrabroad spectral bandwidth associated with ultrashort pulses has made possible diagnostics such as Optical Coherence Tomography (OCT), allowing tissue imaging with micrometer resolution [12].

Solid-state lasers based on vibronic gain materials such as Ti:Sapphire, Cr:Forsterite and Cr:YAG have so far been delivering the best performances in terms of femtosecond pulse durations, very high peak power and low jitter [13]. For example, pulses as short as 5fs can be directly produced from a Kerr-lens mode-locked Ti:sapphire laser [14] and up to 60W of average power has been generated in femtosecond pulses from a thin-disk Yb:YAG laser [15]. However, these laser systems present intrinsic limitations that have been preventing their widespread use in industrial and medical applications [16]. Ultrafast solid-state lasers can be very expensive and cumbersome optical sources. Despite some efforts on the miniaturisation of these

sources, the footprint of these systems is still very significant and integration in ultra-compact setups is virtually impossible. They are not electrically pumped, and a second laser system has to be used as an optical pump, which often needs a cooling system. Ultrafast solid-state lasers are multi-element systems, comprising at least a crystal, lenses, output couplers and mirrors, all critically aligned between them. Most of these lasers also incorporate intracavity and extra-cavity dispersion compensation in order to achieve femtosecond pulse durations. Solid-state lasers are thus complex to operate and optimise, requiring a highly-skilled user. The crystals used in these lasers have usually low gain, and therefore the necessary minimum crystal length limits the obtainable pulse repetition frequency. Electrical control of the output characteristics such as pulse duration and emission wavelength is not yet possible in ultrafast solid-state lasers. Moreover, these lasers can not be easily synchronised with an external electrical signal.

In contrast, ultrafast semiconductor laser diodes offer the potential for the ultimate in compactness and integrability along with direct electrical control and higher efficiency. There are several techniques for generating short pulses in semiconductor lasers: gain-switching, Q-switching and mode locking [17]. Mode locking is usually the preferred technique as it allows for shorter pulses and higher repetition rates. The mode locking of laser diodes (at the present moment, mainly based on quantum-well heterostructures) by active and passive modulation of cavity losses is a well-developed technique for the generation of ultrashort and high-repetition-rate optical pulses in the near-infrared spectral range [17]. In many cases, it is possible to incorporate the components required for passive mode locking directly into the device structure, thereby further simplifying the fabrication techniques. Semiconductor lasers can not yet directly generate the sub-100fs pulses routinely available from diode-pumped crystal-based lasers, but they represent the most compact and efficient sources of picosecond and sub-picosecond pulses. Furthermore, the bias can be easily adjusted to determine the pulse duration and the optical power, thus offering, to some extent, electrical control of the characteristics of the output pulses. These lasers also offer the best option for the generation of high-repetition rate trains of pulses, owing to their small cavity size. Ultrafast diode lasers have thus been favoured over other laser sources for high-frequency applications such as optical data/tele-communications. Being much cheaper to fabricate and operate, ultrafast semiconductor lasers also offer the potential for dramatic cost savings in a number of applications that traditionally use

solid-state lasers. The deployment of high-performance ultrafast diode lasers would therefore have a significant economic impact, by enabling ultrafast applications to become more profitable, and even facilitate the emergence of new applications.

The physical mechanisms underlying the generation of short pulses from diode lasers are very different from vibronic lasers. Semiconductors have a higher nonlinear refractive index than other gain media. The interaction of the pulse with the gain and the resulting large changes in the nonlinear refractive index lead to a phase change across the pulse, owing to the coupling between gain and index, which is regulated via the linewidth enhancement factor, or α-factor. This effect results in significant self-phase modulation, imparting an up-chirp to the pulses[1], which combined with the positive dispersion of the gain material, leads to substantial pulse broadening. This mechanism has been one of the major limitations in obtaining pulse durations of the order of 100fs *directly* from the diode lasers, with picosecond pulses being the norm. Furthermore, a strong saturation of the gain also results in a stabilisation of pulse energy, which limits the average and peak power to much lower levels than in vibronic lasers. Output average power levels for mode-locked laser diodes are usually between 0.1-100mW, while peak power levels remain between 10mW-1W. Only with additional amplification/compression setups, can the peak power reach the kW level [18].

Until very recently, ultrafast laser diodes have been solely based on bulk and quantum-well semiconductors. Since 2001 [19], quantum-dot materials have been generating much interest, because they offer specific advantages when integrated in ultrafast lasers. The next section explains how a lower dimensionality can result in completely new optoelectronic properties.

1.1.2. The role of dimensionality in semiconductor lasers

The history of semiconductor laser materials has been punctuated by dramatic revolutions. Everything started with the proposal of *p-n* junction semiconductor lasers in 1961, followed by experimental realisation on different semiconductor materials [20,21]. However, the lasers fabricated at that time exhibited an extremely low efficiency due to high optical and electrical losses. In fact, until mid-60s, only bulk materials were used in semiconductor devices, which were functionalised by introducing a doping profile. At the time, pioneers like Zhores I. Alferov and Herbert

[1] In passive mode-locked lasers, the chirp is usually an up-chirp (or positive chirp).

Kroemer independently considered the hypothesis of building heterostructures, consisting of layers of different semiconductor materials [22]. The classic heterostructure example consists of a lower bandgap layer surrounded by a higher bandgap semiconductor material. Such design results in electronic and optical confinement, because a higher bandgap semiconductor also exhibits a higher refractive index. The enhanced confinement improved notably the operational characteristics of laser diodes, in particular the threshold current density J_{th}, which decreased by two orders of magnitude.

But another revolution was about to come when it was realised that the confinement of electrons in lower dimensional semiconductor structures translated into completely new optoelectronic properties, when compared to bulk semiconductors. And how small should this confinement be? In order to answer this question, let us recall the concept of the de Broglie wavelength of thermalised electrons, λ_B:

$$\lambda_B = \frac{h}{p} = \frac{h}{\sqrt{2m^* E}} \tag{1.1}$$

where h is Planck's constant, p is the electron momentum, m^* is the electron effective mass, and E is the energy. In the case of III-V compound semiconductors, λ_B is typically of the order of tens of nanometres [23]. If one of the dimensions of a semiconductor is comparable or less than λ_B, the electrons will be strongly confined in one dimension, while moving freely in the remaining two dimensions - this is the case of a quantum well. A quantum wire is a one-dimensionally confined structure, while a quantum dot is confined in all the three dimensions. Quantum dots are thus tiny clusters of semiconductor material with dimensions of only a few nanometres.

The spatial confinement of the carriers in lower dimensional semiconductors leads to dramatically different energy-momentum relations in the directions of confinement, which results in completely new density of states, when compared to the bulk case, as depicted in Fig. 1.1. As dimensionality decreases, the density of states is no longer continuous or quasi-continuous but becomes quantised. In the case of quantum dots, the charge carriers occupy only a restricted set of energy levels rather like the electrons in an atom, and for this reason, quantum dots are sometimes referred to as 'artificial atoms'.

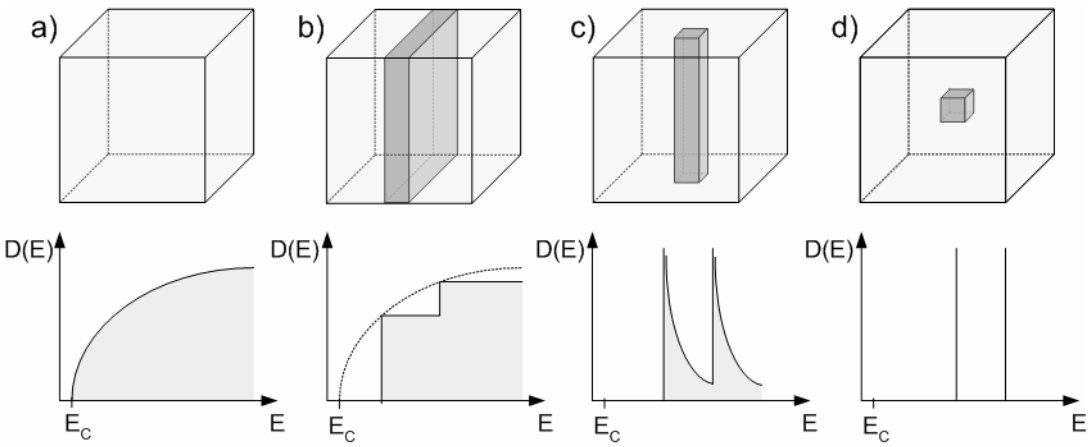

Fig. 1.1 – Schematic structures of bulk and low-dimensional semiconductors and corresponding density of states: (a) bulk; (b) quantum well; (c) quantum wire; (d) quantum dot.

For a given energy range, the number of carriers necessary to fill out these states reduces substantially as the dimensionality decreases, which implies that it becomes easier to achieve transparency and inversion of population - with the resulting reduction of threshold current density J_{th}. In fact, the reduction in J_{th} has been quite spectacular over the years, with sudden jumps whenever the dimensionality is decreased, as shown in Fig. 1.2 (a).

Low-dimensional lasers also exhibit reduced temperature sensitivity of J_{th}. Theoretical values are shown in Fig. 1.2 (b). In the case of quantum dots, an infinite characteristic temperature has even been predicted.

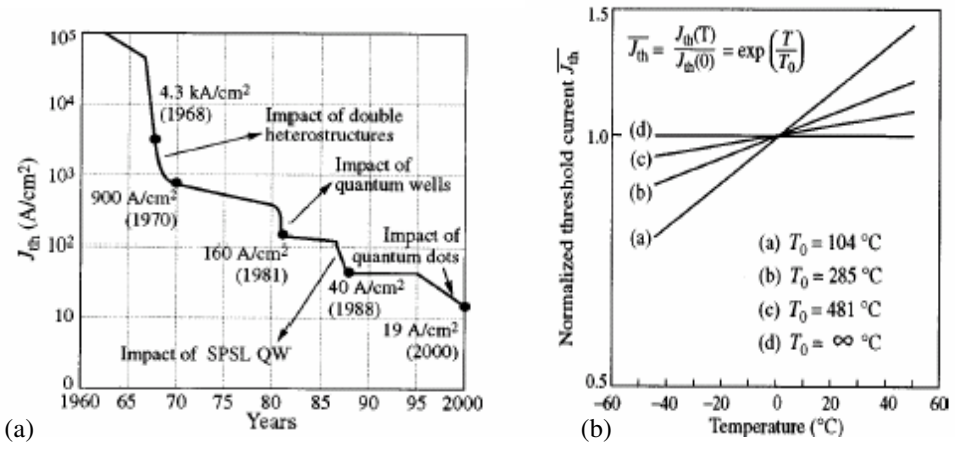

Fig. 1.2 – (a) Evolution of the threshold current of semiconductor lasers. (b) Normalized (theoretical) dependence of the threshold current for various double heterostructure lasers with: (a) bulk; (b) quantum wells; (c) quantum wires; (d) quantum dots. [22]

1.1.3. Quantum dots: materials and growth

The group of quantum-dot materials that has shown particular promise is based on III-V quantum dots epitaxially grown on a semiconductor substrate. For instance, InGaAs/InAs quantum dots on a GaAs substrate emit in the 1-1.3μm wavelength range, and which can be extended to 1.55μm. Alternatively, InGaAs/InAs quantum dots can be grown on an InP substrate, that covers the 1.4-1.9μm wavelength range [24].

The remarkable achievements in quantum dot (QD) epitaxial growth have enabled the fabrication of QD lasers, amplifiers and saturable absorbers offering excellent performance characteristics. To date, the most promising results have been achieved using the spontaneous formation of three-dimensional islands during strained layer epitaxial growth in a process known as the Stranski-Krastanow mechanism [24,25]. In this process, when a film A is epitaxially grown over a substrate B, the initial growth occurs layer by layer, but beyond a certain critical thickness, three-dimensional islands start to form – the quantum dots. A continuous film lies underneath the dots, and is called the wetting layer. The most important condition in this technique is that the lattice constant of the deposited material is larger than the one of the substrate. This is the case of an InAs film (lattice constant of 6.06Å) on a GaAs substrate (lattice constant of 5.64Å), for example.

Even being an extremely complex process, the Stranski-Krastanow mode is now widely used in the self-assembly of quantum dots. An advantage of this technique is that films can be grown using the well-known techniques of Molecular Beam Epitaxy (MBE) and Metal Organic Chemical Vapor Deposition (MOCVD), and therefore the science of quantum dots growth has benefited immensely from all the previous knowledge gained with this technology. These are also good news for commercialisation, because manufacturers do not have to invest in new epitaxy equipment to fabricate these structures.

Due to the statistical fluctuations occurring during growth, there is a distribution in dot size, height and composition but, at the moment, epitaxy techniques have evolved to such an extent that the amount of fluctuations can be reasonably controlled, and can be as small as a few percent.

If the dots are grown in a plane surface, their lateral positions will be random. An example of such structure is shown in Fig. 1.3 a). In the self-assembly process, there is

not a standard way of arranging the dots in a planar ordered way, unless they are encouraged to grow at particular positions in a pre-patterned substrate.

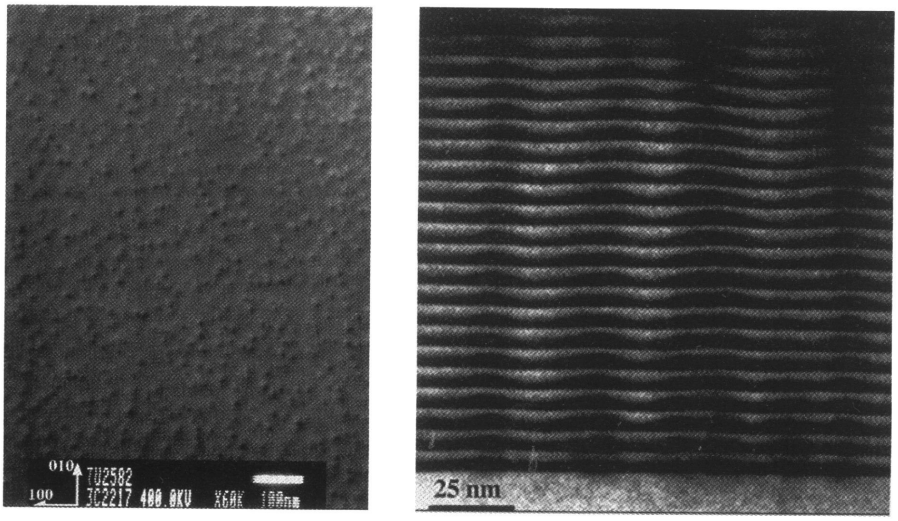

(a) (b)

Fig. 1.3 – (a) A TEM image of a single sheet of InAs quantum dots grown on GaAs. (b) A TEM image of a cross-section of a 25-layer thick stack of InGaAs quantum dots (thicker dark regions) grown on GaAs substrate (lighter area in the bottom of the picture and surrounding the InGaAs layers). The QDs are connected within the layers by the wetting layers (thin dark regions). [26]

At the present, the densities of quantum dots lie typically between $10^{9}\,cm^{-2}$ and $10^{11}\,cm^{-2}$. The sparse distribution of quantum dots results in a low value of gain. Thus, the levels of gain and optical confinement provided by a single layer of quantum dots may not be enough for the optimal performance of a laser. In order to circumvent this problem, quantum dots can also be grown in stacks, which allows an increase in the modal gain without increasing the internal optical mode loss [27]. A cross-section of a multi-stacked structure is shown in Fig. 1.3 b). In this figure (and in most cases), the various layers are separated by GaAs (lighter regions). The GaAs separators are responsible for transmitting the tensile strain from layer to layer, inducing the formation of ordered arrays of quantum dots aligned on the top of each other. Further optical confinement is enabled through the cladding of such arrays within layers of higher refractive index and bandgap energy, therefore forming a heterostructure.

1.1.4. Quantum-dot lasers – ultrafast characteristics

A QD laser was proposed in 1976 [28] and the first theoretical treatment was published in 1982 [29]. The main motivation was to conceive a design for a low-threshold, single-frequency and temperature-insensitive laser, owing to the discrete nature of the

density of states. In fact, practical devices exhibit the predicted outstandingly low thresholds [30,31], but the spectral bandwidths of such lasers are significantly broader than those of conventional quantum-well lasers [32]. This results from the self-organised growth of quantum dots, leading to a Gaussian distribution of dot sizes, with a corresponding Gaussian distribution of emission frequencies. Additionally, lattice strain may vary across the wafer, thus further affecting the energy levels in the quantum dots. These effects lead to the inhomogeneous broadening of the gain - a useful phenomenon in the context of ultrafast applications, because a very wide bandwidth is available for the generation, propagation and amplification of ultrashort pulses. The effects of inhomogeneous broadening on the density of states are schematically illustrated in Fig. 1.4. However, it is important to stress that a highly inhomogeneously broadened gain also encompasses a number of disadvantages, because it partially defeats the purpose of a reduced dimensionality, by broadening the density of states. Indeed, the fluctuation in the size of the QDs has the effect of increasing the transparency current and reducing the modal and differential gain [33,34]. Therefore, much effort has been put into improving the dots uniformisation by engineering the growth and post-growth processes [24].

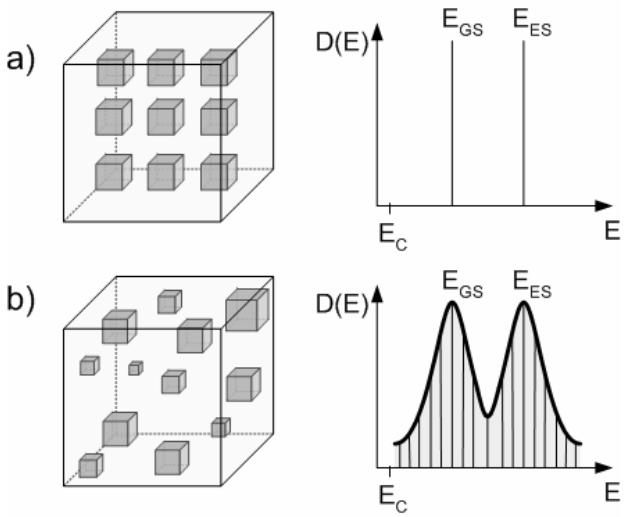

Fig. 1.4 - Schematic morphology and density of states for charge carriers in: (a) an ideal quantum-dot system and (b) a real quantum-dot system, where inhomogeneous broadening is illustrated.

Importantly, QD structures exhibit ultrafast recovery time (<1ps), both under absorption and gain conditions [35]. The fast recovery time is particularly useful for enabling saturable absorbers to mode lock lasers at high-repetition rates, where the

absorption recovery should occur within the round-trip time of the cavity. Crucially, the shaping mechanism of the fast absorption recovery also enhances the shortening of the mode-locked pulses, and thus QD lasers have the potential for generating shorter pulses than their quantum-well counterparts. QDs also exhibit a 2-5 times lower absorption saturation fluence than quantum-well materials [36], which helps the self-start of mode locking.

The investigations of the amplification of the femtosecond pulses and the ultrafast carrier dynamics of quantum-dot structures imply that such structures could be used simultaneously as an efficient broadband gain media and as fast saturable absorbers, either independently or monolithically. In Chapter 2, we will explore further the particular advantages that QD structures bring to ultrafast technology.

1.2. Emerging applications of ultrafast quantum-dot lasers

Owing to the flexibility of QD growth, the emission wavelength can be engineered over a wide span, and laser sources operating at room temperature can be made available at any wavelength from 1.0μm to 1.65μm, with similar operational properties [24]. QD lasers operating at 1.9μm have also been demonstrated [37], but at low temperatures (T=77K). This spectral flexibility can match a range of applications that have specific wavelength requirements, which the versatility of QD lasers can address.

1.2.1. Optical communications

QD mode-locked lasers are particularly interesting for applications in communication systems. The possibility to generate pulses at very high repetition rate and with record-low jitter is very desirable for optical time division multiplexing systems (OTDM), where a mode-locked QD laser can be used either as a pulse source or in a clock recovery circuit. In OTDM, different slow data signals are interleaved to form a single faster signal. If a shorter pulse duration is used, the switching window is narrowed, enabling higher bit rates.

On the other hand, the broad spectral bandwidth offered by QD structures can be deployed in wavelength division multiplexing systems (WDM). In this transmission format, each signal is assigned a different wavelength, enabling the independent

propagation down the fibre. By engineering the inhomogeneous broadening caused by the size distribution of QDs, a very broad laser emission spectrum can be obtained with nearly-uniform intensity distribution. Using slicing techniques, this spectrum can be converted into an array of different equally spaced wavelengths, which is a cost-effective technique to use WDM, without resorting to the use of several laser sources. In fact, a uniform 93-channel multiwavelength QD laser has been demonstrated recently [38], over a wavelength range from 1638 to 1646nm. The 93 channels were generated directly from the single monolithic chip, without external components or slicing setups, as the channel/mode spacing was simply determined by the length of the cavity (4.5mm). The stability of the laser modes was attributed to the inhomogeneous broadened nature of the gain.

QD lasers would be particularly suitable for metro networks that operate in the O-band (1260-1360 nm), which coincides with the spectral window of lowest dispersion in optical fibres. Indeed, QD lasers emitting around 1300nm can now be routinely grown on GaAs substrates. This represents a significant advantage over previous technology, because QW lasers emitting at the same wavelength have to be grown on InP, with the associated poor performance due to high nonradiative Auger recombination. The telecomm optical band of 1550nm has also been addressed, with much research done on this topic in recent times [39].

With the additional features of low threshold and resilience to temperature, QD lasers have become suitable candidates for the next generation of telecommunication sources, either fibre-based or free-space. In fact, the use of QD lasers in space applications is very promising, as they also exhibit enhanced radiation hardness, when compared to QW materials [40,41]. Due to the cluster-like nature of QD gain material and enhanced carrier confinement, the impact of high-energy radiation on active layers and the consequent generation of defects is less likely to decrease the efficiency of the material, as the carriers are spatially confined. This greatly enhances the reliability of the lasers used in spaceborne applications, such as intersatellite communications.

1.2.2. Datacomms

Mode-locked semiconductor lasers can also be used as optical interconnects for clock distribution, either on-chip or at an inter-chip/inter-board level [6]. In recent years, there has been much interest in lower repetition rate mode-locked lasers (5GHz and

less) that have potential as optical clocks for computer motherboards, a technology that is being developed to avoid interaction with electrical signal lines. In order to achieve such low repetition rates, it is necessary to fabricate lasers with very long cavities, around 8mm or more. Technologically, it is less of a challenge to fabricate these long lasers from QD materials as it is with QW lasers, because they exhibit comparatively lower internal optical losses (and thus lower threshold). This relaxes the need of insertion of a low-loss passive waveguide to minimise threshold current and pulse duration, as it is common practice with long-cavity QW lasers [42]. Long cavity mode-locked QD lasers have been reported since 2004 [43,44], and their fabrication has reached a level of maturity such that they are now commercially available through Innolume GmBH . This company has recently announced its commitment to the application of QD lasers in silicon-based photonics, as the emission range of 1064-1310nm coincides with the transparency window of silicon.

1.2.3. Biophotonics and medical applications

Telecoms and datacoms are two particular niches of applications that semiconductor ultrafast laser diodes have been traditionally designed to address [17,45]. The ultimate goal is to access applications that have been mainly in the domain of solid-state lasers. Such is the case of biophotonics and medical applications in particular, where compact, rugged and turnkey sources are crucial for the deployment of sophisticated and non-invasive optical diagnostics and therapeutics. In this respect, compact and simple semiconductor ultrafast sources based on QD materials can offer a number of advantages.

Optical Coherence Tomography (OCT) – a technique that enables imaging with resolutions up to the micrometre level - is one of the medical diagnostics that may benefit in the near-future from developments in QD ultrafast lasers. The resolution achieved by this technique is determined by the wavelength and spectral bandwidth of the optical source, and it is desirable to achieve as high a bandwidth as possible. The optical source used in OCT should also have a short coherence length. All these requirements can be satisfied by mode-locked lasers, which have been the best performing sources deployed for OCT, in particular Ti:Sapphire lasers (800nm) and Cr:Forsterite and fibre lasers (1300nm). However, in order to turn OCT an interesting and practical tool, it is crucial to decrease the footprint and complexity of the laser

system. Superluminescent diodes have been used to this end, but power levels can be very low.

An alternative could be to use QD-based mode-locked lasers. The spectral range that is most routinely accessed with QD lasers (around 1.3μm) can penetrate deeper into biological tissue [46,47], as it suffers less scattering and absorption than at 800nm. In fact, the use of this longer wavelength has allowed imaging depths of 3mm in non-transparent tissues [48].

In order to become competitive sources, QD lasers will have to generate a spectral bandwidth at least comparable to what has been obtained directly by Cr:Forsterite and fibre lasers (~100nm). The possibility of engineering the inhomogeneous broadening in QD laser devices could afford some potential in the fabrication of inexpensive and efficient alternative sources for OCT, as revealed by the recent demonstration of a 75nm-broad spectrum from a cw QD laser [32].

1.3. Research goals and thesis outline

One of the main goals of this thesis was to investigate what are the ultimate advantages and unique characteristics of mode-locked QD lasers that will make these optical sources competitive, when compared to QW lasers. The aim was to understand more of the particular mechanisms behind mode locking in QD lasers, in order to exploit these effects in the robust generation of ultrashort pulses from these devices.

Several directions of investigation were taken for this purpose. A comprehensive characterisation of the mode-locking regime in several QD lasers was performed, in order to more easily track performance patterns that could bring further insight into the physics of mode-locked QD lasers (Chapter 3). This approach allowed the systematic study of several mode-locking regimes in different conditions, as for instance with increasing temperature (Chapter 6). The motivation for evaluating the mode-locking performance with temperature was two-fold. First, and from a device point of view, it was important to verify if the temperature resilience characteristic of QD lasers was extensive to pulse generation, and thus determine if these sources are suitable for applications in harsh environments. Second, using an extra variable such as temperature would allow us to gain more insights into the carrier mechanisms that are relevant in the generation of short pulses in QD lasers. For this purpose, it was particularly

important to interlink the experimental results with theoretical simulations, that resulted from a collaboration with the Group of Theoretical Nonlinear Optics at the *Université Libre de Bruxelles*.

Throughout this work, novel regimes of mode locking in QD lasers were also investigated - by using an unconventional approach, the role of excited-state transitions was exploited. Indeed, due to the quantum nature of these nanostructures, laser emission can occur via ground-state or excited-state transitions. Although the presence of the excited state is a unique feature of QD lasers, the potential of excited-state transitions had not been considered until now. In this thesis the following two main questions were addressed:

- Does the excited state plays any influence in the mode locking via ground state?

- Is it possible to achieve mode locking via the excited-state transitions? And how different is excited-state mode locking from ground-state mode locking?

These two questions will be addressed in Chapters 4 and 5, respectively.

The next Chapter starts with an introduction to mode locking in semiconductor lasers. The challenges inherent to the generation of ultrashort pulses from these lasers are described. The discussion of these challenges will put into context the advantages of QD materials for ultrafast applications, which are explained in detail. A review of the state of the art in the field of QD mode-locked lasers is provided.

1.4. References

[1] *http://nobelprize.org/nobel_prizes/chemistry/laureates/1999/index.html*.

[2] *http://nobelprize.org/nobel_prizes/physics/laureates/2005/index.html*.

[3] A. H. Zewail, "Femtochemistry: Atomic-Scale Dynamics of the Chemical bond using ultrafast lasers - (Nobel lecture)," *Angewandte Chemie-International Edition*, vol. 39, pp. 2587-2631, 2000.

[4] W. H. Knox, "Ultrafast technology in telecommunications," *IEEE J. Sel. Topics Quantum Electron.*, vol. 6, pp. 1273-1278, 2000.

[5] T. Morioka, "Ultrafast optical technologies for large-capacity TDM/WDM photonic networks," *J. Optical and Fiber Comm. Rep.*, vol. 4, pp. 14-40, 2007.

[6] G. A. Keeler, B. E. Nelson, D. Agarwal, C. Debaes, N. C. Helman, A. Bhatnagar, and D. A. B. Miller, "The benefits of ultrashort optical pulses in optically interconnected systems," *IEEE J. Sel. Topics Quantum Electron.*, vol. 9, pp. 477-485, 2003.

[7] J. A. Valdmanis and G. Mourou, "Subpicosecond electrooptic sampling - principles and applications," *IEEE J. Quantum Electron.*, vol. 22, pp. 69-78, 1986.

[8] P. W. Juodawlkis, J. C. Twichell, G. E. Betts, J. J. Hargreaves, R. D. Younger, J. L. Wasserman, F. J. O'Donnell, K. G. Ray, and R. C. Williamson, "Optically sampled analog-to-digital converters," *IEEE Trans. Microwave Theory Tech.*, vol. 49, pp. 1840-1853, 2001.

[9] P. J. Delfyett, C. DePriest, and T. Yilmaz, "Signal processing at the speed of lightwaves," *IEEE Circuits & Devices*, vol. 18, pp. 28-35, 2002.

[10] S. Nolte, "Micromachining," in *Ultrafast Lasers - Technology and Applications*, M. E. Fermann, A. Galvanauskas, and G. Sucha, Eds. New York: Marcel Dekker, Inc., 2003, pp. 359-394.

[11] M. Niemz, *Laser-Tissue Interactions: Fundamentals and Applications*. Berlin: Springer-Verlag, 1996.

[12] J. G. Fujimoto, M. Brezinski, W. Drexler, I. Hartl, F. Kartner, X. Li, and U. Morgner, "Optical Coherence Tomography," in *Ultrafast Lasers - Technology and Applications*, M. E. Fermann, A. Galvanauskas, and G. Sucha, Eds. New York: Marcel Dekker, Inc., 2003, pp. 712-743.

[13] C. T. A. Brown, M. A. Cataluna, A. A. Lagatsky, E. U. Rafailov, M. B. Agate, C. G. Leburn, and W. Sibbett, "Compact laser-diode-based femtosecond sources," *New J. Phys.*, vol. 6, pp. 175, 2004.

[14] R. Ell, U. Morgner, F. X. Kartner, J. G. Fujimoto, E. P. Ippen, V. Scheuer, G. Angelow, T. Tschudi, M. J. Lederer, A. Boiko, and B. Luther-Davies, "Generation of 5-fs pulses and octave-spanning spectra directly from a Ti : sapphire laser," *Opt. Lett.*, vol. 26, pp. 373-375, 2001.

[15] E. Innerhofer, T. Sudmeyer, F. Brunner, R. Haring, A. Aschwanden, R. Paschotta, C. Honninger, M. Kumkar, and U. Keller, "60-W average power in 810-fs pulses from a thin-disk Yb : YAG laser," *Opt. Lett.*, vol. 28, pp. 367-369, 2003.

[16] G. Sucha, "Overview of Industrial and Medical Applications of Ultrafast Lasers," in *Ultrafast Lasers - Technology and Applications*, M. E. Fermann, A. Galvanauskas, and G. Sucha, Eds. New York: Marcel Dekker, Inc., 2003, pp. 323-358.

[17] P. Vasil'ev, *Ultrafast Diode Lasers: Fundamentals and Applications*. Boston: Artech House, 1995.

[18] K. Kim, S. Lee, and P. J. Delfyett, "1.4kW high peak power generation from an all semiconductor mode-locked master oscillator power amplifier system based on eXtreme Chirped Pulse Amplification(X-CPA)," *Opt. Express*, vol. 13, pp. 4600-4606, 2005.

[19] X. D. Huang, A. Stintz, H. Li, L. F. Lester, J. Cheng, and K. J. Malloy, "Passive mode-locking in 1.3 μm two-section InAs quantum dot lasers," *Appl. Phys. Lett.*, vol. 78, pp. 2825-2827, 2001.

[20] N. G. Basov, O. N. Krokhin, and Y. M. Popov, "The possibility of use of indirect transitions to obtain negative temperature in semiconductors," *Soviet Physics JETP*, vol. 12, pp. 1033, 1961.

[21] N. G. Basov, "Nobel Lecture: Semiconductor lasers," *http://www.nobel.se/physics/laureates/1964/basov-lecture.html*, 1964.

[22] Z. I. Alferov, "Nobel Lecture: The double heterostructure concept and its applications in physics, electronics, and technology," *Reviews of Modern Physics*, vol. 73, pp. 767, 2001.

[23] B. E. A. Saleh and M. C. Teich, *Fundamentals of Photonics*. New York: Wiley, 1991.

[24] V. M. Ustinov, A. E. Zhukov, A. Y. Egorov, and N. A. Maleev, *Quantum Dot Lasers*. New York: Oxford University Press, 2003.

[25] L. Goldstein, F. Glas, J. Y. Marzin, M. N. Charasse, and G. L. Roux, "Growth by molecular beam epitaxy and characterization of InAs/GaAs strained-layer superlattices," *Appl. Phys. Lett.*, vol. 47, pp. 1099-1101, 1985.

[26] P. Yu and M. Cardona, *Fundamentals of Semiconductors: physics and materials properties*, 3rd ed. Heidelberg: Springer-Verlag, 2001.

[27] P. M. Smowton, E. Herrmann, Y. Ning, H. D. Summers, P. Blood, and M. Hopkinson, "Optical mode loss and gain of multiple-layer quantum-dot lasers," *Appl. Phys. Lett.*, vol. 78, pp. 2629-2631, 2001.

[28] N3982207 R. Dingle and C. H. Henry, 1976.

[29] Y. Arakawa and H. Sakaki, "Multidimensional quantum well laser and temperature dependence of its threshold current," *Appl. Phys. Lett.*, vol. 40, pp. 939-941, 1982.

[30] A. R. Kovsh, N. N. Ledentsov, S. S. Mikhrin, A. E. Zhukov, D. A. Livshits, N. A. Maleev, M. V. Maximov, V. M. Ustinov, A. E. Gubenko, I. M. Gadjiev, E. L. Portnoi, J. S. Wang, J. Chi, D. Ouyang, D. Bimberg, and J. A. Lott, "Long-wavelength (1.3-1.5 μm) quantum dot lasers based on GaAs," *Physics and Simulation of Optoelectronic Devices XII*, *Proc. SPIE*, 31-45, Bellingham, 2004.

[31] H. Y. Liu, D. T. Childs, T. J. Badcock, K. M. Groom, I. R. Sellers, M. Hopkinson, R. A. Hogg, D. J. Robbins, D. J. Mowbray, and M. S. Skolnick, "High-performance three-layer 1.3-μm InAs-GaAs quantum-dot lasers with very low continuous-wave room-temperature threshold currents," *IEEE Photon. Technol. Lett.*, vol. 17, pp. 1139-1141, 2005.

[32] A. Kovsh, I. Krestnikov, D. Livshits, S. Mikhrin, J. Weimert, and A. Zhukov, "Quantum dot laser with 75 nm broad spectrum of emission," *Opt. Lett.*, vol. 32, pp. 793-795, 2007.

[33] O. Qasaimeh, "Effect of inhomogeneous line broadening on gain and differential gain of quantum dot lasers," *IEEE Trans. Electron Devices*, vol. 50, pp. 1575-1581, 2003.

[34] H. Dery and G. Eisenstein, "The impact of energy band diagram and inhomogeneous broadening on the optical differential gain in nanostructure lasers," *IEEE J. Quantum Electron.*, vol. 41, pp. 26-35, 2005.

[35] P. Borri, S. Schneider, W. Langbein, and D. Bimberg, "Ultrafast carrier dynamics in InGaAs quantum dot materials and devices," *J. Opt. A*, vol. 8, pp. S33-S46, 2006.

[36] M. G. Thompson, C. Marinelli, Y. Chu, R. L. Sellin, R. V. Penty, I. H. White, M. Van Der Peol, D. Birkedal, J. Hvam, V. M. Ustinov, M. Lammlin, and D. Bimberg, "Properties of InGaAs quantum dot saturable absorbers in monolithic mode-locked lasers," *IEEE 19th International Semiconductor Laser Conference*, 53-54, Matsue Shi, Japan, 2004.

[37] V. M. Ustinov, A. E. Zhukov, A. Y. Egorov, A. R. Kovsh, S. V. Zaitsev, N. Y. Gordeev, V. I. Kopchatov, H. N. Ledentsov, A. F. Tsatsul'nikov, B. V. Volovik, P. S. Kop'ev, Z. I. Alferov, S. S. Ruvimov, Z. Liliental-Weber, and D. Bimberg, "Low threshold quantum dot injection laser emitting at 1.9 μm," *Electron. Lett.*, vol. 34, pp. 670-672, 1998.

[38] J. Liu, Z. Lu, S. Raymond, P. J. Poole, P. J. Barrios, G. Pakulski, D. Poitras, G. Xiao, and Z. Zhang, "Uniform 90-channel multiwavelength InAs/InGaAsP quantum dot laser," *Electron. Lett.*, vol. 43, pp. 458-460, 2007.

[39] J. P. Reithmaier, A. Somers, S. Deubert, R. Schwertberger, W. Kaiser, A. Forchel, M. Calligaro, P. Resneau, O. Parillaud, S. Bansropun, M. Krakowski, R. Alizon, D. Hadass, A. Bilenca, H. Dery, V. Mikhelashvili, G. Eisenstein, M. Gioannini, I. Montrosset, T. W. Berg, M. van der Poel, J. Mork, and B. Tromborg, "InP based lasers and optical amplifiers with wire-/dot-like active regions," *J. Phys. D*, vol. 38, pp. 2088-2102, 2005.

[40] F. Guffarth, R. Heitz, M. Geller, C. Kapteyn, H. Born, R. Sellin, A. Hoffmann, D. Bimberg, N. A. Sobolev, and M. C. Carmo, "Radiation hardness of InGaAs/GaAs quantum dots," *Appl. Phys. Lett.*, vol. 82, pp. 1941-1943, 2003.

[41] S. Marcinkevicius, J. Siegert, R. Leon, B. Cechavicius, B. Magness, W. Taylor, and C. Lobo, "Changes in luminescence intensities and carrier dynamics induced by proton irradiation in $In_xGa_{1-x}As$/GaAs quantum dots," *Phys. Rev. B*, vol. 66, pp. 235314, 2002.

[42] F. Camacho, E. A. Avrutin, P. Cusumano, A. S. Helmy, A. C. Bryce, and J. H. Marsh, "Improvements in mode-locked semiconductor diode lasers using monolithically integrated passive waveguides made by quantum-well intermixing," *IEEE Photon. Technol. Lett.*, vol. 9, pp. 1208-1210, 1997.

[43] A. Gubenko, D. Livshits, I. Krestnikov, S. Mikhrin, A. Kozhukhov, A. Kovsh, N. Ledentsov, A. Zhukov, and E. Portnoi, "High-power monolithic passively modelocked quantum-dot laser," *Electron. Lett.*, vol. 41, pp. 1124-1125, 2005.

[44] L. Zhang, L. Cheng, A. L. Gray, S. Luong, J. Nagyvary, F. Nabulsi, L. Olona, K. Sun, T. Tumolillo, R. Wang, C. Wiggins, J. Zilko, Z. Zou, P. M. Varangis, H. Su, and L. F. Lester, "Low timing jitter, 5 GHz optical pulses from monolithic two-section passively mode-locked 1250/1310 nm quantum dot lasers for high-speed optical interconnects," *Optical Fiber Communication Conference*, *Technical Digest*, OWM4, Anaheim, USA, 2005.

[45] E. A. Avrutin, J. H. Marsh, and E. L. Portnoi, "Monolithic and multi-GigaHertz mode-locked semiconductor lasers: Constructions, experiments, models and applications," *IEE Proc. Optoel.*, vol. 147, pp. 251-278, 2000.

[46] M. E. Brezinski and J. G. Fujimoto, "Optical coherence tomography: High-resolution imaging in nontransparent tissue," *IEEE J. Sel. Topics Quantum Electron.*, vol. 5, pp. 1185-1192, 1999.

[47] P. Fischer, A. McWilliam, C. T. A. Brown, K. Wood, M. MacDonald, W. Sibbett, and K. Dholakia, "Deep tissue penetration of radiation: 3D modelling and experiments," *European Conference on Lasers and Electro-Optics*, *Technical Digest*, CL-4-Wed, 641-641, Munich, Germany, 2005.

[48] M. E. Brezinski, G. J. Tearney, B. E. Bouma, J. A. Izatt, M. R. Hee, E. A. Swanson, J. F. Southern, and J. G. Fujimoto, "Optical coherence tomography for optical biopsy - Properties and demonstration of vascular pathology," *Circulation*, vol. 93, pp. 1206-1213, 1996.

2. MODE-LOCKED QUANTUM-DOT LASERS: PHYSICS AND STATE OF THE ART

In this chapter, the necessary background information is presented on short pulse generation from diode lasers and quantum-dot materials. The concept of mode locking is introduced, and an overview of the mode locking techniques available for semiconductor lasers is provided. Passive mode locking – the chosen technique used in this project - is explained in greater detail. The unique properties of quantum-dot materials and their suitability for ultrashort-pulse diode lasers are exploited. Finally, a review of the state of the art in the field of QD mode-locked lasers is provided.

2.1. Introduction to mode locking in semiconductor lasers

2.1.1. Basics of mode locking

Mode locking is a technique that involves the locking of the phases of the longitudinal modes in a laser. This results in the generation of a sequence of pulses with a repetition rate corresponding to the cavity round-trip time. This well established technique enables the production of the shortest pulse durations and the highest repetition rates available from ultrafast lasers, whether they are semiconductor or crystal-based laser systems. In a standing-wave resonator, the pulse repetition rate f_R is given by:

$$f_R = \frac{c}{2nL} \tag{2.1}$$

where c is the speed of light in vacuum, n is the refractive index and L is the length of the laser cavity.

In terms of Fourier analysis, there is an inverse proportionality between the duration of a mode-locked pulse and the corresponding bandwidth of its optical spectrum. The product of both the pulse duration $\Delta\tau$ and the optical frequency bandwidth $\Delta\nu$ is called the time-bandwidth product (TBWP). For a given frequency bandwidth, there is a minimum corresponding pulse duration – if this is the case and the optical spectrum is symmetrical, then the pulse is said to be transform-limited, and the TBWP equals a constant K, whose value depends on the shape of the pulse, whether it is Gaussian, hyperbolic secant squared or Lorentzian. By measuring the full-width at half maximum from an optical spectrum $\Delta\lambda$, it is straightforward to calculate the TBWP of a given pulse:

$$\Delta\nu \cdot \Delta\tau = K \quad \Rightarrow \quad \frac{c}{\lambda^2}\Delta\lambda \cdot \Delta\tau = K \tag{2.2}$$

Another important property of mode-locked lasers is that the energy that was dispersed in several modes while in cw operation, is now concentrated in short pulses of light. This implies that although the output average power P_{av} may be low, the pulse peak power P_{peak} can be significantly higher:

$$P_{peak} = \frac{E_p}{\Delta\tau} \quad \Rightarrow \quad P_{peak} = \frac{1}{\Delta\tau} \cdot \frac{P_{av}}{f_R} \tag{2.3}$$

where E_p is the pulse energy.

2.1.2. Mode-locking techniques in semiconductor lasers

In recent years, mode-locked laser diodes have been at the centre of a quest for ultrafast, transform-limited and high-repetition-rate lasers. To achieve these goals, a variety of mode locking techniques and semiconductor device structures have been demonstrated and optimised [1]. The three main forms of mode locking can be described as active, passive and hybrid techniques, as outlined below.

Active mode locking relies on the direct modulation of the gain with a frequency equal to the repetition frequency of the cavity, or to a sub-harmonic of this frequency. The main advantages of this approach are the resultant low jitter and the ability to synchronise the laser output with the modulating electrical signal. These features are especially relevant for optical transmission and signal processing applications. However, high repetition frequencies are not readily obtained through directly driven modulation of lasers because fast RF modulation of the drive current becomes progressively more difficult with increase in frequency.

The frequency limitation imposed by electronic drive circuits can be overcome by employing passive mode locking techniques. This scheme typically utilises a saturable absorbing region in the laser diode. In a saturable absorber, the loss decreases as the optical intensity increases. This feature acts as a discriminator between cw and pulsed operation and can facilitate a self-starting mechanism for mode locking. Most importantly, saturable absorption plays a crucial role in shortening the duration of the circulating pulses, as will be explained, thus providing the shortest pulses achievable by all three techniques and the absence of a RF source simplifies the fabrication and operation considerably. Passive mode locking also allows for higher pulse repetition rates that are determined solely by the cavity length.

Inspired by active and passive mode locking, the technique of hybrid mode locking meets the best of both worlds because the pulse generation is initiated by an RF current imposed in the gain or absorber section, while further shaping and shortening is

assisted by saturable absorption. Throughout this work, passive mode locking was used and the next section explores in more detail the physical mechanisms behind this technique[2].

2.1.3. Passive mode locking: physics and devices

So far a simple frequency-domain picture for mode locking has been provided, where the relative phases are of primary relevance. A physical model for passive mode locking can alternatively and equivalently be described in terms of the temporal broadening and narrowing mechanisms.

Upon start-up of laser emission, the laser modes initially oscillate with relative phases that are random such that the radiation pattern consists of noise bursts. If one of these bursts is energetic enough to provide a fluence that matches the saturation fluence of the absorber, it will bleach the absorption. This means that around the peak of the burst where the intensity is higher, the loss will be smaller, while the low-intensity wings become more attenuated. The pulse generation process is thus initiated by this family of intensity spikes that experience lower losses within the absorber carrier lifetime.

The dynamics of absorption and gain play a crucial role in pulse shaping. In steady state, the unsaturated losses are higher than the gain. When the leading edge of the pulse reaches the absorber, the loss saturates more quickly than the gain, which results in a net gain window, as depicted in Fig. 2.1. The absorber then recovers from this state of saturation to the initial state of high loss, thus attenuating the trailing edge of the pulse. It is thus easy to understand why the saturation fluence and the recovery time of the absorber are of primary importance in the formation of mode-locked pulses.

This temporal scenario can be connected to the previously described frequency domain description of mode locking. The burst of noise is the result of an instantaneous phase locking occuring among a number of modes. The self-saturation at the saturable absorber then helps to sustain and strengthen this favourable combination, by discriminating it against the lower power cw noise.

[2] From this point, mode locking will implicitly mean passive mode locking, unless otherwise stated.

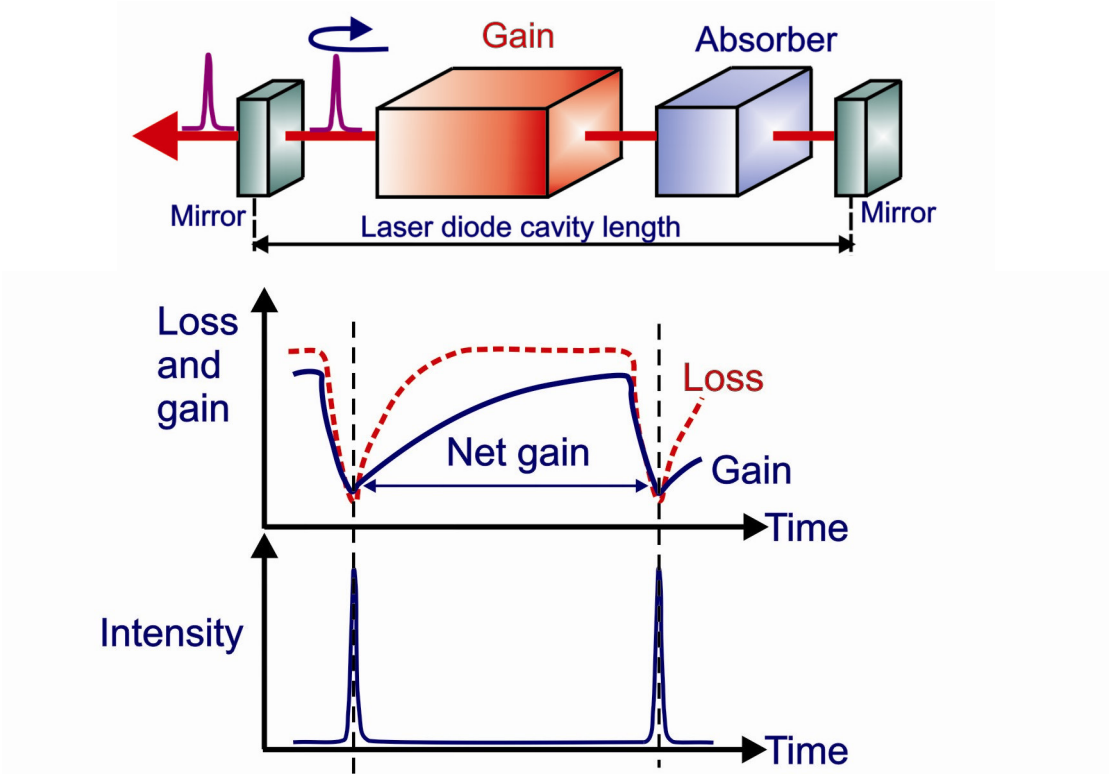

Fig. 2.1 – A schematic diagram of the main components that form a two-section laser diode (top). Loss and gain dynamics which lead to pulse generation (bottom).

In practical terms, a saturable absorber can be integrated monolithically into a semiconductor laser, by electrically isolating one section of the device. By applying a reverse bias to this section, the carriers that are photo-generated by the pulses can be more efficiently swept out of the absorber, thus enabling the saturable absorber to recover more quickly to its initial state of high loss. An increase in the reverse bias serves to decrease the absorber recovery time, and this will have the effect of further shortening the pulses.

Alternatively, a saturable absorber can also be implemented through ion implantation on one of the facets of the laser. The defects generated in the semiconductor provide a channel for the nonradiative recombination of the photocarriers, thus enabling the recovery of the absorption at relatively short times [2].

2.1.4. Requirements for successful passive mode locking

Ultrafast carrier dynamics are fundamental for successful mode locking in semiconductor lasers, particularly in the saturable absorber, because the absorption should saturate faster and recover faster. Indeed, the absorption recovery time is one of

the determining factors for obtaining ultrashort pulses. In particular, for high-repetition-rate lasers, the absorber recovery time should be much shorter than the cavity period so that the absorber can return to a state of total attenuation prior to the incidence of each incoming pulse. The fast absorption recovery also prevents the appearance of satellite pulses within the window of the net gain. On the other hand, the gain recovery time should be shorter than the cavity round-trip time. Thus, for lasers operating at pulse repetition rates of 20GHz or more, this means that the recovery times of both gain and absorption should be much shorter than 40ps.

The saturation dynamics represent another crucial aspect for successful mode locking, as shown schematically in Fig. 2.1. Such dynamics can be translated in terms of saturation fluence F_{sat} or saturation energy $E_{sat} = A \cdot F_{sat}$, where A is the optical mode cross-sectional area. The saturation energy is an indication of how much energy is necessary to saturate the absorption or the gain. Indeed, to achieve robust mode locking, the saturation energy of the absorber E_{sat}^{a} should be as small as possible and smaller than the saturation energy of the gain E_{sat}^{g}:

$$E_{sat}^{a} = \frac{h\nu A}{\frac{\partial a}{\partial N}} < E_{sat}^{g} = \frac{h\nu A}{\frac{\partial g}{\partial N}} \tag{2.4}$$

where h is Planck's constant, ν is the optical frequency, $\partial a/\partial N$ and $\partial g/\partial N$ are the differential loss and gain, respectively. This condition implies that the absorber will saturate faster than the gain for a given pulse fluence to suit the net gain window as already mentioned. The ratio between saturation energies should also be as large as possible to ensure that the losses saturate more strongly than the gain. The special dependence of the loss/gain with carrier density in a semiconductor laser allows for $\partial a/\partial N > \partial g/\partial N$, as shown in Fig. 2.2.

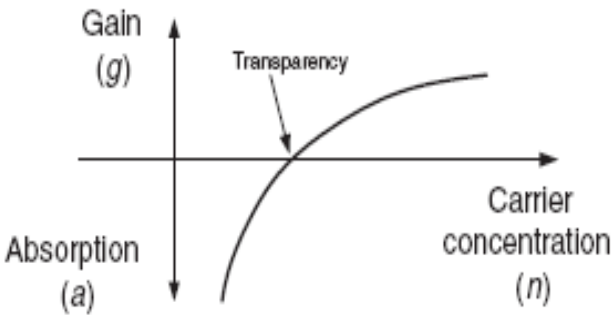

Fig. 2.2 – Dependence of absorption/gain with carrier concentration in a semiconductor laser.

2.2. Limiting factors in ultrashort-pulse generation in semiconductor lasers

2.2.1. Gain bandwidth

A natural gain narrowing usually occurs during laser operation, owing to mode competition in a semiconductor laser, particularly if the gain material is homogeneously broadened, because the mode intensities follow the peak gain at the centre of the spectral profile. This means that even with very broad gain bandwidth, the effective spectral bandwidth involved in laser emission can be narrowed significantly. Additionally, a wide frequency spacing between modes in the short semiconductor laser cavities implies that a relatively small number of modes is available to lock in phase. This phenomenon may hinder the generation of ultrashort pulses that require wide operating bandwidths.

Intracavity spectral shaping has been much explored in external cavity configurations so as to prevent gain narrowing [3,4]. The intracavity spectrum can be artificially broadened by means of an etalon, which is tuned to promote minimum transmission at the peak of the gain and two maximum transmission peaks in the wings of the gain curve, resulting in a flat and broader spectrum. An actively mode-locked laser using an intracavity etalon and external dispersion compensation generated pulses with durations around 330fs [3].

Nevertheless, although a wide bandwidth is a desirable feature, it may not be playing the most limiting effect, as even homogeneously broadened QW lasers may exhibit a spectral bandwidth large enough to support pulse durations of 200fs [5].

2.2.2. Gain saturation and recovery

The gain evolves dynamically as an optical pulse propagates in the cavity. On one hand, the optical pulse experiences gain, but on the other hand, it can also induce transitions of the carriers to higher energy levels, resulting in a gain reduction owing to free carrier absorption and two-photon absorption [6]. Being a dynamic phenomenon, the gain depletion may distort and broaden the pulse shape, as the leading part experiences more gain than the peak.

Dynamic gain saturation also plays a role in the maximum extractable energy from the medium, playing a detrimental effect in the pulse energy and thus contributing to the low peak power observed in semiconductor mode-locked lasers. The gain recovery time/gain saturation can also have an impact on the pulse shape. If there is a slow gain recovery with a time constant much larger than the pulse duration, then the trailing edge of the pulse will not be amplified, and as such could indirectly help to shorten the pulse by shaping the trailing edge.

2.2.3. Self-phase modulation and dispersion

In a semiconductor material, the refractive index and gain (or loss) depend on the carrier density and are thus strongly coupled. As the pulse propagates in the gain section[3], the carrier density and thus the gain is depleted across the pulse, as the carriers recombine through stimulated emission. This leads to a dynamic increase of the refractive index, which then introduces a phase modulation on the pulse, changing the instantaneous frequency across the pulse. This phenomenon is called self-phase modulation and is one of the main nonlinear effects associated with pulse propagation in semiconductor media.

To understand the mechanism of self-phase modulation (SPM), consider the simple and illustrative example of a plane wave $E(t,x)$:

$$E(t,x) = E_0 \exp i\Phi(t) = E_0 \exp i(\omega_0 t - kx), \qquad k = \frac{\omega_0}{c} n(t) \tag{2.5}$$

[3] In the following discussion reference is made mostly to gain to simplify the description. However, all this reasoning can be applied equally well to the absorber.

where the $\Phi(t)$ is the time-varying phase, k is the wave vector, ω_0 is the optical carrier frequency, c is the speed of light and $n(t)$ is the time-varying refractive index.

The instantaneous frequency is the time derivative of the phase and thus can be written as:

$$\omega(t) = \frac{\partial}{\partial t}\Phi(t) = \omega_0 - \frac{\omega_0}{c}\frac{\partial n(t)}{\partial t}x \tag{2.6}$$

From this expression, it is clear that if the refractive index varies with time, then the instantaneous frequency of the plane wave will vary relative to ω_0 and in a manner proportional to the temporal derivative of the index. The time dependence of this instantaneous frequency is called the frequency chirp. An up-chirp[4] (down-chirp) means that the frequency increases (decreases) with time. An example of a frequency up-chirped pulse is illustrated in Fig. 2.3.

Self-phase modulation is not dispersive in itself, but the pulse will not remain transform-limited when it propagates in a dispersive material such as the laser medium. For an up-chirped pulse, the frequency is higher in the trailing edge than in the leading edge. When the pulse propagates through a material exhibiting positive (normal) dispersion, the trailing edge of the pulse propagates more slowly than the leading edge of the pulse and so this results in a temporal broadening of the pulse.

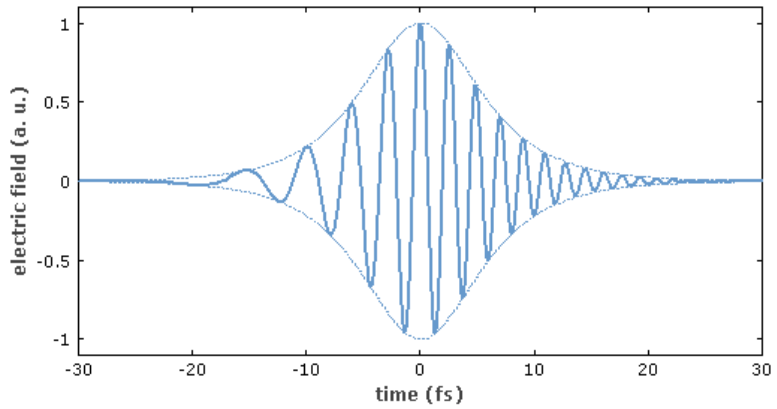

Fig. 2.3 – Illustration of an electric field of a strongly up-chirped pulse, where the instantaneous frequency increases with time.

[4] Up-chirp is also known as blue-chirp or positive chirp.

In a monolithic two-section mode-locked semiconductor laser, where a saturable absorber and a gain section coexist, the resulting chirp is a balance between the effects caused by the absorber and the gain. In the gain section, a frequency up-chirp results, while the saturable absorber helps to further shape the pulse by contributing with a negative chirp, as shown in Fig. 2.4. With a suitable balance between both sections, the chirp can be close to zero thereby leading to transform-limited pulses. Unfortunately, this is the exception rather than the rule, because this usually only occurs for a limited set of bias conditions and/or for given ratios of absorber/gain lengths. Therefore, up-chirp prevails for passively mode-locked lasers, leading to significant pulse broadening as the pulse propagates. The combined effect of self-phase modulation and dispersion impose the strongest limitation in the achievable shortest duration of pulses from mode-locked semiconductor diode lasers.

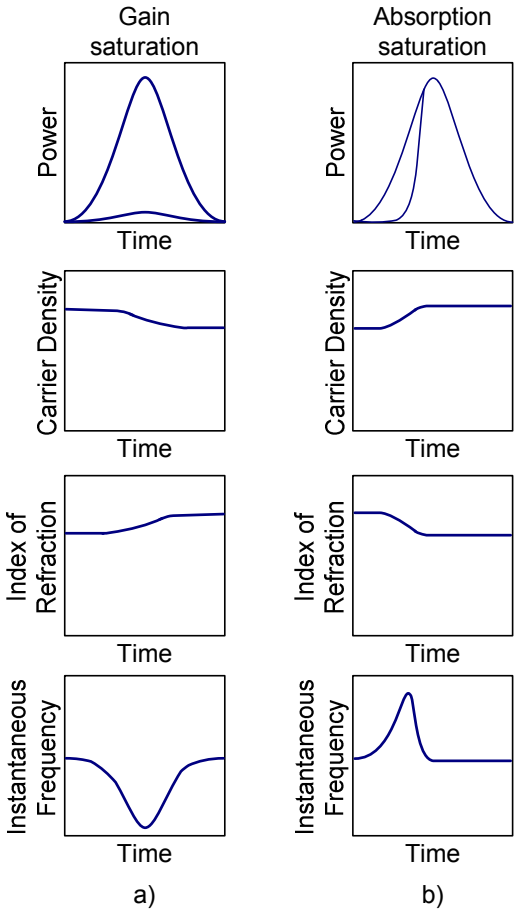

Fig. 2.4 – Effects of self-phase modulation in a mode-locked semiconductor laser, due to (a) gain saturation and (b) absorption saturation [7].

The mechanism of SPM implies that in addition to the original frequency ω_0, there are now more frequencies inside the pulse envelope. This richer spectral content is not necessarily unhelpful because it can provide bandwidth support for shorter pulses, if the chirp of a pulse can be removed by provision of a suitable dispersion-induced chirp of the opposite sign. For up-chirped pulses, a dispersion compensation setup can be configured such that a negative (anomalous) group velocity dispersion is able to slow down the leading edge of the pulse and speed the blue-shifted trailing edge to such an extent that at a certain point both edges propagate simultaneously and the pulse is shorter. This is illustrated in Fig. 2.5.

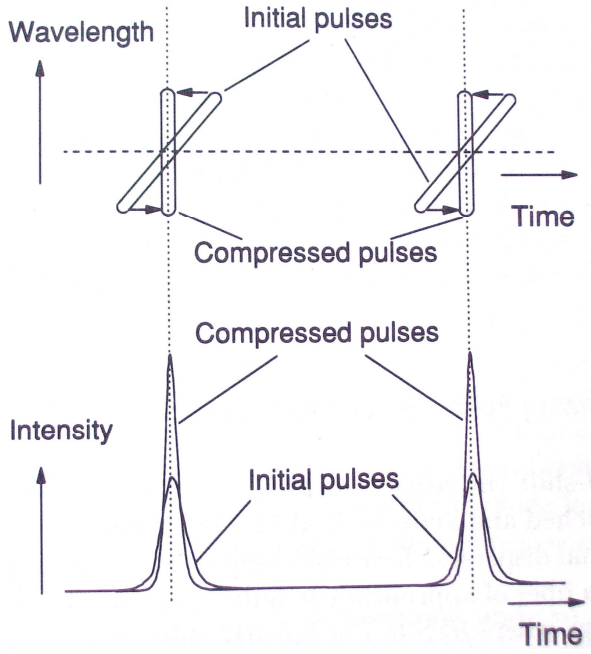

Fig. 2.5 – Illustration of the principle of optical pulse compression of linearly chirped pulses [1].

In ultrafast solid-state lasers, for example, there is also SPM, but of a different type. It is called fast SPM because it arises from an essentially instantaneous phenomenon, - an intensity dependence of the refractive index due to the optical Kerr effect[5]. In these lasers, SPM is useful to enlarge the spectral bandwidth. However, to generate femtosecond pulses, intracavity dispersion compensation is necessary, so as to balance the resulting pulse broadening effects.

[5] Fast SPM depends on the pulse duration and on the propagation distance.

In semiconductor lasers, the SPM associated with the recovery of the gain or absorption saturation is essentially a slow-SPM[6] given that it depends on the carrier density. Without dispersion compensation, it is difficult to obtain transform-limited pulses with durations shorter than 1ps directly from a monolithic device. Unfortunately, extracavity dispersion compensation setups will necessarily increase the footprint and complexity of the laser system and the monolithic integration of dispersion compensation has only recently been proposed [8].

To routinely generate pulses that are nearly transform-limited, an alternative could be found in the choice of a material that exhibits lower coupling between refractive index and gain, as described by linewidth enhancement factor, or α-factor:

$$\alpha = -\frac{4\pi}{\lambda}\frac{dn/dN}{dg/dN} \tag{2.7}$$

A higher α-factor implies a more significant coupling between gain and refractive index changes with carrier concentration and thus the possibility for higher levels of SPM and frequency chirp.

2.2.4. Low peak power

The outputs from mode-locked semiconductor diode lasers are usually characterised by low peak power. The combination of low average powers (typically in the mW scale), relatively long-duration pulses (in the picosecond range) and high pulse repetition frequencies (up to tens of GHz) is particularly detrimental in this respect. Gain saturation poses a serious limit to the achievable pulse energy. Higher-power pulses can be obtained, at the expense of increasing the average power, but this may limit some applications where high average power could result in undesirable thermal effects. Furthermore, SPM and other nonlinear effects become more important at elevated peak power levels and these can give rise to induced frequency chirp and distortion in the pulses.

Up until now, one of the most reliable techniques for achieving high peak power pulses has been to combine a diode laser oscillator with an amplifier and a pulse compressor. Delfyett has proposed a “recipe” for high-power ultrafast semiconductor

[6] Slow SPM is independent of pulse duration and the length of the gain medium.

lasers [6], using a principle similar to Chirped Pulse Amplification (CPA). In the oscillator, the optimum situation corresponds to the generation of broad and linearly chirped pulses, to avoid gain saturation effects. The power is then boosted using external amplification of the chirped pulses – thus avoiding again the detrimental gain saturation effects. The resulting pulses are finally compressed using an appropriate dispersion compensation setup to remove the linear chirp. The philosophy behind this approach is that it is easier to amplify long pulses, as they can extract more energy than shorter pulses (<1 ps), by minimising carrier heating effects. Through the use of these external amplification schemes, the peak output power can reach tens of kW but at the expense of relatively complicated arrangements. Furthermore, the pulse quality degrades as it goes through sequential stages of amplification and compression. More practical and efficient schemes for the generation of ultrashort and high power pulses are therefore desirable.

2.3. Quantum dots: distinctive advantages for ultrafast diode lasers

2.3.1. Broad gain bandwidth

Quantum-dot (QD) semiconductor structures are particularly exciting materials for the generation and amplification of femtosecond pulses because one of the key parameters that influences the emission spectrum and the optical gain in QD devices is the spectral broadening associated with the distribution of dot sizes. The extremely broad bandwidth available in QD mode-locked lasers offers potential for generating sub-100fs pulses provided all of the bandwidth can be engaged coherently and dispersion effects suitably minimised.

Indeed, it has been shown that there is usually some gain narrowing/filtering effects in mode-locked QW lasers [3]. With the inhomogeneously broadened gain bandwidth exhibited by QDs, there is support for more bandwidth and this can oppose the effect of pulse broadening that may arise from spectral narrowing. Additionally, due to the particular nature of QD lasers, many possibilities open up in respect of the

exploitation of ground-state (GS) and excited-state (ES) bands[7], thereby enabling multiple-wavelength-band switchable mode locking, as described in Chapter 5 of this thesis [9]. On the other hand, the interplay between GS and ES can be deployed in novel mode-locking regimes, as explored in Chapter 4 [10]. Using an external cavity, it is possible to set up tunable mode-locked sources, that can operate in the wavelength range that extends from the GS to the ES transition bands [11].

The inhomogeneous nature of the gain can also bring some advantages regarding the generation of low jitter pulses. In fact, the inhomogeneously broadened gain may lead to a lower mode partition noise, enabling the generation of individual comb components with reduced relative intensity noise [12].

However, high levels of inhomogeneous broadening entail a number of disadvantages, due to the resulting low levels of gain. In order to achieve reasonable optical power levels, the cavity length needs to be longer, which implies a higher level of dispersion - and thus further broadening of the pulse duration.

2.3.2. Ultrafast carrier dynamics

In the initial studies of QD materials, it was thought that their carrier dynamics would be significantly slower than those in QW materials due to a phonon bottleneck effect [13]. Interestingly, experiments have demonstrated quite the opposite. As a consequence of access to a number of recombination paths for the carriers, QD structures exhibit ultrafast recovery both under absorption and gain conditions [14]. In two evaluations, the absorber dynamics of surface and waveguided QD-structures were investigated by using a pump-probe technique [15,16]. This showed the existence of at least two distinct time constants for the recovery of the absorption (Fig. 2.6). A fast recovery of around 1ps is followed by a slower recovery process that extends over 100ps [15].

[7] Ground and excited states are also available in quantum wells. However, the δ-like density of states associated with quantum dots enables an easier access to the ES, owing to the faster saturation of the GS in quantum dots.

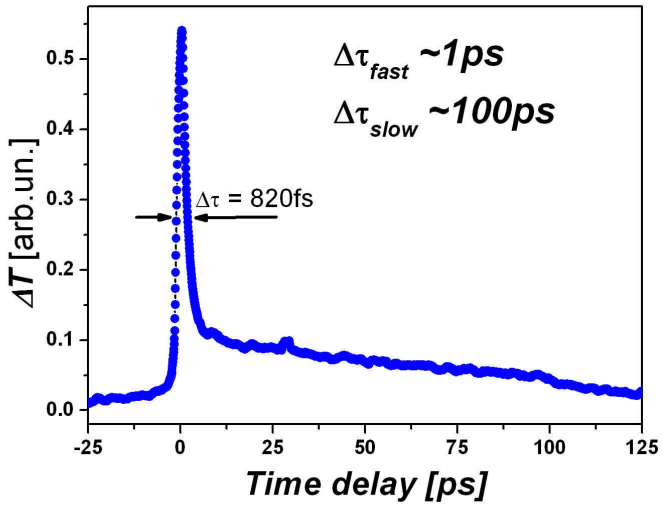

Fig. 2.6 – Pump-probe measurement of carrier lifetime in a QD waveguided device. [15]

More recently, sub-picosecond carrier recovery was measured directly in a QD absorption modulator when a reverse bias was applied [17]. Absorption recovery times ranged from 62ps down to 700fs and showed a decrease by nearly two orders of magnitude when the reverse bias applied to the structure was changed from 0V to -10V. This important observation provides significant promise for ultrafast modulators that can operate above 1THz and for the optimisation of saturable absorbers used for the passive mode locking of semiconductor lasers, where an integrated saturable absorber should be fast enough to accommodate the high-repetition-rate pulses generated by QD-lasers.

2.3.3. Lower absorption saturation fluence

QD-based saturable absorbers exhibit lower saturation fluence than QW-based materials due to their δ-like density of states. For example, in a quantum dot one electron is enough to achieve transparency and two to achieve inversion. This characteristic facilitates the self-starting of mode locking at modest pulse energies. This feature is particularly important in high-repetition rate lasers where the optical energy available in each pulse is small. Indeed, it has also been observed that the saturation power is at least 2-5 times smaller for a QD saturable absorber than for a QW-based counterpart when integrated in a monolithic mode-locked laser [18]. In this paper, the authors pointed out that saturation would further depend on the density of dots, reverse bias and inhomogeneous broadening.

It is noteworthy to mention that the required specifications of a saturable absorber may be more stringent if the absorber is integrated into a semiconductor mode-locked laser. First of all, the optical peak power is usually much lower than in mode-locked vibronic lasers. Moreover, in a monolithic configuration, the usual ridge waveguide geometry of the two-section laser imposes a similar mode area on both the gain and absorber sections, which inhibits a flexible optimization of the saturation fluence in the absorber. To overcome this limitation, the use of a flared waveguide has been investigated in a QD monolithic laser, enabling the generation of 790fs-pulses [19].

2.3.4. Low threshold current

As devices, QD diode lasers have the advantage of requiring a very low threshold current to initiate lasing [20]. This attribute applies also to operation in the mode-locking regime, because most QD lasers exhibit mode-locked operation right from the threshold of laser emission. (Bistability between the non-lasing state and the onset of lasing/mode-locking might be present, as has been shown experimentally [19,21] and numerically [22].) A low threshold current is clearly advantageous because this can represent a device that is compatible as an efficient and compact source of ultrashort pulses where the demand for electrical power can be very low. Furthermore, having a low threshold avoids the need for higher carrier densities for pumping the laser and this implies less amplified spontaneous emission and reduced optical noise in the generated pulse sequences.

2.3.5. Low temperature sensitivity

Due to the discrete nature of their density of states, QD lasers exhibit low temperature sensitivity [23], making them excellent candidates for applications in optical communications, for example. If the need for thermo-electric coolers can be avoided, then there is scope for cheap, compact, lightweight and lower power systems. More importantly, QD lasers can also show resilience to temperature effects while in mode-locked operation, as reported in Chapter 5 of this thesis.

2.3.6. Suppressed carrier diffusion

Owing to the clustered nature of QDs, carrier diffusion in the gain material is strongly suppressed, compared with QW materials [24]. This feature facilitates the fabrication of laser devices because there are no or few defects created in the sidewalls of mesas and so there are likely to be only a few centres of nonradiative recombination at the surface or interface of the active material. This feature has allowed routine processing that involves etching through the active layer, without imposing a heavy penalty on the threshold current of laser devices [25,26]. The ease of integrating deeply-etched structures opens up wide and appealing opportunities for integrating a greater range of structures into QD mode-locked lasers, such as photonic bandgap structures, chirped mirrors for dispersion compensation and distributed-feedback (DFB) structures. The fabrication process of etching through the active layer brings significant advantages for efficient fibre coupling in narrow stripe lasers because the stronger index guiding of the optical mode that is possible results in a quasi-symmetric far-field [27]. Moreover, better light confinement also improves the saturation of the absorber.

Etch-through fabrication has another advantage in respect of the direct modulation of the laser. This is important in hybrid mode locking where an RF electrical signal is injected either into the absorber or into the gain section. It has been demonstrated that an etch-through mesa exhibits a much lower parasitic capacitance than a shallow-etched mesa and so this enhances the electrical performance of the laser diode at high frequencies [27]. This feature is of key importance in active and hybrid mode-locked configurations.

Finally, another positive aspect of the lower diffusion of carriers, when associated with a low linewidth enhancement factor, is that it reduces the likelihood of beam filamentation in contrast to QW lasers [28,29]. This affords some additional potential for upgrading the optical power of QD mode-locked lasers without degrading beam quality – something that has been proven difficult for QW lasers. Indeed, QD mode-locked lasers with ridges as wide as 24μm or 30μm are possible [30,31], and a tapered-waveguide mode-locked laser with a 100μm wide front facet has been demonstrated [19]. The absence of carrier diffusion to the end facets may also concur to the higher threshold of optical catastrophic damage. This implies that QD lasers can withstand higher values of current injection than their QW counterparts, without degradation of the facet mirrors and thus higher power levels can be achieved [32].

2.3.7. Lower level of amplified spontaneous emission

Pulse generation in semiconductor ultrafast lasers can be affected by timing jitter, in particular in passively mode-locked devices, due to the lack of synchronisation with an electrical signal [33]. Amplified spontaneous emission (ASE) is the primary cause of jitter because it generates random fluctuations in photon density, gain and index of refraction, which contribute to variations in the round-trip time [1]. Longer devices are particularly prone to such problems because there is a build-up of spontaneous emission along the length of the active material. QD-based materials could make a difference in this respect, as these nanostructures exhibit lower levels of ASE [34], compared to QW, due to the discrete nature of their energy levels. On the other hand, because QD lasers usually have a lower threshold current, less carriers will be involved in non-stimulated emission [35].

2.3.8. Possibility of low-linewidth enhancement factors

One of the main motivations for the enthusiastic investigation of QD materials in the last few years has been the theoretically predicted potential for very low values of linewidth enhancement factor (LEF), owing to the symmetry of the gain associated with QD structures. The possibility of a low LEF is very attractive for a number of performance aspects, such as lower frequency chirp in directly modulated lasers, lower sensitivity to optical feedback effects and suppressed beam filamentation. The potential of a lower effect of self-phase modulation in QD lasers also held a promise for the generation of transform-limited pulses. However, disparate reports have been published in the last three years, with some reports of LEF values of nearly zero [36], and others with values of LEF similar [37] or significantly higher than in QW structures [38]. Throughout this thesis further reference will be made to this topic as the experimental results are presented.

2.4. Mode-locked quantum-dot lasers: state of the art

The first demonstration of a QD mode-locked laser was reported in 2001, with pulse durations of ~17ps at 1.3μm and repetition rate of 7.4GHz, using passive mode locking [21]. Hybrid mode locking at the same wavelength was demonstrated in 2003, by the Cambridge University group [31], reporting an upper limit estimation of 14.2ps for the shortest pulses measured at a repetition rate of 10GHz. Later in 2004, the same group demonstrated Fourier-transform-limited 10ps pulses at a 18GHz repetition rate, using passive mode locking [30].

In 2004, in collaboration with Dr Rafailov at the University of St Andrews, I participated in the demonstration of the generation of sub-picosecond pulses directly from a QD laser[8] where the shortest pulse durations were measured to be 390fs (Fig. 2.7), without any form of supplementary pulse compression [39,40]. These pulses were generated by a two-section passively mode-locked QD laser and this was the first time that sub-picosecond pulses were generated directly from such a monolithic laser. Owing to the excellent electrical characteristics of the device, it was possible to apply very high values of current and reverse bias (up to 10V), which provided some latitude for exploring a wider range of these parameters. (It is important to recall that until then, mode-locked lasers were being operated close to threshold and with relatively low values of reverse bias (< 3V).

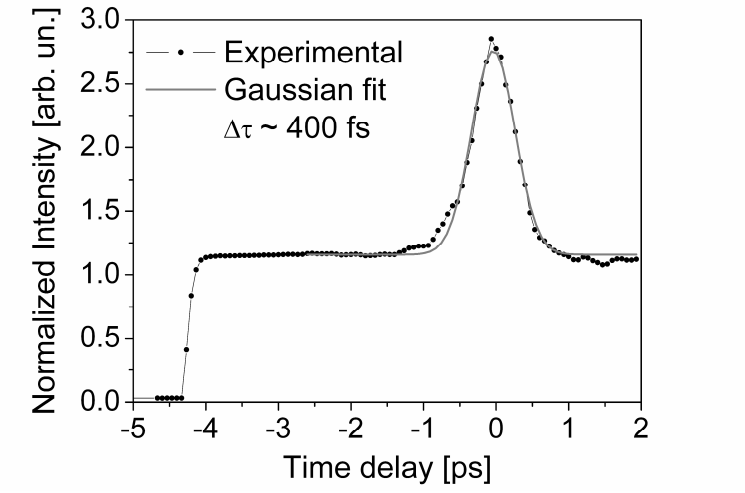

Fig. 2.7 – Intensity autocorrelation trace indicating a contrast ratio close to 3:1.

[8] My contribution to this work consisted in building a collinear autocorrelator based on a two-photon semiconductor photodiode to measure the pulse durations.

In this laser, mode-locked operation was observed over a broad range of injection currents from above laser threshold (~30mA) up to 360mA and over a relatively wide range of reverse bias levels on the absorber section (from 4.5V to 10V). The deduced time-bandwidth product of about one indicated some residual frequency chirp in these pulses. The spectrum was also the broadest generated to date (14nm). However, at the moment the physical mechanisms behind these results are still not understood and a plausible hypothesis is that the unintentional presence of some defects in the absorber could have decreased significantly the absorption recovery time to a point where significant shortening of the pulses arose.

Given that this laser was operating considerably above threshold, the power level was relatively high, with typical output powers of up to 60mW in the cw and up to 45mW in mode-locked regimes. This exceeded substantially all the previously reported values of output power for this type of laser. It thus became evident that a wider range of operating conditions could be usefully explored to improve the performance of such QD lasers. This became possible as the material growth and device processing was further refined for increased numbers of QD layers.

The generation of sub-picosecond pulses was reported later by several groups [19,41]. In one of these reports (in 2006), Thompson and co-workers demonstrated the generation of pulses as short as 790fs, by using a flared waveguide configuration in a two-section QD laser [19]. Because the beam mode size in the saturable absorber section was much smaller than that in the gain section, the ratio of saturation fluences in the absorber and gain sections was increased. This enhanced the pulse formation mechanisms and allowed for better pulse shaping and shortening. Many other results have been published during the years when my project was under way and in Table 2.1 an overview summary is presented, for mode-locked lasers based on InAs quantum dots grown on a GaAs substrate (the results presented in this thesis are not included in this Table).

There has also been much effort in designing QD-based mode-locked sources that could be deployed in the 1.55μm band [42]. Ultrashort pulse generation has been achieved from single-section lasers based either on InAs quantum dots [43] or quantum dashes [44] grown on an InP substrate. These authors have suggested that there are no fundamental differences between the quantum dots and dashes in the context of mode-locked laser sources.

QD-based materials have also been gaining status as low-noise sources because of their reduced values of ASE [34], as already mentioned, when compared with other higher-dimensional materials. To achieve ultra-low noise performance, a QD laser in a ring-cavity configuration with active harmonic mode locking was used to generate ultrashort pulses at a repetition rate of 12.8GHz [45]. The external cavity configuration, together with the electrical synchronisation allowed by active mode locking, resulted in very low residual timing jitter values of 7.5fs. This outstanding result represents the lowest timing jitter reported so far for mode-locked semiconductor lasers, thereby confirming the importance of QD materials in the pursuit of low-noise pulsed laser sources. This enhanced performance has also been observed in monolithic passively and hybridly mode-locked QD lasers. Sub-picosecond timing jitter was demonstrated for the first time in 2005 [35], for a monolithic passively mode-locked QD laser. A timing jitter value of 390fs has been reported [46], which is nearly thirty times lower than that for a similar passively mode-locked QW laser [33]. Record low values for jitter between mode-locked pulses followed, when 291fs and 124fs were reported for passive and hybrid mode locking, respectively [47].

Table 2.1 - Performance of mode-locked InAs/GaAs quantum-dot lasers using different configurations (results presented by chronological order). τ_p: pulse duration. λ_0: central wavelength. $\Delta\lambda$: spectral bandwidth. f_{rep}: repetition frequency. P_{peak}: peak power. N.A.: data not available.

Number of QD layers	Setup	ML Regime	τ_p [ps]	λ_0 [nm]	$\Delta\lambda$ [nm]	f_{rep} [GHz]	P_{peak} [mW]	Ref
2	Monolithic	Passive	17	1278	1	7.4	7	[21]
3	Monolithic	Hybrid/Passive	<14.2	1107	0.8	10	4	[31]
10	Monolithic	Passive	10	1291	0.2	18	2.5	[30]
5	Monolithic	Hybrid / Passive	12 / 7	1286	0.18	20 / 35	N.A. / 6	[48]
5	Monolithic	Passive	2	1260	14	21	1100	[39,40]
5	Monolithic	Passive	**0.39**	1260	8	21	**3000**	[39,40]
5	Monolithic	Passive	3	1281	0.8	50	6	[27]
5	Monolithic	Passive	1.7	1277	0.86	9.7	57	[49]
N.A.	Monolithic	Passive	5.7	1264	4.5	5.2	290	[35]
3	Monolithic	Colliding-pulse	7	1107	0.32	20	13	[50]
5	Monolithic (using flared waveguide)	Passive	0.79	1276	3.6	24	500	[19]
10	External cavity + SOA + compressor	Passive	1.2	1268	3.1	4.95	1220	[51]
15	Monolithic + SOA	Hybrid	0.7	1300	8.5	20	130	[41]
15	Monolithic + SOA	Hybrid	3.3	1300	6.5	20	26	[41]
15	Monolithic + SOA	Hybrid	1.9	1300	2.2	40	14	[41]
15	Monolithic + SOA	Passive	2.2	1300	4.2	80	11	[41]
5	Monolithic	Harmonic mode-locking	1.3	1280	1.4	**238**	10	[52]
6	Monolithic	Harmonic mode-locking	6.4	1216	1.8	42.4	234	[53]

To achieve higher repetition rates in mode-locked lasers it is necessary to decrease the cavity length. This poses a significant challenge to QD lasers because of their lower gain and the operation in short cavities may shift the emission to the excited-state band [54]. To avoid this problem, a higher number of QD layers should be deployed in the active region. Using this simple approach, the highest repetition rate directly generated from a passively mode-locked QD two-section laser was 80GHz [41], when a 15-layer structure was used. Another method to boost the repetition rate of mode-locked lasers is to use colliding-pulse mode-locking. This technique is similar to passive mode locking, but the saturable absorber region is placed at the precise centre of the gain section. Two counter-propagating pulses from each outer gain section therefore meet in the saturable absorber region, bleaching it much more efficiently than if just one pulse was present. This process can also result in shorter and more stable pulses. Owing to the device geometry, mode locking is achieved at the second harmonic of the fundamental (round-trip) frequency, and the pulse repetition rate is doubled. A variation of colliding pulse mode locking is harmonic mode locking, where more than two pulses circulate in the cavity, the number being equal to the harmonic.

Colliding-pulse mode-locking was first demonstrated for QD lasers in 2005 [50], resulting in a modest repetition rate of 20GHz. Harmonic mode locking has also been demonstrated with repetition rates of approximately 40GHz, 80GHz, 120GHz and 240GHz [52]. Although these data offer further evidence of the extreme speed of the absorber recovery time, it is still early to foresee if QD lasers will be able to beat the performance of high-repetition-rate lasers based on bulk and quantum-well materials. One of the earliest reports of colliding-pulse mode-locking dates from 1991 [55] and the results obtained are still astonishing today: a monolithic multiple quantum well InGaAsP laser was able to generate transform-limited pulses of 640fs, at 350GHz. Terahertz-rate pulse generation was achieved in 1994 [56], by the harmonic mode-locking of a self-colliding-pulse diode laser having a distributed-Bragg-reflector (an in-depth study of this experiment can also be found in reference [57]). The 40^{th} harmonic number of the fundamental repetition frequency was obtained, yielding 260fs transform-limited pulses, at a 1.54THz-rate.

In terms of pulse duration, the results presented in the literature show that only *monolithic passively mode-locked* QD lasers [19,40] can slightly exceed the performance of quantum-well and bulk lasers with similar geometry (but not using

colliding-pulse mode locking). Indeed, pulse durations as short as 650fs have been obtained directly from a bulk InGaAsP/InP laser, where the saturable absorber regions were formed by deep implantation of heavy ions into the diode facets [58].

In this thesis, the passive mode-locking regime of QD lasers has been investigated thoroughly, as reported in Chapter 3, to get a clearer understanding of the limitations and potential of ultrafast QD lasers. However, as will be shown, the results did not surpass those that are reported in Table 1, in terms of pulse duration or peak power. Another approach has therefore been adopted here that involved an investigation of the additional unique aspects of QD lasers that could give them a competitive edge over QW lasers. One such aspect is the innovative use of the excited-state transitions in the ultrafast operation of QD lasers, which was proposed for the first time during this research. Two novel mode-locking regimes stemmed from this research direction and these are described in Chapters 4 and 5.

The other aspect that was considered was the temperature resilience of QD lasers and this was extended to ultrafast operation which is of relevance to commercial applications (Chapter 6). Moreover, the use of temperature as an investigative tool enabled further crucial information to be obtained on the carrier dynamics that is relevant to the mode locking of QD lasers.

2.5. References

[1] P. Vasil'ev, *Ultrafast Diode Lasers: Fundamentals and Applications*. Boston: Artech House, 1995.

[2] E. L. Delpon, J. L. Oudar, N. Bouche, R. Raj, A. Shen, N. Stelmakh, and J. M. Lourtioz, "Ultrafast excitonic saturable absorption in ion-implanted InGaAs/InAlAs multiple quantum wells," *Appl. Phys. Lett.*, vol. 72, pp. 759-761, 1998.

[3] P. J. Delfyett, H. Shi, S. Gee, C. P. J. Barty, G. Alphonse, and J. Connolly, "Intracavity spectral shaping in external cavity mode-locked semiconductor diode lasers," *IEEE J. Sel. Topics Quantum Electron.*, vol. 4, pp. 216-223, 1998.

[4] S. Gee, G. A. Alphonse, J. C. Connolly, C. Barty, and P. J. Delfyett, "Ultrashort pulse generation by intracavity spectral shaping and phase compensation of external-cavity modelocked semiconductor lasers," *IEEE J. Quantum Electron.*, vol. 36, pp. 1035-1040, 2000.

[5] F. Futami, Y. Takushima, and K. Kikuchi, "Generation of 10GHz, 200fs Fourier-transform-limited optical pulse train from modelocked semiconductor laser at 1.55 μm by pulse compression using dispersion-flattened fibre with normal group-velocity dispersion," *Electron. Lett.*, vol. 34, pp. 2129-2130, 1998.

[6] P. J. Delfyett, "Ultrafast Single and Multiwavelength Modelocked Semiconductor Lasers: Physics and Applications," in *Ultrafast Lasers - Technology and Applications*, M. E. Fermann, A. Galvanauskas, and G. Sucha, Eds. New York: Marcel Dekker, Inc., 2003, pp. 219-321.

[7] D. J. Derickson, R. J. Helkey, A. Mar, J. R. Karin, J. G. Wasserbauer, and J. E. Bowers, "Short pulse generation using multisegment mode-locked semiconductor-lasers," *IEEE J. Quantum Electron.*, vol. 28, pp. 2186-2202, 1992.

[8] T. J. Karle, Y. J. Chai, C. N. Morgan, I. H. White, and T. F. Krauss, "Observation of pulse compression in photonic crystal coupled cavity waveguides," *J. Lightwave Technol.*, vol. 22, pp. 514-519, 2004.

[9] M. A. Cataluna, W. Sibbett, D. A. Livshits, J. Weimert, A. R. Kovsh, and E. U. Rafailov, "Stable mode locking via ground- or excited-state transitions in a two-section quantum-dot laser," *Appl. Phys. Lett.*, vol. 89, pp. 81124-3, 2006.

[10] M. A. Cataluna, A. D. McRobbie, W. Sibbett, D. A. Livshits, A. R. Kovsh, and E. U. Rafailov, "New mode-locking regime in a quantum-dot laser: enhancement by simultaneous CW excited-state emission," *Conference on Lasers and Electro-Optics/Quantum Electronics and Laser Science Conference*, *Technical Digest*, CThH3, Long Beach, USA, 2006.

[11] J. Kim, M. T. Choi, W. Lee, and P. J. Delfyett, "Wavelength tunable mode-locked quantum-dot laser," *Enabling Photonics Technologies for Defense, Security, and Aerospace Applications II*, *Proc. SPIE*, 62430M, M2430-M2430, Kissimmee, FL, 2006.

[12] P. J. Delfyett, M. T. Choi, S. Gee, J. Kim, W. Lee, S. Ozharar, and F. Quinlan, "Recent advances in stabilized ultrafast modelocked semiconductor diode lasers for high speed information based applications," *The 19th Annual Meeting of the IEEE Lasers and Electro-Optics Society*, *Technical Digest*, 791, Montreal, Canada, 2006.

[13] K. Mukai, N. Ohtsuka, H. Shoji, and M. Sugawara, "Phonon bottleneck in self-formed $In_xGa_{1-x}As/GaAs$ quantum dots by electroluminescence and time-resolved photoluminescence," *Phys. Rev. B*, vol. 54, pp. R5243-R5246, 1996.

[14] P. Borri, S. Schneider, W. Langbein, and D. Bimberg, "Ultrafast carrier dynamics in InGaAs quantum dot materials and devices," *J. Opt. A*, vol. 8, pp. S33-S46, 2006.

[15] E. U. Rafailov, S. J. White, A. A. Lagatsky, A. Miller, W. Sibbett, D. A. Livshits, A. E. Zhukov, and V. M. Ustinov, "Fast quantum-dot saturable absorber for passive mode-locking of solid-state lasers," *IEEE Photon. Technol. Lett.*, vol. 16, pp. 2439-2441, 2004.

[16] P. Borri, W. Langbein, J. M. Hvam, F. Heinrichsdorff, M. H. Mao, and D. Bimberg, "Spectral hole-burning and carrier-heating dynamics in InGaAs quantum-dot amplifiers," *IEEE J. Sel. Topics Quantum Electron.*, vol. 6, pp. 544-551, 2000.

[17] D. B. Malins, A. Gomez-Iglesias, S. J. White, W. Sibbett, A. Miller, and E. U. Rafailov, "Ultrafast electroabsorption dynamics in an InAs quantum dot saturable absorber at 1.3 μm," *Appl. Phys. Lett.*, vol. 89, pp. 171111-3, 2006.

[18] M. G. Thompson, C. Marinelli, Y. Chu, R. L. Sellin, R. V. Penty, I. H. White, M. Van Der Peol, D. Birkedal, J. Hvam, V. M. Ustinov, M. Lammlin, and D. Bimberg, "Properties of InGaAs quantum dot saturable absorbers in monolithic mode-locked lasers," *IEEE 19th International Semiconductor Laser Conference*, 53-54, Matsue Shi, Japan, 2004.

[19] M. G. Thompson, A. Rae, R. L. Sellin, C. Marinelli, R. V. Penty, I. H. White, A. R. Kovsh, S. S. Mikhrin, D. A. Livshits, and I. L. Krestnikov, "Subpicosecond high-power mode locking using flared waveguide monolithic quantum-dot lasers," *Appl. Phys. Lett.*, vol. 88, pp. 133119-3, 2006.

[20] V. M. Ustinov, A. E. Zhukov, A. Y. Egorov, and N. A. Maleev, *Quantum Dot Lasers*. New York: Oxford University Press, 2003.

[21] X. D. Huang, A. Stintz, H. Li, L. F. Lester, J. Cheng, and K. J. Malloy, "Passive mode-locking in 1.3 μm two-section InAs quantum dot lasers," *Appl. Phys. Lett.*, vol. 78, pp. 2825-2827, 2001.

[22] E. A. Viktorov, P. Mandel, A. G. Vladimirov, and U. Bandelow, "Model for mode locking in quantum dot lasers," *Appl. Phys. Lett.*, vol. 88, pp. 201102-3, 2006.

[23] S. S. Mikhrin, A. R. Kovsh, I. L. Krestnikov, A. V. Kozhukhov, D. A. Livshits, N. N. Ledentsov, Y. M. Shernyakov, I. I. Novikov, M. V. Maximov, V. M. Ustinov, and Z. I. Alferov, "High power temperature-insensitive 1.3 μm InAs/InGaAs/GaAs quantum dot lasers," *Semiconductor Sci. Tech.*, vol. 20, pp. 340-342, 2005.

[24] S. A. Moore, L. O'Faolain, M. A. Cataluna, M. B. Flynn, M. V. Kotlyar, and T. F. Krauss, "Reduced surface sidewall recombination and diffusion in quantum-dot lasers," *IEEE Photon. Technol. Lett.*, vol. 18, pp. 1861-1863, 2006.

[25] D. Ouyang, N. N. Ledentsov, D. Bimberg, A. R. Kovsh, A. E. Zhukov, S. S. Mikhrin, and V. M. Ustinov, "High performance narrow stripe quantum-dot lasers with etched waveguide," *Semiconductor Sci. Tech.*, vol. 18, pp. L53-L54, 2003.

[26] D. Ouyang, N. N. Ledentsov, S. Bognar, F. Hopfer, R. L. Sellin, I. N. Kaiander, and D. Bimberg, "Impact of the mesa etching profiles on the spectral hole burning effects in quantum dot lasers," *Semiconductor Sci. Tech.*, vol. 19, pp. L43-L47, 2004.

[27] M. Kuntz, G. Fiol, M. Lammlin, D. Bimberg, M. G. Thompson, K. T. Tan, C. Marinelli, A. Wonfor, R. Sellin, R. V. Penty, I. H. White, V. M. Ustinov, A. E. Zhukov, Y. M. Shernyakov, A. R. Kovsh, N. N. Ledentsov, C. Schubert, and V. Marembert, "Direct modulation and mode locking of 1.3 μm quantum dot lasers," *New J. Phys.*, vol. 6, pp. 181, 2004.

[28] C. Ribbat, R. L. Sellin, I. Kaiander, F. Hopfer, N. N. Ledentsov, D. Bimberg, A. R. Kovsh, V. M. Ustinov, A. E. Zhukov, and M. V. Maximov, "Complete suppression of filamentation and superior beam quality in quantum-dot lasers," *Appl. Phys. Lett.*, vol. 82, pp. 952-954, 2003.

[29] E. Gehrig, O. Hess, C. Ribbat, R. L. Sellin, and D. Bimberg, "Dynamic filamentation and beam quality of quantum-dot lasers," *Appl. Phys. Lett.*, vol. 84, pp. 1650-1652, 2004.

[30] M. G. Thompson, K. T. Tan, C. Marinelli, K. A. Williams, R. V. Penty, I. H. White, M. Kuntz, D. Ouyang, D. Bimberg, V. M. Ustinov, A. E. Zhukov, A. R. Kovsh, N. N. Ledentsov, D. J. Kang, and M. G. Blamire, "Transform-limited optical pulses from 18 GHz monolithic modelocked quantum dot lasers operating at 1.3 μm," *Electron. Lett.*, vol. 40, pp. 346-347, 2004.

[31] M. G. Thompson, C. Marinelli, K. T. Tan, K. A. Williams, R. V. Penty, I. H. White, I. N. Kaiander, R. L. Sellin, D. Bimberg, D. J. Kang, M. G. Blamire, F. Visinka, S. Jochum, and S. Hansmann, "10 GHz hybrid modelocking of monolithic InGaAs quantum dot lasers," *Electron. Lett.*, vol. 39, pp. 1121-1122, 2003.

[32] M. Grundmann, F. Heinrichsdorff, N. N. Ledentsov, C. Ribbat, D. Bimberg, A. E. Zhukov, A. R. Kovsh, M. V. Maximov, Y. M. Shernyakov, D. A. Lifshits, V. M. Ustinov, and Z. I. Alferov, "Progress in quantum dot lasers: 1100 nm, 1300 nm, and high power applications," *Jpn. J. Appl. Phys.*, vol. 39, pp. 2341-2343, 2000.

[33] D. J. Derickson, P. A. Morton, J. E. Bowers, and R. L. Thornton, "Comparison of timing jitter in external and monolithic cavity mode-locked semiconductor-lasers," *Appl. Phys. Lett.*, vol. 59, pp. 3372-3374, 1991.

[34] T. W. Berg and J. Mork, "Quantum dot amplifiers with high output power and low noise," *Appl. Phys. Lett.*, vol. 82, pp. 3083-3085, 2003.

[35] L. Zhang, L. Cheng, A. L. Gray, S. Luong, J. Nagyvary, F. Nabulsi, L. Olona, K. Sun, T. Tumolillo, R. Wang, C. Wiggins, J. Zilko, Z. Zou, P. M. Varangis, H. Su, and L. F. Lester, "Low timing jitter, 5 GHz optical pulses from monolithic two-section passively mode-locked 1250/1310 nm quantum dot lasers for high-speed optical interconnects," *Optical Fiber Communication Conference*, *Technical Digest*, OWM4, Anaheim, USA, 2005.

[36] T. C. Newell, D. J. Bossert, A. Stintz, B. Fuchs, K. J. Malloy, and L. F. Lester, "Gain and linewidth enhancement factor in InAs quantum-dot laser diodes," *IEEE Photon. Technol. Lett.*, vol. 11, pp. 1527-1529, 1999.

[37] A. A. Ukhanov, A. Stintz, P. G. Eliseev, and K. J. Malloy, "Comparison of the carrier induced refractive index, gain, and linewidth enhancement factor in quantum dot and quantum well lasers," *Appl. Phys. Lett.*, vol. 84, pp. 1058-1060, 2004.

[38] B. Dagens, A. Markus, J. X. Chen, J. G. Provost, D. Make, O. Le Gouezigou, J. Landreau, A. Fiore, and B. Thedrez, "Giant linewidth enhancement factor and purely frequency modulated emission from quantum dot laser," *Electron. Lett.*, vol. 41, pp. 323-324, 2005.

[39] E. U. Rafailov, M. A. Cataluna, W. Sibbett, N. D. Il'inskaya, Y. M. Zadiranov, A. E. Zhukov, V. M. Ustinov, D. A. Livshits, A. R. Kovsh, and a. N. N. Ledentsov, "High-power ultrashort pulses output from a mode-locked two-section quantum-dot laser," *Conference on Lasers and Electro-Optics/International Quantum Electronics Conference*, *Technical Digest*, CPDB5, post-deadline, 1031-1032, San Francisco, 2004.

[40] E. U. Rafailov, M. A. Cataluna, W. Sibbett, N. D. Il'inskaya, Y. M. Zadiranov, A. E. Zhukov, V. M. Ustinov, D. A. Livshits, A. R. Kovsh, and N. N. Ledentsov, "High-power picosecond and femtosecond pulse generation from a two-section mode-locked quantum-dot laser," *Appl. Phys. Lett.*, vol. 87, pp. 81107-3, 2005.

[41] M. Laemmlin, G. Fiol, C. Meuer, M. Kuntz, F. Hopfer, A. R. Kovsh, N. N. Ledentsov, and D. Bimberg, "Distortion-free optical amplification of 20-80 GHz modelocked laser pulses at 1.3 μm using quantum dots," *Electron. Lett.*, vol. 42, pp. 697-699, 2006.

[42] F. Lelarge, B. Dagens, J. Renaudier, R. Brenot, A. Accard, F. van Dijk, D. Make, O. Le Gouezigou, J. G. Provost, F. Poingt, J. Landreau, O. Drisse, E. Derouin, B. Rousseau, F. Pommereau, and G. H. Duan, "Recent advances on InAs/InP quantum dash based, semiconductor lasers and optical amplifiers operating at 1.55 mu m," *IEEE J. Sel. Topics Quantum Electron.*, vol. 13, pp. 111-124, 2007.

[43] J. Renaudier, R. Brenot, B. Dagens, F. Lelarge, B. Rousseau, F. Poingt, O. Legouezigou, F. Pommereau, A. Accard, P. Gallion, and G. H. Duan, "45 GHz self-pulsation with narrow linewidth in quantum dot Fabry-Perot semiconductor lasers at 1.5 μm," *Electron. Lett.*, vol. 41, pp. 1007-1008, 2005.

[44] C. Gosset, K. Merghem, A. Martinez, G. Moreau, G. Patriarche, G. Aubin, A. Ramdane, J. Landreau, and F. Lelarge, "Subpicosecond pulse generation at 134 GHz using a quantum-dash-based Fabry-Perot laser emitting at 1.56 μm," *Appl. Phys. Lett.*, vol. 88, pp. 241105-3, 2006.

[45] M.-T. Choi, J.-M. Kim, W. Lee, and P. J. Delfyett, "Ultralow noise optical pulse generation in an actively mode-locked quantum-dot semiconductor laser," *Appl. Phys. Lett.*, vol. 88, pp. 131106-3, 2006.

[46] A. R. Rae, M. G. Thompson, R. V. Penty, I. H. White, A. R. Kovsh, S. S. Mikhrin, D. A. Livshits, and I. L. Krestnikov, "Absorber length optimisation for sub-picosecond pulse generation in passively mode-locked 1.3 μm Quantum-Dot Laser Diodes," *Semiconductor Lasers and Laser Dynamics II*, *Proc. SPIE*, 61841F, F1841-F1841, 2006.

[47] M. G. Thompson, D. Larson, A. Rae, K. Yvind, R. Penty, I. H. White, J. Hvam, A. Kovsh, S. Mikhrin, D. A. Livshits, and I. Krestnikov, "Monolithic hybrid and passive mode-locked 40GHz quantum dot laser diodes," *32nd European Conference on Optical Communication*, *Technical Digest*, We4.6.3, Nice, France, 2006.

[48] M. Kuntz, G. Fiol, M. Lammlin, D. Bimberg, M. G. Thompson, K. T. Tan, C. Marinelli, R. V. Penty, I. H. White, V. M. Ustinov, A. E. Zhukov, Y. M. Shernyakov, and A. R. Kovsh, "35 GHz mode-locking of 1.3 μm quantum dot lasers," *Appl. Phys. Lett.*, vol. 85, pp. 843-845, 2004.

[49] A. E. Gubenko, L. M. Gadjiev, N. D. Il'inskaya, Y. M. Zadiranov, A. E. Zhukov, V. M. Ustinov, Z. I. Alferov, E. L. Portnoi, A. R. Kovsh, D. A. Livshits, and N. N. Ledentsov, "Mode-locking at 9.7 GHz repetition rate with 1.7 ps pulse duration in two-section QD lasers," *19th IEEE International Semiconductor Laser Conference*, *Technical Digest*, 51-52, Matsue Shi, Japan, 2004.

[50] M. G. Thompson, C. Marinelli, X. Zhao, R. L. Sellin, R. V. Penty, I. H. White, I. N. Kaiander, D. Bimberg, D. J. Kang, and M. G. Blamire, "Colliding-pulse modelocked quantum dot lasers," *Electron. Lett.*, vol. 41, pp. 248-250, 2005.

[51] M. T. Choi, W. Lee, J. M. Kim, and P. J. Delfyett, "Ultrashort, high-power pulse generation from a master oscillator power amplifier based on external cavity mode locking of a quantum-dot two-section diode laser," *Appl. Phys. Lett.*, vol. 87, pp. 221107-3, 2005.

[52] A. R. Rae, M. G. Thompson, R. V. Penty, I. H. White, A. R. Kovsh, S. S. Mikhrin, D. A. Livshits, and I. L. Krestnikov, "Harmonic mode-locking of a quantum-dot laser diode," *The 19th Annual Meeting of the IEEE Lasers and Electro-Optics Society*, *Technical Digest*, ThR5, 874-875, Montreal, Canada, 2006.

[53] Y. C. Xin, Y. Li, V. Kovanis, A. L. Gray, L. Zhang, and L. F. Lester, "Reconfigurable quantum dot monolithic multi-section passive mode-locked lasers," *Opt. Express*, vol. 15, pp. 7623-7633, 2007.

[54] A. Markus, J. X. Chen, C. Paranthoen, A. Fiore, C. Platz, and O. Gauthier-Lafaye, "Simultaneous two-state lasing in quantum-dot lasers," *Appl. Phys. Lett.*, vol. 82, pp. 1818-1820, 2003.

[55] Y. K. Chen, M. C. Wu, T. Tanbunek, R. A. Logan, and M. A. Chin, "Subpicosecond Monolithic Colliding-Pulse Mode-Locked Multiple Quantum-Well Lasers," *Appl. Phys. Lett.*, vol. 58, pp. 1253-1255, 1991.

[56] S. Arahira, S. Oshiba, Y. Matsui, T. Kunii, and Y. Ogawa, "Terahertz-Rate Optical Pulse Generation from a Passively Mode-Locked Semiconductor-Laser Diode," *Opt. Lett.*, vol. 19, pp. 834-836, 1994.

[57] S. Arahira, Y. Matsui, and Y. Ogawa, "Mode-locking at very high repetition rates more than terahertz in passively mode-locked distributed-Bragg-reflector laser diodes," *IEEE J. Quantum Electron.*, vol. 32, pp. 1211-1224, 1996.

[58] A. G. Deryagin, D. V. Kuksenkov, V. I. Kuchinskii, E. L. Portnoi, and I. Y. Khrushchev, "Generation of 110 GHz train of subpicosecond pulses in 1.535 mm spectral region by passively modelocked InGaAsP/InP laser diodes," *Electron. Lett.*, vol. 30, pp. 309-311, 1994.

3. CHARACTERISATION OF MODE-LOCKED OPERATION IN QUANTUM-DOT LASERS

The present chapter will start by discussing how ultrashort pulses can be measured using autocorrelation techniques. A brief theoretical description is given and certain practical issues are discussed. The design of an autocorrelator is explored and the details on the actual experimental setup used in this work are given. The mode-locking performance of two sets of lasers is extensively characterised at room temperature, and the effects of the bias conditions on the mode-locking regime are discussed.

3.1. Techniques for characterisation of mode-locked operation

3.1.1. Pulse duration measurements

The most immediate and simple technique to measure a pulse duration would be to use a sampling oscilloscope. However, an optical pulse with a duration of 1ps would require a bandwidth of several 100GHz for an accurate recovery of the pulse shape. A lower bandwidth leads to the detection of a broadened pulse envelope, restricting the resolution of the detector. The bandwidth of fast sampling oscilloscopes is limited due to the required conversion from optical to electrical signals. The bandwidth of commercially available photodiodes in the NIR region are currently specified to 70GHz [1]. Optical pulses with a pulse duration of 1ps, measured with such photodiodes and an electrical sampling oscilloscope would result in a trace with a pulse duration of 10ps. Furthermore, the lack of an appropriate trigger for passively mode-locked high-repetition-rate lasers makes it difficult to visualise the generated pulses in the oscilloscope, even for extremely long pulses.

To overcome the bandwidth limitations imposed by the photodetectors, optical oscilloscopes can be used. These instruments can measure the pulse directly without the need of an electrical signal transmission line. Nevertheless, the best temporal resolution available from optical sampling systems is 18ps at the moment [2].

An alternative direct method would involve using a streak camera, which can offer a better temporal resolution, although currently limited to 200fs [2]. Therefore a measurement of a 1ps pulse would deliver only 5 measurement points.

The best resolution available at the moment is only accessible via an indirect all-optical technique called autocorrelation, where the pulse interacts with a delayed replica of itself. The good temporal resolution and the low cost of an autocorrelation setup make this technique one of the most widely used methods for measuring ultrashort pulse durations.

In an autocorrelation setup, the incoming pulse with temporal intensity profile $I(t)$ is split into two replicas $I(t)$ and $I(t-\tau)$ to be compared within an interferometer. An adjustable arm imbalance of Δx between the two paths in the interferometer introduces the temporal delay τ, thus changing the temporal overlap between the pulses, as shown in Fig. 3.1. The two replicas are then combined and focused into a nonlinear medium to produce a mixing signal whose strength depends on

the extent of mutual overlap. The resulting mixing signal - the autocorrelation function - is thus measured as a function of the delay τ, which can be controlled in the setup. Based on a time-space transformation, a light pulse takes one picosecond to travel 300 μm in air – and this distance can be easily measured and calibrated. Therefore, the temporal resolution available from this method can be as good as few fs, corresponding to a spatial accuracy of few microns.

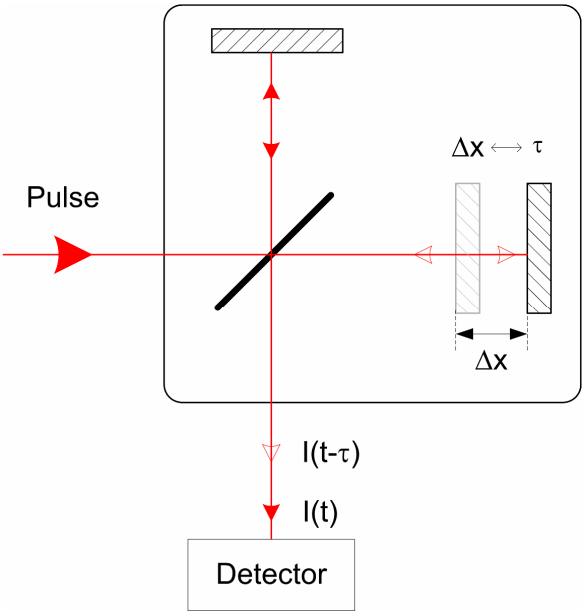

Fig. 3.1 – Basic principle of autocorrelation.

In order to extract the information of the pulse duration, it is necessary to access the higher orders of the autocorrelation function beyond the first. Usually, a second-order autocorrelation function of an optical pulse is measured, as it is easily implemented using two-photon nonlinear optical processes, such as second-harmonic generation (SHG) in a nonlinear crystal or two-photon absorption in a semiconductor photodiode. Throughout the course of this work, both processes were used. A collinear autocorrelator based on two-photon absorption in a photodiode was firstly developed and used to measure the results regarding the pulse duration of 400fs [3]. A commercial autocorrelator was later purchased, based on a SHG crystal and photomultiplier tube. This noncollinear setup was used to measure the pulse durations presented in this work, and will be explained in more detail in Section 3.2.1. It is important to remark that the autocorrelation of the pulses generated by mode-locked laser diodes can prove very challenging, owing to the low peak power of the pulses (10-100mW), which results

from the low average power (0.1-10mW), picosecond pulse durations and high repetition rates (10-100GHz).

A second-order autocorrelation function of a pulse with an electrical field $E(t)$ is proportional to:

$$\int_{-\infty}^{+\infty} \left| \left[E(t) + E(t+\tau) \right]^2 \right|^2 dt \tag{3.1}$$

In a system with insufficient bandwidth to resolve the interference fringes resulting from the combination of the two replicas, an intensity autocorrelation profile is obtained.

If the two replicas are collinearly aligned, the nonlinear signal intensity as read by the detector will be given by:

$$f(\tau) = 1 + 2 \frac{\int_{-\infty}^{+\infty} I(t) I(t-\tau) dt}{\int_{-\infty}^{+\infty} I(t)^2 dt} \tag{3.2}$$

where $I(t)$ is the pulse intensity. In this type of autocorrelation, a peak-to-background ratio of 3 to 1 is observed for an optical pulse.

In the case of a noncollinear setup, the autocorrelation is background-free, because the individual beams do not contribute to the detector signal. The resulting second harmonic of each beam will have the same direction of the beams and will thus be spatially filtered. It is only the second harmonic resulting from the interaction of both beams that will hit the detector, as a result of momentum conservation (phase matching) in the crystal. In this case, the background-free autocorrelation function f_{zb} takes the form:

$$f_{zb}(\tau) = \frac{\int_{-\infty}^{+\infty} I(t) I(t-\tau) dt}{\int_{-\infty}^{+\infty} I(t)^2 dt} \tag{3.3}$$

The resulting outputs from these functions are illustrated in Fig. 3.2, depending on the degree of stability of the pulse generation.

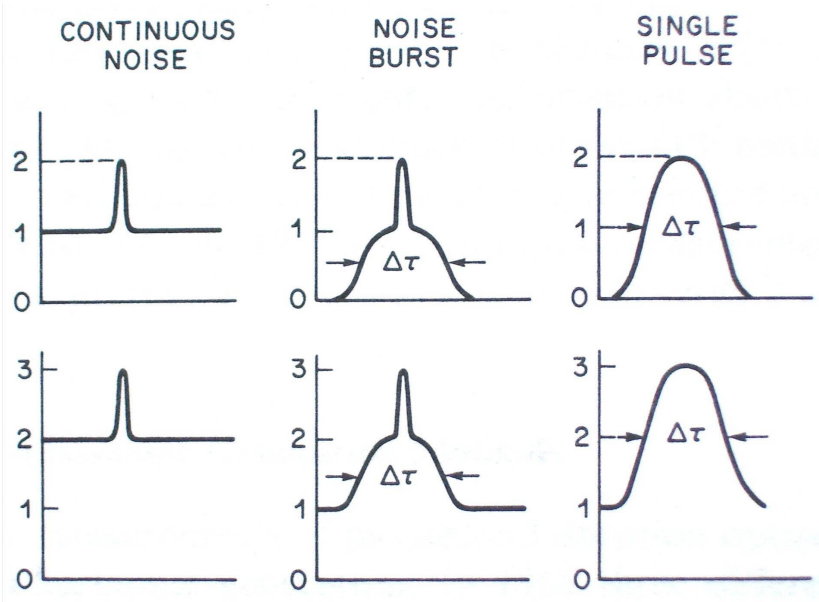

Fig. 3.2 – Theoretical intensity autocorrelation functions $f(\tau)$ and $f_{zb}(\tau)$ for various optical inputs [4].

In order to extract an actual pulse duration, an assumption has to be made about the shape of the actual pulse – a function that can be assumed after a best-fit to the acquired autocorrelation. The most commonly found shapes in literature are Gaussian, hyperbolic sech and Lorentzian. Depending on the type of pulse shape, the full width at half maximum (FWHM) of the autocorrelation trace should be multiplied by a given factor in order to obtain the pulse duration. The time-bandwidth product is also different for each function type. Throughout this work, it was found that for all the characterised lasers, the pulses and the optical spectra were best fitted assuming a Gaussian pulse shape. For a Gaussian function, the FWHM of the autocorrelation should be multiplied by 0.707 in order to obtain the pulse duration. In the case of a Gaussian function, the minimum time-bandwidth product is 0.441.

Autocorrelation is not without its disadvantages. The autocorrelation function is by definition a symmetrical function $f(\tau) = f(-\tau)$, and thus conceals any information about the symmetry properties of the original pulse. Also, no information about the phase and the chirp of the pulse is available from intensity autocorrelations. Different

pulses can result in similar autocorrelation functions, so there is a certain degree of ambiguity on matching a pulse shape to the autocorrelation trace [5].

3.1.2. RF characterisation as a measure of mode locking stability

The pulse repetition frequency can be accurately measured by an electrical spectrum analyzer, after converting the optical signal into an RF signal by a photodiode with a suitable bandwidth. The signal-to-noise ratio of the trace and the -3dB bandwidth provide an indication of mode-locking stability. For instance, if there is a strong noise component around the carrier, this translates into a broader pedestal. This means that overall, the jitter is also higher, because the pulse repetition frequency oscillates in a range of values. Mode locking was considered to be stable when this pedestal was narrow and the signal-to-noise ratio was higher than 15dB.

The RF spectrum can thus be used as quick monitor to assess the stability of mode locking. Automated acquisitions of RF spectra further enabled to get this info at a glance, allowing the identification of the best parameters of stable mode locking – a broad RF spectrum corresponds to unstable mode locking, while a narrow one corresponds to stable mode locking.

3.2. Experimental setup

The gain section of the lasers was biased using a Melles Griot diode laser driver, while the reverse bias was applied using a HP 3631E power supply. Unless otherwise specified, a Peltier cooler was used to maintain a constant temperature of 25 ^{o}C for all the tested lasers.

After appropriate collimation, the beam traversed a Linos optical isolator (FI-1310-4SL) with more than 35dB isolation. This component prevented unintentional reflections from the optical fibre facet and other setup components from being coupled back into the laser chip. It is crucial to avoid uncontrolled optical feedback, as it can significantly affect the mode-locking regime, which becomes unstable and with lower average power.

Using several beamsplitters, the laser output could be simultaneously monitored by all the diagnostic equipments (Fig. 3.3).

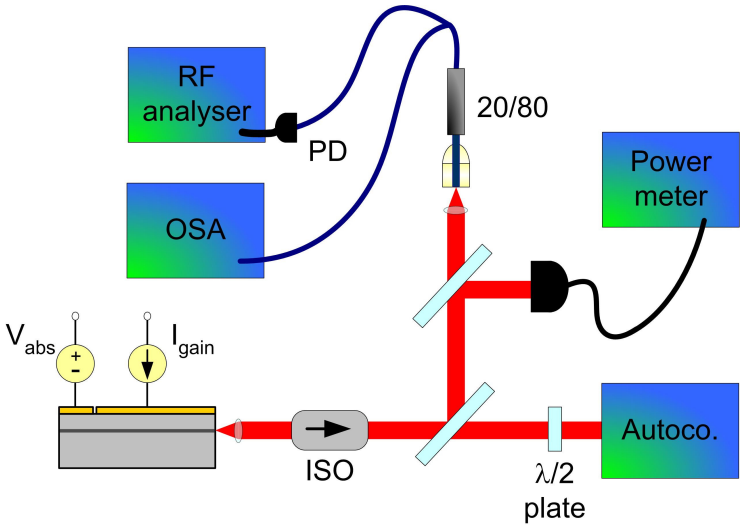

Fig. 3.3 – Schematic of the experimental setup used to characterise mode locking.
Legend: PD – photodetector; OSA – optical spectrum analyser; ISO – optical isolator.

Part of the beam was focused into an optical fibre, which included a 20/80 beamsplitter, separating the output into two further fibre arms. One of the fibre connectors was coupled into an optical spectrum analyser (HP 86140). The other was coupled into a fast photodetector with a (voltage) bandwidth up to 30GHz (Newport DF-15). The output of the photodetector was then connected to a RF spectrum analyser, able to measure frequencies up to 40GHz (Rohde & Schwarz FSP 40). The average power was monitored by a Melles Griot power meter. The pulse duration was measured via a commercial Femtochrome autocorrelator (FR-103MN). The resulting electrical trace was read out by an oscilloscope (TDS 3032). A computer controlled all the equipments, using GPIB protocol (General Purpose Interface Bus). In the following sections, we describe with more detail some of the setup blocks.

3.2.1. Autocorrelator

The autocorrelator used a combination of a second-harmonic generation crystal and photomultiplier tube. The noncollinear geometry resulted in a background-free autocorrelation measurement. The scanning arm consisted of a pair of parallel mirrors centred about a rotating axis [6], as shown in Fig. 3.4. The rotation of this assembly leads to an increase (or decrease) of the path length for a traversing beam – implying that the transmitted pulse train is delayed (or advanced) about the reference (zero delay) position. The rotation of the mirror set leads to a repetitive generation of linear delay,

sweeping the total optical path with a 10Hz periodicity. This rapid and repetitive scanning enables real-time visualisation of the autocorrelation function of the pulses, when the photomultiplier output is connected to a standard high-impedance oscilloscope, with the trigger synchronised to the rotation of the mirrors. A calibration procedure allowed the calculation of a multiplication factor to convert the millisecond timebase displayed in the oscilloscope into the picosecond scale of the scan. The measurements were re-calibrated for each major re-alignment, as for example after changing the experimental setup, or the laser being characterised.

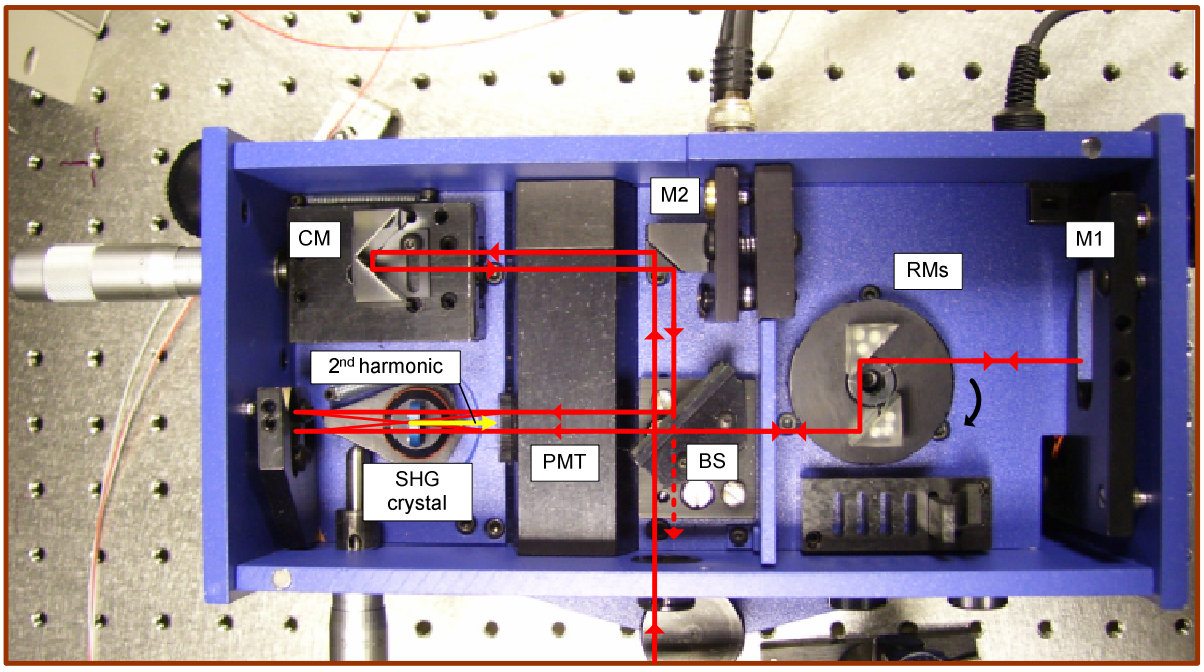

Fig. 3.4 – Autocorrelator top view. The optical path is highlighted in red.
Legend: BS – beamsplitter; RMs - rotating mirrors; M1/M2 – mrrors 1/2; CM – corner mirror; PMT – photomultiplier tube; SHG crystal – second-harmonic generation crystal.

The material used for second-harmonic generation was a $LiIO_3$ crystal, that can be deployed in a spectral range from 700nm up to 1800nm. The crystal had to meet the conditions of phase-matching for a bandwidth centred at a particular wavelength. This requirement has several implications. On one hand, the phase-matching angle had to be optimised for each major change in the emission wavelength (Fig. 3.5), as for example for each different value of temperature, or for measuring the pulse duration of the pulses generated using the excited-state band (~1190nm). The angle was easily adjustable via a micrometric knob that enabled angular displacement.

Due to the constraints of low peak power associated with the picosecond pulses generated by mode-locked laser diodes, the initial phase of alignment of the autocorrelator is particularly critical and difficult to undertake. At this stage, it was necessary to ensure that the laser was mode-locked in a very stable regime (which could be verified using the RF analyser), and that the average power level was at a minimum of 7-8mW. After achieving the correct alignment, autocorrelation traces with good signal-to-noise ratio could be obtained with an average power as low as 2-3mW.

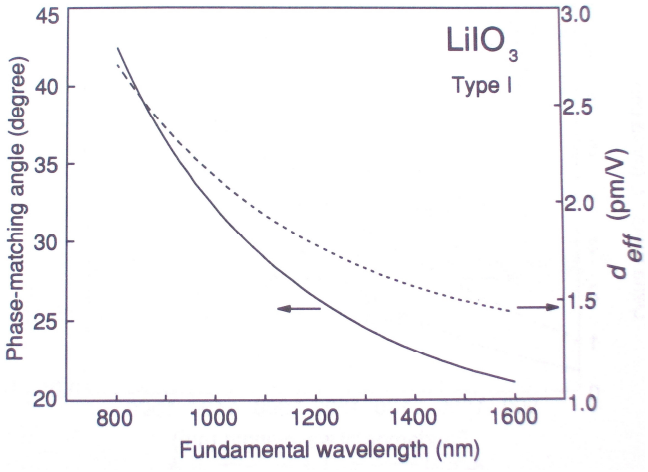

Fig. 3.5 – Theoretical phase-matching angle and the effective nonlinear coefficient d_{eff} in $LiIO_3$ at room temperature [7].

On the other hand, there is a finite spectral bandwidth over which phase-matching occurs, as depicted in Fig. 3.6.

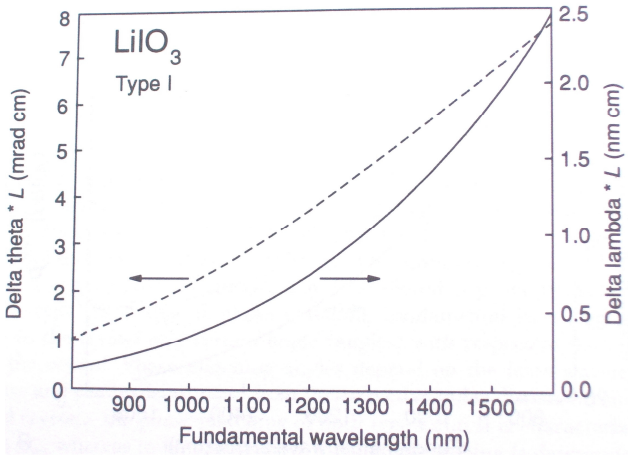

Fig. 3.6 – Calculated product $\Delta\lambda \cdot L$ (axis on the right), for $LiIO_3$ at room temperature [7].

This phase matching bandwidth depends on the type and thickness of crystal (in this case, 1.0 mm). From the graph in Fig. 3.6, it can be observed that for an emission wavelength centred at ~1300nm, the bandwidth should not exceed 10nm, to guarantee an accurate measurement. As the spectral bandwidth generated from the studied QD lasers did not exceed this value, we believe it did not pose any risk of spectral filtering (and thus pulse broadening) by the crystal.

The orientation of the crystal also had to be matched to the polarisation direction of the beam. Instead of tuning the crystal orientation, a half-waveplate was placed immediately before the autocorrelator so as to tune the polarisation and match it with the polarisation of the crystal. This minimised the direct interaction with the fragile crystal, preventing accidental damage.

Finally, it is important to remark that the relatively large thickness of the crystal was also of importance to generate a strong second-harmonic signal and enhance the overall sensitivity of the autocorrelator. Thinner crystals can result in a better resolution, however the generated signal can be very weak and result in a poor measurement sensitivity. In this particular case - for pulse durations quite above 100fs, the resolution is more than enough for accurate measurements.

3.2.2. Measurements automation

Most of the equipments available in the experimental setup were controllable via GPIB, allowing the automation of the measurements acquisition. Specific Labview programs were designed in order to setup and control the equipments and acquire data, enabling us to probe the performance of the laser in a nearly continuous fashion, as the bias conditions were changed. Optical and RF spectra, autocorrelations and optical power were scanned with changing current/reverse bias. The automation was crucial in the sense that it made possible a multi-dimensional mapping of the operation of the laser and the discovery of new mode-locking regimes (described in chapters 4 and 5), which would have been more difficult to identify with a discrete measurement approach. It also enabled a more complete study of the general trends and behaviour of the lasers, allowing to correlate spectral and temporal information, for example. This will be more clearly illustrated in the following sections.

Post-processing of data was also automatised using additional Labview programs. By automatically fitting the traces of each acquired autocorrelation or spectrum, it was

possible to generate comprehensive graphs of the pulse characteristics such as pulse duration, peak power and time-bandwidth product.

More recently, the acquisition programs were improved in order to scan both current and reverse bias and process the data, allowing the straightforward generation of 2-D maps of the performance of the commercial modules which will be described later in this chapter.

3.2.3. Power measurements

The optical power of the laser output was measured using a Melles Griot germanium detector head, interfaced by a Melles Griot universal optical power meter controller. The germanium head is sensitive over a wide bandwidth, ranging from 800nm to 1800nm, and can measure from 10μW up to 200mW. However, the responsivity of this detector head is strongly dependent on wavelength – this was experimentally measured in the spectral range of interest for this work, and is shown in Fig. 3.7. The power meter controller thus requires the user to input a value for the wavelength at which the power will be measured.

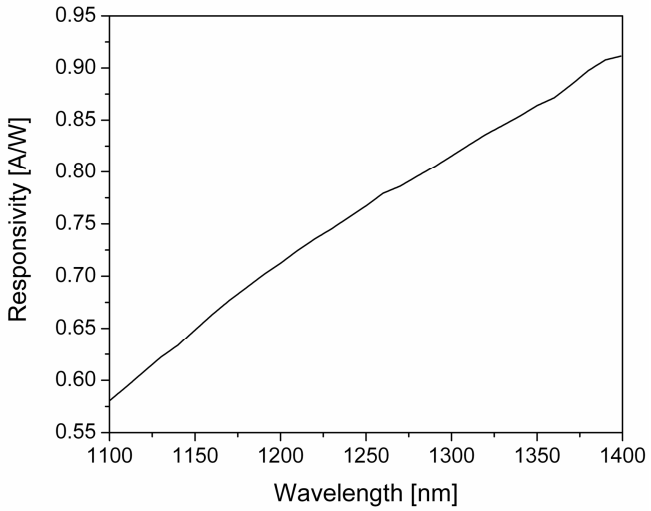

Fig. 3.7 – Measured responsivity of the germanium detector head used to characterise the optical power.

However, during the course of the experiments, the value of the wavelength would vary frequently. As will be evidenced in this and the following chapters, the inhomogeneously broadened emission spectrum of the QD lasers can vary significantly in shape, bandwidth and peak wavelength with the bias conditions. This becomes even more relevant when automated scans within a wide span of bias conditions are

performed. The emission spectra also changes significantly with increasing temperature.

In order to ensure the accuracy and robustness of the automated measurements, a procedure was implemented, in order to determine, point-by-point, the best wavelength value to be input to the power meter controller. In automated measurements, this implied an acquisition of the optical spectrum for each set of bias conditions and the determination of the wavelength, prior to each power measurement.

The criterion to find the correct wavelength was not immediate. The simplest criterion would be to consider the peak wavelength of each spectrum. However, the emission spectra from QD lasers are very often asymmetric or multimoded. In this case, the peak does not correspond to the point around which the pulse energy is concentrated. For this reason, the centroid of each optical spectrum was calculated – what we believe to be the correct value at which the optical power should be measured.

The presented results of average and peak power correspond to the output power of front facet only, corresponding to the gain section.

Finally, it is important to stress that for each change in the experimental setup, the optical power was re-calibrated according to the optical path and corresponding attenuation imposed by optical elements such as collimating lens, optical isolator, and beamsplitters.

3.3. Experimental results

The mode-locking performance is significantly affected by bias conditions. In the following sections an assessment of the mode-locking performance is provided for several lasers. The autocorrelation traces throughout this thesis were always best fitted to a Gaussian function. For some of the lasers where unstable mode-locking regions are present (evidenced by shaded/patterned regions in the graphs), the value of the pulse duration corresponded to the best fit obtained from that pulse - it is important to stress that these values are shown only to illustrate trends. The optical spectra were also fitted to a Gaussian function, although in the vast majority of cases, the spectra tended to be asymmetric, with a tendency to red-shift.

All the characterised lasers were two-section devices, similar to the one depicted in Fig. 3.8. Under conditions of a cw current supplied to the gain section and with a reverse bias on the saturable absorber section, the lasers emitted pulses with a repetition

period determined by the cavity round-trip time. The lasers' output facet was on the side of the gain section. The improved resilience of QD lasers has enabled their operation under cw bias conditions, unlike previously tested QW lasers, that would have to operate in a pulsed regime. Thus, we have chosen to perform all the measurements under cw bias, as these are the operating conditions that are closer to those found in "real-life" operation. This has also improved significantly the sensitivity of the autocorrelation measurements.

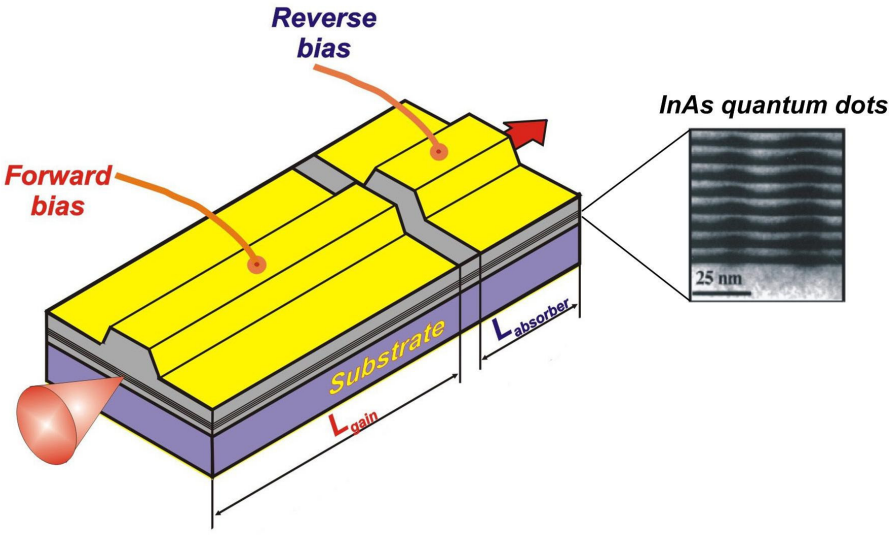

Fig. 3.8 – Schematic of a two-section semiconductor laser, similar to the lasers studied in this work.

The lasers studied in this work originated from two different suppliers who have been collaborating with St Andrews for a number of years: the Ioffe Institute (St Petersburg, Russia) and Innolume (Dortmund, Germany), formerly known as NanoSemiconductor (a spin-off from Ioffe Institute).

3.3.1. Ioffe laser

The Ioffe laser is a two-section device with a total length of 2.1mm, where the saturable absorber length is 0.3mm, generating pulses with a repetition frequency of 21GHz. The shallow-etched ridge waveguide was 6μm wide. The Ioffe laser contains a separate optical confinement double heterostructure. The detailed epitaxial structure of the Ioffe QD material is depicted in Table 3.1[9]. The cladding layers together with the GaAs

[9] It was not possible to obtain the details of the epitaxial structure for the commercial Innolume laser devices.

waveguide provide the optical confinement, whereas the confinement of carriers is provided by the quantum dots and the adjacent wetting layers. The active region consists of five layers of self-organised InAs QDs in InGaAs quantum-wells, each layer separated from the other by GaAs spacers with a thickness of 33nm. In order to decrease interface roughness, several transition layers were also introduced to the structure, such as graded AlGaAs layers. Between the cladding layers and the waveguide, $Al_{0.35}Ga_{0.65}As$/GaAs short-period super-lattices were also deposited to ensure good growth conditions for the QDs and to keep the surface roughness on top of the QDs at a minimum. The doping was performed with Si and C, respectively, for n- and p-type conductivity.

Table 3.1 - The composition of the Ioffe laser material.

Thickness (nm)	Repeats	Description	Composition	Doping
400		Cap/contact layer	GaAs:C	$p=1x10^{19}$
50		Graded AlGaAs	$Al_xGa_{1-x}As$, 0.05<x<0.8	$p=2x10^{18}$
1200		Top cladding	$Al_{0.8}Ga_{0.2}As$	$p=5x10^{17}$
50		Graded AlGaAs	$Al_xGa_{1-x}As$, 0.35<x<0.8	$p=1x10^{17}$
2/2	10	Super-lattice	$Al_{0.35}Ga_{0.65}As$/GaAs	undoped
20		Waveguide ↓	GaAs	undoped
5	5	QD-in-QW	InAs/InGaAs	undoped
33	5	Barrier	GaAs	undoped
53		Waveguide↑	GaAs	undoped
2/2	13	Super-lattice	$Al_{0.35}Ga_{0.65}As$/GaAs	undoped
50		Graded AlGaAs	$Al_xGa_{1-x}As$, 0.35<x<0.8	$n=1x10^{17}$
55/10	17	Lower cladding	$Al_{0.8}Ga_{0.2}As$/GaAs	$n=5x10^{17}$
50		Graded AlGaAs	$Al_xGa_{1-x}As$, 0.05<x<0.3	$n=1x10^{18}$
300		Buffer layer	GaAs	$n=2x10^{18}$
		Substrate	GaAs:Si (100)	n+

The Ioffe laser's front facet was anti-reflection-coated on the side of the gain section and high-reflection-coated on the absorber facet. The laser was wire-bonded, and the substrate had been thinned down to few hundreds of microns. The device was mounted p-side up on a copper heat sink, and a Peltier cooler was used to maintain a constant operating temperature of 25°C. A close-up photo of the laser mount is shown in Fig. 3.9.

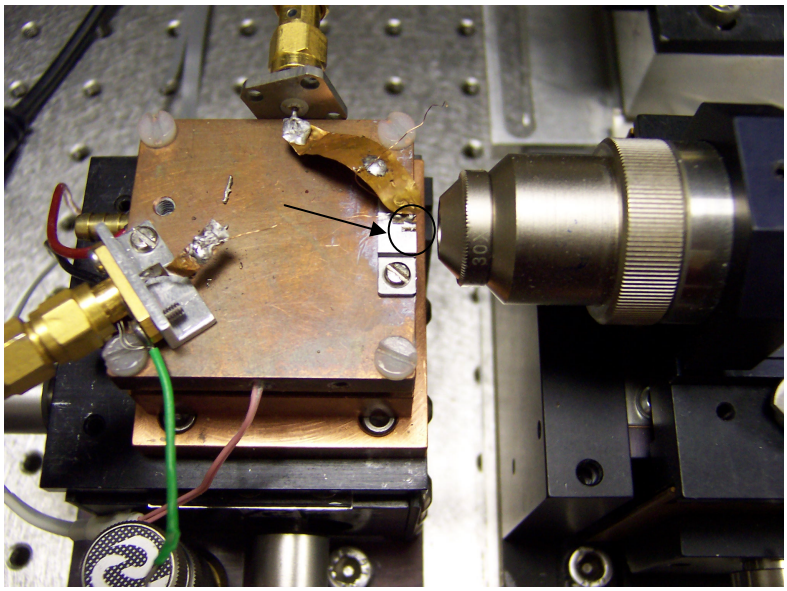

Fig. 3.9 – Close-up of the Ioffe laser (highlighted with an arrow), mounted on the copper mount.

The typical light-current characteristics for the Ioffe laser under cw (0V) and mode-locked operation (8.9V) are shown in Fig. 3.10.

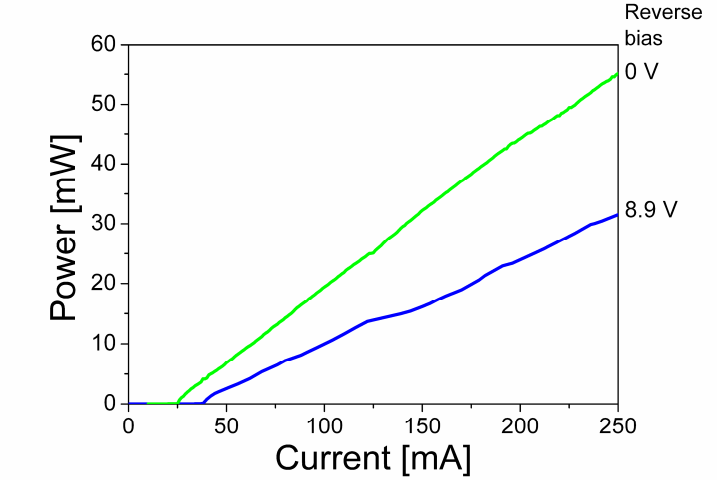

Fig. 3.10 – Light-current characteristic of the Ioffe laser, for reverse bias values of 0 V and 8.9 V.

The threshold current increases with reverse bias, owing to an increase of non-saturated losses. No pronounced hysteresis was observed on the light-current characteristic on either of the devices that were investigated. Average output powers up to 35mW were obtained for operation in the mode-locked regime. Importantly, no thermal rollover with increasing current was observed in the light-current characteristics. This improved thermal resilience was crucial for testing the lasers under cw bias conditions (in the aforementioned range).

In order to achieve mode-locked operation, the reverse bias level had to fall in the range between 6.5V and 10V, depending on the current level. Within this range, mode-locked operation involving the ground-state spectral band (~1260nm) was observed at injection currents just above laser threshold and up to 250mA / 300mA. Current was applied up to 400mA in a later stage[10]. Absorber voltages higher than 10/11V were not applied in order to avoid a failure due to a breakdown of the laser *p-n* junction.

Over the next two pages, an assessment of mode-locking performance is presented for two situations: a fixed reverse bias and increasing current (Fig. 3.11), and a fixed current and increasing reverse bias (Fig. 3.12).

For low values of reverse bias, the absorption recovery in the saturable absorber is not yet fast enough for generating a stable mode-locked output. As the reverse bias increases, the stable mode locking is achieved and the pulse duration decreases overall. The only region of unstable mode locking occurs in the region between 6.5V and 7.1V, where a simultaneous ultra-broad optical spectrum can be observed (Fig. 3.13), when a transition occurs between emission at the spectral bands of 1257nm and 1265nm, and both seem to be simultaneously present (Fig. 3.12). A similar phenomenon is observed in the evolution of mode-locking performance with increasing current, where one of the regions of unstable mode-locking also corresponds to an intermediate situation of transition with dual spectral bands (for a bias current around 140mA). In the corresponding RF spectra, two weak signals can be distinguished at distinct RF frequencies. The relatively wide spectral gap between these two modes and the corresponding difference between refractive indices results in different cavity round-trip times, thus resulting in distinct RF peaks. This implies that both distinct spectral bands are competing for mode locking, but fail to be coherently coupled together.

[10] In the next chapter, more details will be presented on a new mode-locking regime that involves the excited state, and which is observed under very high injection currents (>300 mA).

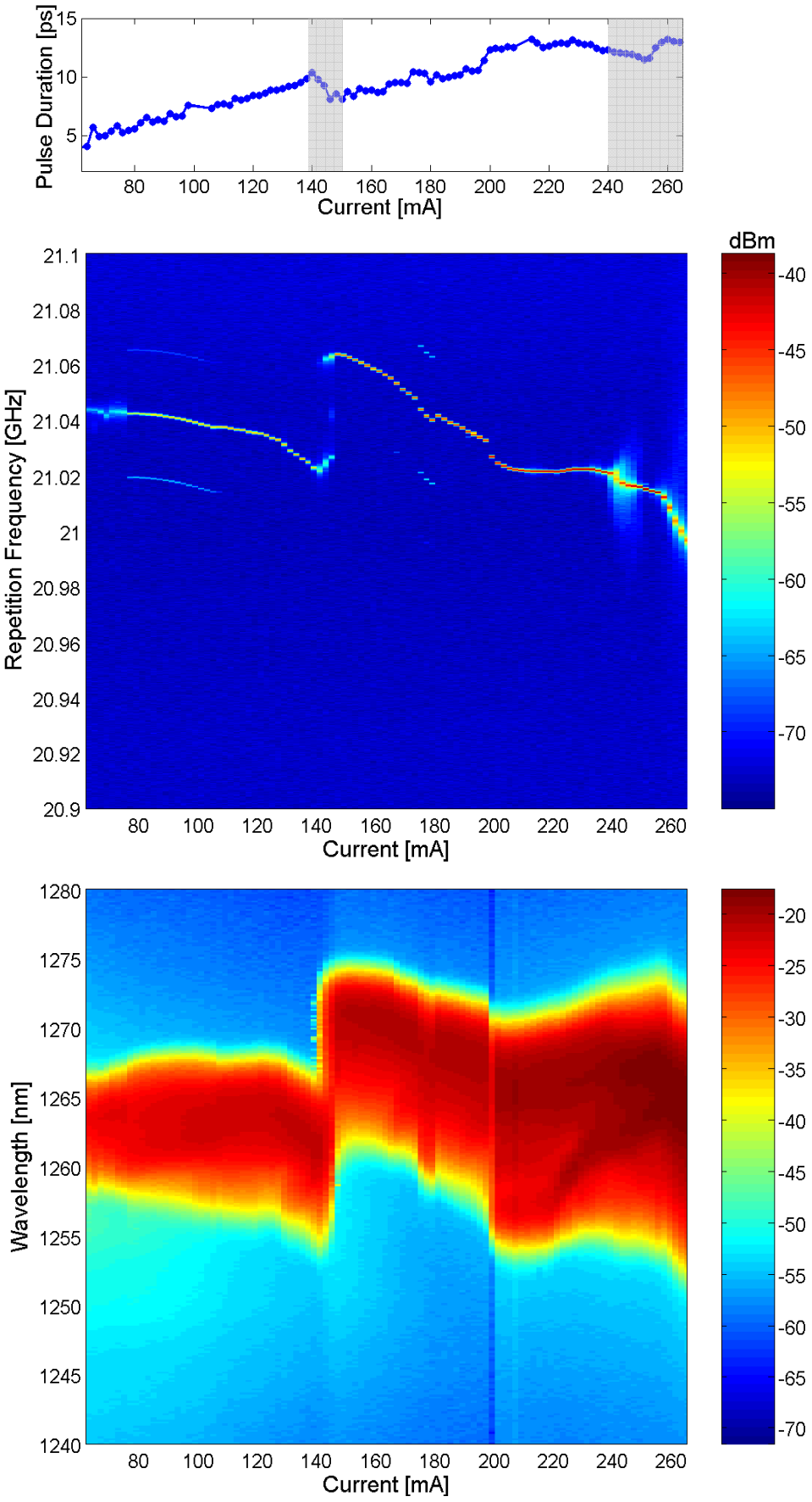

Fig. 3.11 - Performance of the Ioffe laser with increasing current: pulse duration (top), RF spectra (middle) and optical spectra (bottom). The reverse bias level was kept constant at 8.9V.

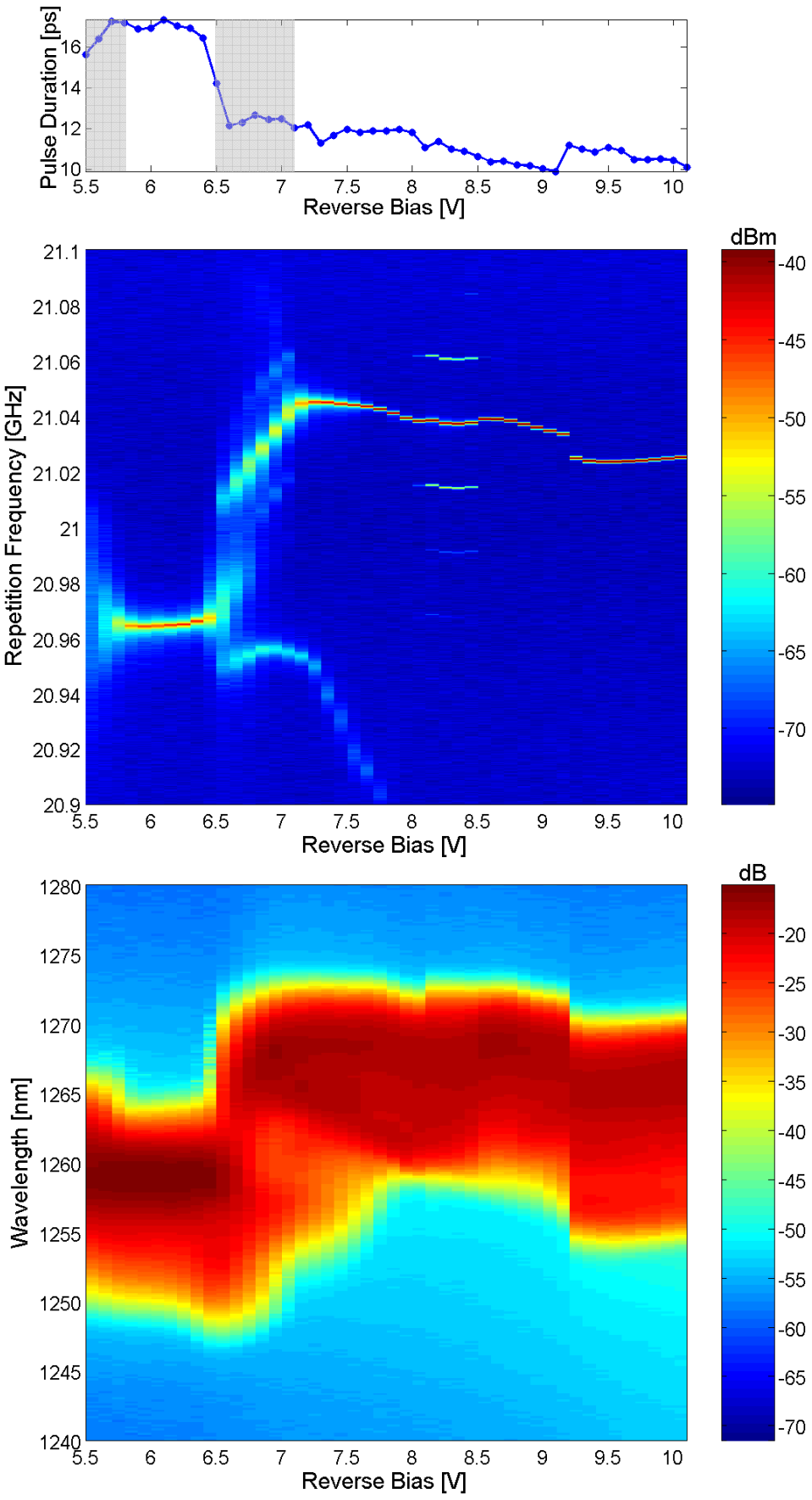

Fig. 3.12 - Performance of the Ioffe laser with increasing reverse bias: pulse duration (top), RF spectra (middle) and optical spectra (bottom). The gain current was kept constant at 190mA.

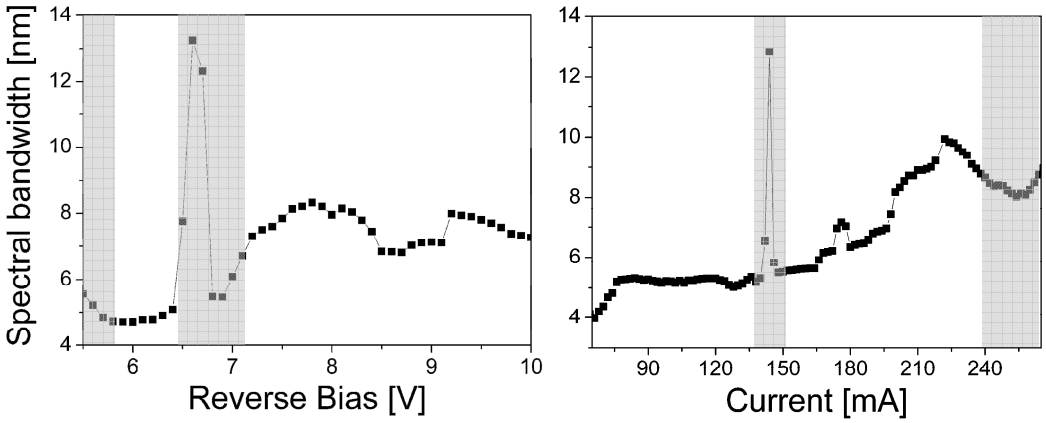

Fig. 3.13 – Evolution of the spectral bandwidth with increasing reverse bias (left) and increasing gain current, for the Ioffe laser.

Additional graphs displaying the time-bandwidth product and peak power for this laser will be presented in the following chapter.

An exemplifying autocorrelation and corresponding spectrum are exhibited in Fig. 3.14.

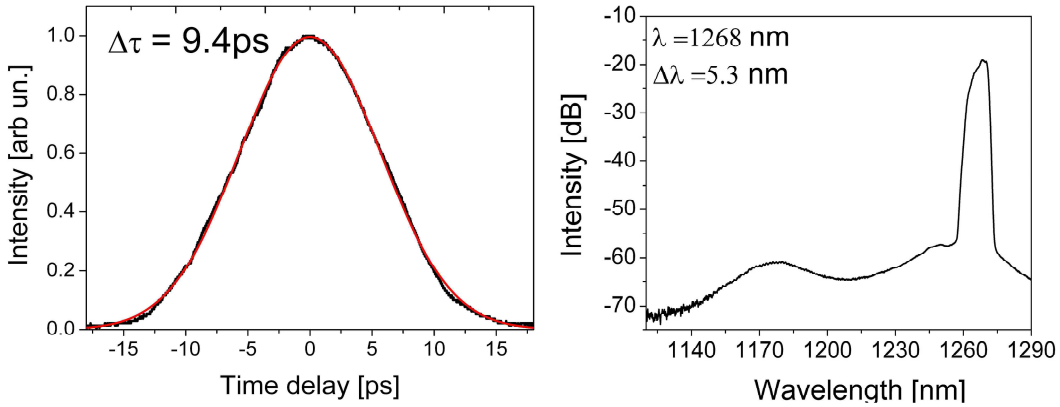

Fig. 3.14 – Exemplifying autocorrelation trace and corresponding optical spectrum, obtained with a bias current of 166mA and a reverse bias of 8.9V.

3.3.2. Innolume lasers

The active region of the two QD lasers provided by Innolume was grown by MBE on a GaAs (100) substrate. The pulse repetition frequency was 5GHz, corresponding to a cavity length of approximately 8mm. Because the laser modules provided by Innolume are commercially available, the disclosed information about these devices was very limited.

The Innolume modules were made available at the most complete level of integration. The lasers were encapsulated in 14-pin butterfly packages with a thermoelectric cooler. The lasers were coupled to a single mode fibre assembly (representative photo shown in Fig. 3.15).

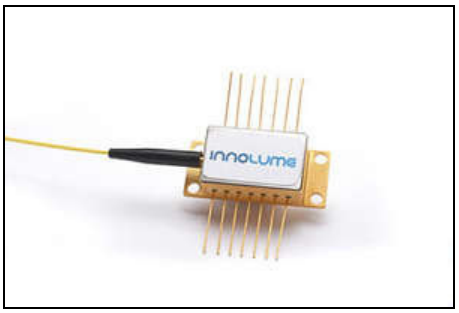

Fig. 3.15 – Representative photo of the laser modules provided by Innolume.

The Innolume modules were evaluated over a full scan of reverse bias and current conditions, enabling a direct mapping of the lasers performance. The maximum reverse bias applied was 8.0V, as advised by the manufacturer. The maximum current tested at this temperature was 180mA, as beyond this value the region of stable mode locking reduced considerably. No hysteresis effects were observed for both lasers. The lasers operated in the ground-state spectral band (~1238nm).

As long-cavity devices, the Innolume modules were able to deliver high average power (Fig. 3.16). It is important to stress that this is the output power delivered by the optical fibre, and so the performance of the laser in this aspect is even superior to what is reported as the performance of the module. From this figure, it is also evident how the higher reverse bias increases the threshold of laser emission and, for a given current, the average power decreases accordingly – both effects due to the increasing non-saturable losses imposed by the absorber section, with increasing reverse bias.

As it is also evident from this figure and the following, the range of stable mode locking was broader in the laser Innolume-1 (the patterned areas correspond to unstable mode locking). The laser Innolume-2 also exhibited a more irregular dependence pattern of the measured quantities with the bias conditions than Innolume-1.

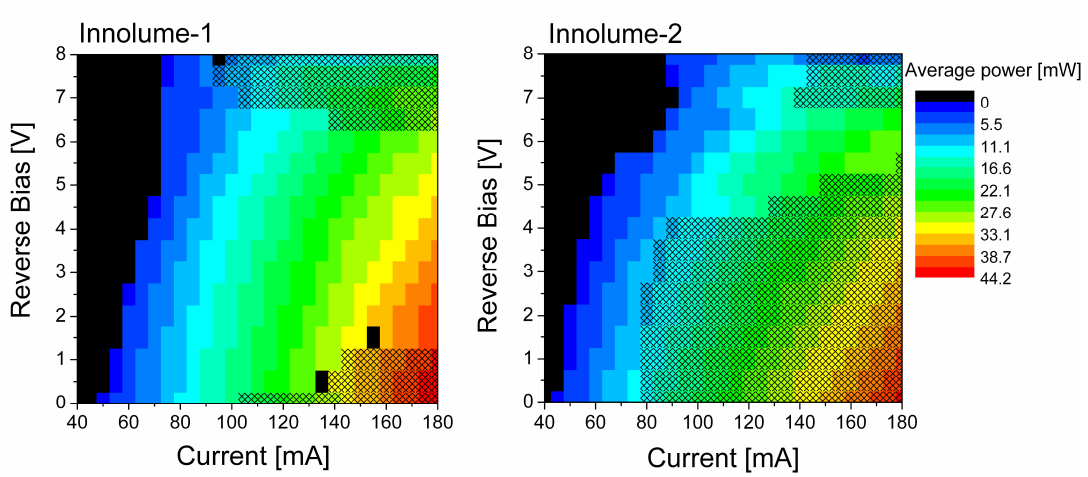

Fig. 3.16 – Measured average power for lasers Innolume-1 and Innolume-2. The patterned areas correspond to unstable mode locking, while the black areas correspond to the regions before laser emission threshold.

The measured pulse duration is displayed in Fig. 3.17. The overall increase of pulse duration with increasing current is evident for laser Innolume-1, as well as the pulse duration decrease with increasing reverse bias. The laser Innolume-2 displays a more irregular pattern at threshold, with slightly longer pulses at threshold for lower values of reverse bias.

It is also relevant to note that the pulses generated by these lasers are longer than the previous ones.

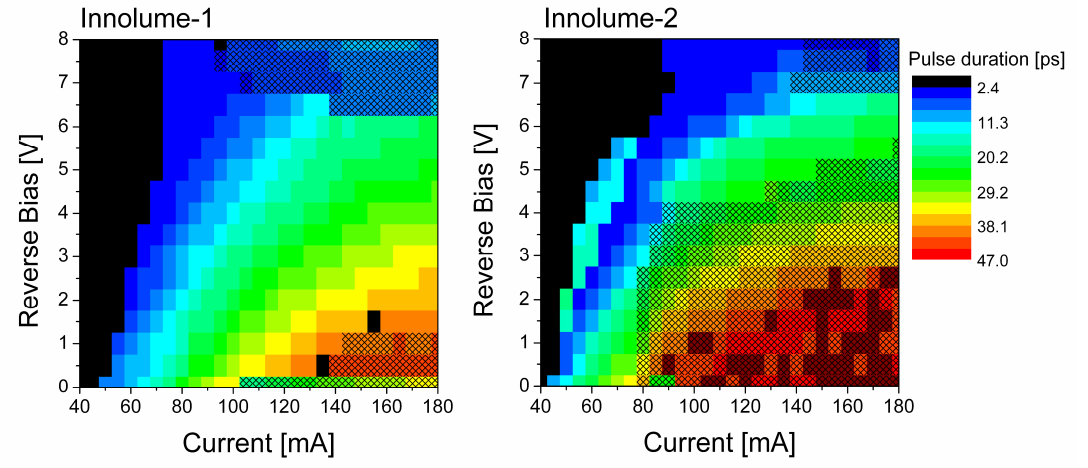

Fig. 3.17 – Measured pulse duration for lasers Innolume-1 and Innolume-2. The patterned areas correspond to unstable mode locking, while the black areas correspond to the regions before laser emission threshold.

The measured spectral bandwidth is displayed in Fig. 3.18. The spectral bandwidth increases both with current and reverse bias, and so the minimum values can be found close to threshold, and for lower values of reverse bias.

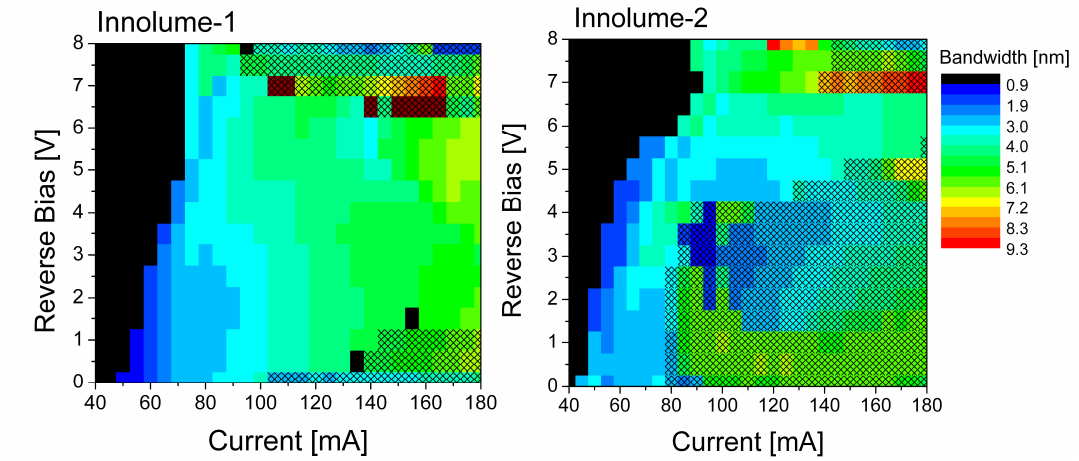

Fig. 3.18 – Measured spectral bandwidth for lasers Innolume-1 and Innolume-2. The patterned areas correspond to unstable mode locking, while the black areas correspond to the regions before laser emission threshold.

The pulses are highly chirped, as depicted in Fig. 3.19. The lowest values for time-bandwidth product can be found close to the threshold frontier.

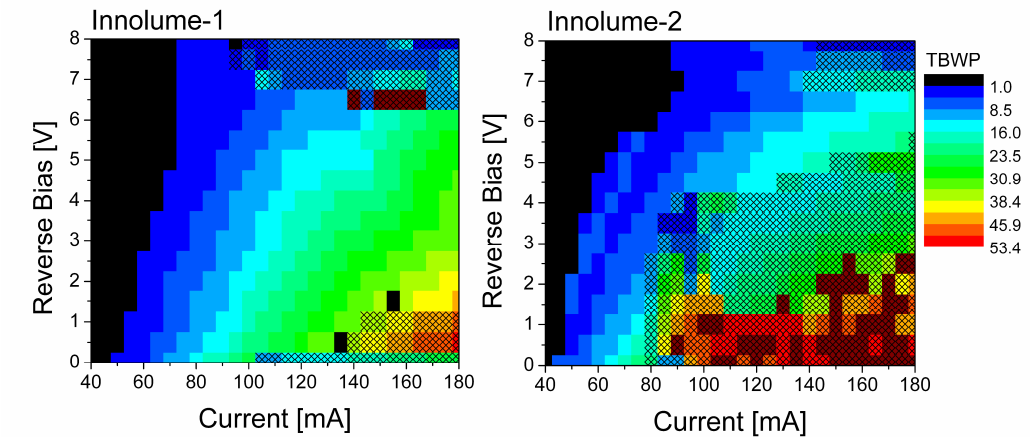

Fig. 3.19 – Measured time-bandwidth product (TBWP) for lasers Innolume-1 and Innolume-2. The patterned areas correspond to unstable mode locking, while the black areas correspond to the regions before laser emission threshold.

The two modules, and particularly Innolume-2, exhibited the highest values of peak power from all the characterised lasers, as their longer length contributed favourably to increase the extracted optical power from the gain, with a lower pulse repetition rate enhancing the obtainable peak power. The highest values of peak power are surprisingly found in a mid-current range, at high reverse bias (Fig. 3.20).

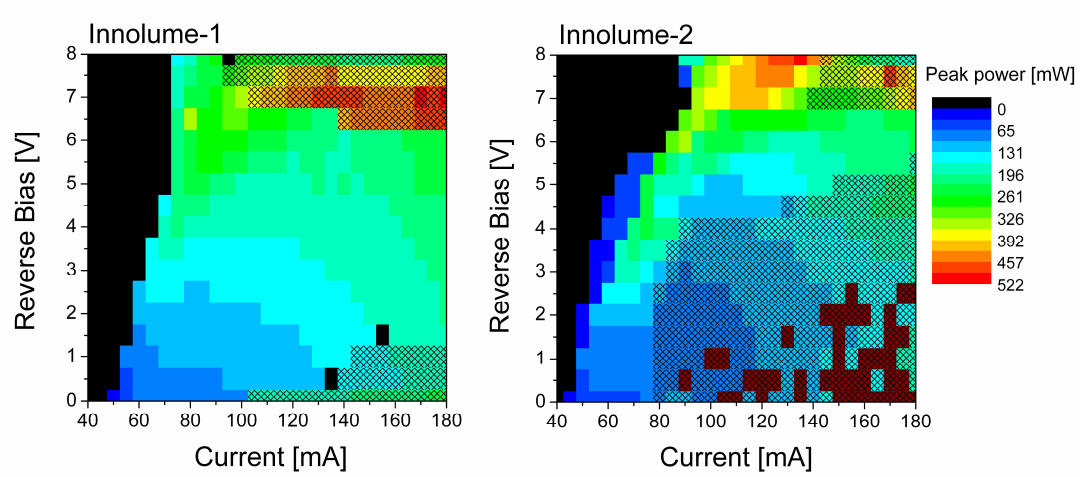

Fig. 3.20 – Measured peak power for lasers Innolume-1 and Innolume-2. The patterned areas correspond to unstable mode locking, while the black areas correspond to the regions before laser emission threshold.

3.4. Discussion of results

3.4.1. Effects contributing to changes in pulse duration

The pulse duration in a passively mode-locked semiconductor laser is determined by two balancing effects: the compression due to the combined effect of the gain and loss, and the broadening due to self-phase modulation in the gain section (SPM), group-velocity dispersion (GVD) and other effects, as explained previously in Section 2.2.

As shown on Fig. 3.11 and Fig. 3.17, the output pulse duration increases with increasing current (as does the TBWP and the optical power). This general trend has been widely reported in literature, in the context of amplification of ultrashort pulses in SOAS and in semiconductor mode-locked lasers based in bulk and QW materials, respectively [8,9], and it has been explained on the basis of SPM and GVD. This effect was equally observed in QD lasers, as recently published [10,11].

The effects of SPM can be minimised by decreasing the optical power of the pulses, thus minimising their impact on gain saturation and refractive index variation. For this reason, shorter pulses are usually found close to threshold, and thus exhibit very low optical power. Owing to GVD, the pulse suffers a significant broadening as it propagates. This effect is indeed dependent on the length of the chip, and thus longer active waveguides result in broader pulses (with the additional effect that longer lasers usually generate higher power levels as well, and therefore the effect of SPM is further

enhanced). This was evident in the experimental results presented in the previous sections, with the long-cavity QD lasers generating longer pulses than the short-cavity laser.

The significant chirp imposed on the pulses implies that the dynamic linewidth enhancement factor is large, particularly at high photon density [10]. Although the linewidth enhancement factor (LEF) was predicted to be low for QD lasers, in practice this has not been observed. During the course of this PhD, many studies have been reported in this sense, and many contradicting results have emerged, owing to the diversity of devices and assessment techniques used [12,13]. There is still not a generalised consensus, but most researchers agree that the linewidth enhancement factor is indeed not an intrinsic property, depending strongly on the material, device, and bias conditions. Below threshold, a small LEF can be measured, but above threshold, LEF increases steadily with current [14,15].

An additional effect takes place as the current increases - the gain recovery becomes faster, as the capture time gets shorter because there are more carriers available. However, a gain recovery faster than the initial pulse duration and faster than the absorber recovery will increase the window of net gain and will not shape the trailing edge, as opposed to slow gain dynamics. The slow dynamics amplifies the leading edge, while reducing the gain for the trailing edge, thus helping to shorten the pulse duration to some extent [16]. A slower gain recovery in the laser might be desirable, as long as it is fast enough to accommodate the next pulse over a round-trip.

The pulse duration decreases with increasing reverse bias – a trend that has been observed in the majority of two-section mode-locked semiconductor lasers, and that is also present in QD lasers, as has also been confirmed by other groups [17]. The main factor contributing to this decrease is the corresponding exponential decrease of the absorber recovery time as the reverse bias is increased [18], which has the effect of narrowing the window of net gain.

While the faster absorber recovery shortens the pulses, the optical power also decreases with increasing reverse bias. The lower power will assist in reducing the effect of SPM on the gain section. A fact that is usually overlooked is that there also exists an associated SPM effect in the absorber, which can counteract the effect of SPM in the gain section, as the phase modulation in the absorber is of opposite signal of that in the gain. The fact that the pulse is shorter and the reverse bias is higher will increase

SPM in the absorber, compensating (to a limited extent) the SPM in the gain section [19]. By having a suitable choice of bias conditions in both sections (high reverse bias in the absorber and low current in the gain section), both effects can cancel each other, rendering it possible to generate transform-limited pulses directly from monolithic passively mode-locked lasers, as demonstrated also in the case of QD-based structures [20]. Unfortunately, this combination of bias conditions leads to very low optical output powers.

Increasing the reverse bias on the saturable absorber is a very convenient bias control to decrease the absorber recovery time, which plays a significant part in reducing the pulse duration. However, there are two main limitations that restrict the boundless increase of reverse bias. First, a very high reverse bias can break down the junction and damage the laser structure, if it exceeds a critical level. Second, for a very high reverse bias, the optical power can become so low, that the pulse has not enough energy to bleach the absorber. This effect is further accentuated by an increase in the absorption saturation energy with reverse bias, an effect that had been verified before in other semiconductor QW-based saturable absorbers. Recently, the saturation energy in QD saturable absorbers lasers has also been shown to increase with reverse bias, albeit to a lesser extent [21]. If the intracavity energy of the pulses becomes comparable to the saturation energy, the discrimination between cw and pulsed operation in the saturable absorber will not be so efficient, and mode locking may even become unstable, as there is no efficient pulse shaping taking place. Such effect was observed in reference [22], where after a certain level of reverse bias, the pulses would start to slightly increase and/or the mode locking would become unstable.

3.4.2. Effects in the spectral bandwidth

For a given reverse bias, the spectral bandwidth increases with increasing current. There are two main factors contributing to the spectral broadening. On one hand, SPM contributes to the generation of new frequencies within the pulse, as previously explained. On the other hand, as the injection current increases, population inversion starts to extend to lateral spectral modes available through inhomogeneous broadening [23]. Therefore, the level of inhomogeneous broadening made available for laser emission is also increasing with current and adds to the increase of TBWP. In this respect, inhomogeneous broadening could be contributing further to the high values of

TBWP, and the extra modes could be failing to lock efficiently. In one paper, for example, a narrower spectrum has been observed upon mode-locked operation than upon cw operation, something that contradicts the usually expected behaviour of mode-locked laser [20].

Another aspect that deserves a comment is the asymmetry present in the vast majority of the acquired optical spectra, and which tends to be more accentuated with increasing current. An exemplifying spectrum is shown Fig. 3.21.

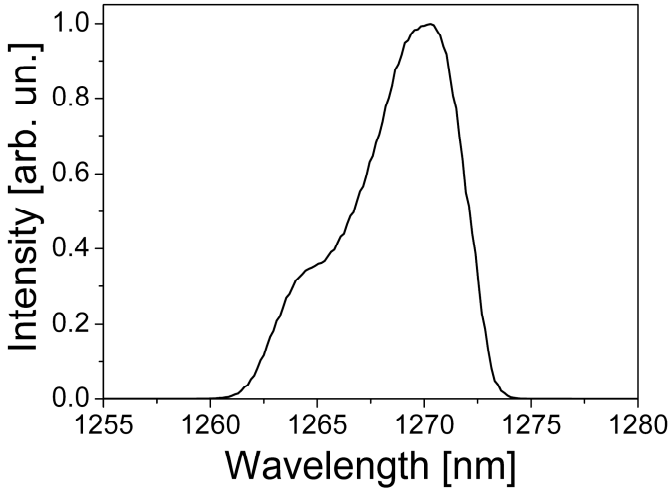

Fig. 3.21 – Linear form of the optical spectrum presented in Fig. 3.14.

The asymmetric spectra imply asymmetric pulses[11]. The steep edge on the red-side of the optical spectra implies a steep leading edge in the short pulses, with longer decaying trailing edges. This suggests that the saturable absorber plays a significant role in shaping the leading edge of the pulse because the saturation dynamics is extremely fast, while the trailing edge is less suppressed, due to the slower absorption recovery and/or fast gain recovery. The amplitude is higher on the red-side of the optical spectrum as it corresponds to a more highly amplified portion of the pulse across the gain section. As mentioned before, the leading edge is more amplified than the trailing edge, due to gain depletion, and thus further contributing to the asymmetry.

[11] This can not be visualised in the autocorrelation traces, as they are intrinsically symmetric.

3.5. Conclusions

A thorough characterisation of the mode-locking regime in several QD lasers was performed. The pulses generated were relatively long (>2ps), despite the wide spectral bandwidth available. The TBWP was significantly higher than the Fourier limit, particularly due to the effects of SPM in the gain section and inhomogeneous broadening of the gain, which increase with increasing current. Indeed, the effect of the bias conditions on the duration and power of the pulses shows that the limitation in achieving simultaneously high output power and short pulses restricts the achievable output peak power. The pulses are found to be shorter in the bias region close to threshold and at high reverse bias values; however, the average power is at its lowest in this range of conditions. Higher power levels seem difficult to attain while in mode-locked operation, as increasingly large contributions from SPM and dispersion make the mode-locking regime become less stable and eventually collapse. The detrimental role of SPM with increasing current is linked to a high LEF observed in QD lasers.

3.6. References

[1] U2t Photonics: www.u2t.de.

[2] Hamamatsu: http://jp.hamamatsu.com.

[3] E. U. Rafailov, M. A. Cataluna, W. Sibbett, N. D. Il'inskaya, Y. M. Zadiranov, A. E. Zhukov, V. M. Ustinov, D. A. Livshits, A. R. Kovsh, and N. N. Ledentsov, "High-power picosecond and femtosecond pulse generation from a two-section mode-locked quantum-dot laser," *Appl. Phys. Lett.*, vol. 87, pp. 81107-3, 2005.

[4] E. P. Ippen and C. V. Shank, "Techniques for Measurement," in *Ultrashort Light Pulses*, S. L. Shapiro, Ed. New York: Springer, 1977, pp. 83-122.

[5] J. H. Chung and A. M. Weiner, "Ambiguity of ultrashort pulse shapes retrieved from the intensity autocorrelation and the power spectrum," *IEEE J. Sel. Topics Quantum Electron.*, vol. 7, pp. 656-666, 2001.

[6] Z. A. Yasa and N. M. Amer, "A rapid-scanning autocorrelation scheme for continuous monitoring of picosecond laser pulses," *Opt. Commun.*, vol. 36, pp. 406-408, 1981.

[7] P. Vasil'ev, *Ultrafast Diode Lasers: Fundamentals and Applications*. Boston: Artech House, 1995.

[8] G. P. Agrawal and N. A. Olsson, "Self-Phase Modulation and Spectral Broadening of Optical Pulses in Semiconductor-Laser Amplifiers," *IEEE J. Quantum Electron.*, vol. 25, pp. 2297-2306, 1989.

[9] M. Y. Hong, Y. H. Chang, A. Dienes, J. P. Heritage, P. J. Delfyett, S. Dijaili, and F. G. Patterson, "Femtosecond self- and cross-phase modulation in semiconductor laser amplifiers," *IEEE J. Sel. Topics Quantum Electron.*, vol. 2, pp. 523-539, 1996.

[10] M. T. Choi, W. Lee, J. M. Kim, and P. J. Delfyett, "Ultrashort, high-power pulse generation from a master oscillator power amplifier based on external cavity mode locking of a quantum-dot two-section diode laser," *Appl. Phys. Lett.*, vol. 87, pp. 221107-3, 2005.

[11] M. Kuntz, G. Fiol, M. Lammlin, D. Bimberg, M. G. Thompson, K. T. Tan, C. Marinelli, R. V. Penty, I. H. White, V. M. Ustinov, A. E. Zhukov, Y. M. Shernyakov, and A. R. Kovsh, "35 GHz mode-locking of 1.3 μm quantum dot lasers," *Appl. Phys. Lett.*, vol. 85, pp. 843-845, 2004.

[12] M. Gioannini, A. Sevega, and I. Montrosset, "Simulations of differential gain and linewidth enhancement factor of quantum dot semiconductor lasers," *Opt. Quantum Electron.*, vol. 38, pp. 381-394, 2006.

[13] S. Melnik and G. Huyet, "The linewidth enhancement factor alpha of quantum dot semiconductor lasers," *Opt. Express*, vol. 14, pp. 2950-2955, 2006.

[14] A. Martinez, A. Lemaitre, K. Merghem, L. Ferlazzo, C. Dupuis, A. Ramdane, J. G. Provost, B. Dagens, O. Le Gouezigou, and O. Gauthier-Lafaye, "Static and dynamic measurements of the alpha-factor of five-quantum-dot-layer single-mode lasers emitting at 1.3 μm on GaAs," *Appl. Phys. Lett.*, vol. 86, pp. 211115, 2005.

[15] H. Su and L. F. Lester, "Dynamic properties of quantum dot distributed feedback lasers: high speed, linewidth and chirp," *J. Phys. D*, vol. 38, pp. 2112-2118, 2005.

[16] P. J. Delfyett, "Ultrafast Single and Multiwavelength Modelocked Semiconductor Lasers: Physics and Applications," in *Ultrafast Lasers - Technology and Applications*, M. E. Fermann, A. Galvanauskas, and G. Sucha, Eds. New York: Marcel Dekker, Inc., 2003, pp. 219-321.

[17] M. G. Thompson, A. Rae, R. L. Sellin, C. Marinelli, R. V. Penty, I. H. White, A. R. Kovsh, S. S. Mikhrin, D. A. Livshits, and I. L. Krestnikov, "Subpicosecond high-power mode locking using flared waveguide monolithic quantum-dot lasers," *Appl. Phys. Lett.*, vol. 88, pp. 133119-3, 2006.

[18] D. B. Malins, A. Gomez-Iglesias, S. J. White, W. Sibbett, A. Miller, and E. U. Rafailov, "Ultrafast electroabsorption dynamics in an InAs quantum dot saturable absorber at 1.3 μm," *Appl. Phys. Lett.*, vol. 89, pp. 171111-3, 2006.

[19] K. Yvind, P. M. W. Skovgaard, J. Mork, A. J. Hanberg, and A. M. Kroh, "Performance of External Cavity Mode-Locked Semiconductor Lasers Employing Reverse Biased Saturable Absorbers," *Physica Scripta*, vol. 101, pp. 129-132, 2002.

[20] M. G. Thompson, K. T. Tan, C. Marinelli, K. A. Williams, R. V. Penty, I. H. White, M. Kuntz, D. Ouyang, D. Bimberg, V. M. Ustinov, A. E. Zhukov, A. R. Kovsh, N. N. Ledentsov, D. J. Kang, and M. G. Blamire, "Transform-limited optical pulses from 18 GHz monolithic modelocked quantum dot lasers operating at 1.3 μm," *Electron. Lett.*, vol. 40, pp. 346-347, 2004.

[21] M. G. Thompson, C. Marinelli, Y. Chu, R. L. Sellin, R. V. Penty, I. H. White, M. Van Der Peol, D. Birkedal, J. Hvam, V. M. Ustinov, M. Lammlin, and D. Bimberg, "Properties of InGaAs quantum dot saturable absorbers in monolithic mode-locked lasers," *IEEE 19th International Semiconductor Laser Conference*, 53-54, Matsue Shi, Japan, 2004.

[22] M. Laemmlin, G. Fiol, C. Meuer, M. Kuntz, F. Hopfer, A. R. Kovsh, N. N. Ledentsov, and D. Bimberg, "Distortion-free optical amplification of 20-80 GHz modelocked laser pulses at 1.3 μm using quantum dots," *Electron. Lett.*, vol. 42, pp. 697-699, 2006.

[23] L. Harris, D. J. Mowbray, M. S. Skolnick, M. Hopkinson, and G. Hill, "Emission spectra and mode structure of InAs/GaAs self-organized quantum dot lasers," *Appl. Phys. Lett.*, vol. 73, pp. 969-971, 1998.

4. INFLUENCE OF THE EXCITED STATE ON GROUND-STATE MODE LOCKING

This chapter presents the exploitation of cw-lasing in the excited-state transitions as a novel means of improving the performance of a QD mode-locked laser. The coexistence of excited-state laser emission with mode locking that involves the ground-state transitions enables the generation of ultrashort and low-noise pulses under the conditions of higher levels of current injection and at higher powers. This chapter shows how this new regime has been achieved in a monolithic two-section QD laser by increasing the dc injection current supplied to the gain section and/or to the absorber section as a reverse bias. A possible underlying mechanism is suggested, based on a lower linewidth enhancement factor in the gain section and a lower absorption saturation energy.

4.1. Introduction

Quantum-dot lasers were theoretically predicted to exhibit very low values of linewidth enhancement factor (LEF). The first measurement of LEF in an InAs QD laser diode in 1999 resulted in a value of 0.1 below threshold [1], which was particularly exciting because it implied the possibility of lower chirp, and Fourier transform-limited pulses. In the past years, there have been some additional experimental demonstrations of low LEF, but limited to a narrow range of bias conditions (below or close to threshold). In practical devices and bias conditions, it has been observed that the LEF increases significantly as the operating current is increased [2,3], which in turn increases the frequency chirp and duration of the pulses generated by mode-locked QD lasers [4]. In fact, LEF can be significantly higher for QD materials than for QW, and a giant LEF of 60 has been measured in a QD laser, the highest ever to be measured in a semiconductor laser [5]. The usual approach to generate shorter and transform-limited pulses is then to operate two-section mode-locked lasers very close to threshold, and at a high reverse bias [6]; however, this limits the output power and constrains the exploitation of their typically high differential efficiency in the generation of high-power ultrashort pulses.

The LEF increase in QD lasers has been attributed to the increasing asymmetry of the gain, as the carrier population is slowly building in the higher levels with increasing current (Fig. 4.1).

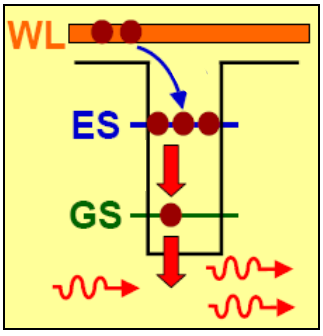

Fig. 4.1 – Scheme of the energy levels present in a QD, corresponding to ground and excited states (GS and ES), and the wetting layer (WL).

Above laser threshold in the ground state (GS), the carrier population in the excited state (ES) is not clamped. As there are a limited number of available GS states where the ES carriers can relax to, they start to accumulate in the ES levels, as the current

increases. A “carrier pile-up” starts to occur – a unique phenomenon in the domain of semiconductor lasers. The carrier pile-up induces a change in the refractive index such that increases the LEF [5].

In this chapter, a technique for depleting the carriers of the ES level via stimulated emission is explored, in order to influence the overall LEF of the laser.

4.1.1. Simultaneous laser emission involving ground and excited states

Laser emission involving the ES has been considered a detrimental effect in QD lasers, particularly in the early days, when the material optimisation was still in progress [7]. ES laser emission implied the presence of a low value of GS saturated gain, which was undesirable for a high-performance laser, and in the past few years much effort has been put into optimising growth techniques to alleviate this effect. Indeed, the excited state levels have higher degeneracy, and consequently higher saturated gain. This means that a transition from the GS to the ES can be achieved by increasing loss [8].

Optical loss can be varied by changing the cavity length, as demonstrated in the first studies of the physics behind simultaneous ES and GS laser emission [9]. In this paper, the length of the device was used as a control to obtain laser emission in the GS (longer laser) or ES (shorter laser). With an optimised length, simultaneous laser emission for both GS and ES was observed. The operating temperature can also play an effect on the saturation of the GS gain, and as will be shown in Chapter 6, this can force a transition to the ES spectral band. During the course of this work, the availability of a saturable absorber was used as a convenient control, enabling the introduction and manipulation of losses, that allowed to overturn the balance between GS gain and loss in favour of ES emission.

4.2. Experimental results

4.2.1. Experimental setup

The laser characterised in this chapter was the Ioffe laser[12], previously described in Section 3.3.1. The train of output pulses from this laser exhibited a pulse repetition rate of 21GHz, involving the GS spectral band, with a central wavelength of emission around 1260nm. The ES spectral band was centred at 1180-1190nm.

The experimental setup was very similar to what has already been described in the previous Section 3.2, with an added diffraction grating that was used to separate the two spectral bands, for independent power measurement. Two identical power meters were used for this purpose (their sensitivity was measured and proved to be the same). The measured optical power was re-calibrated for both GS and ES, as they suffered different levels of attenuation/dispersion along the optical path in the setup. The mode-locking stability was monitored using the RF analyser, while the pulse durations were simultaneously measured with the noncollinear autocorrelator.

The RF spectrum and the autocorrelation were crucial to clarify that the pulses were solely generated via GS transitions, while the ES was emitting on a continuous manner. First, in the RF spectrum, a single spectral signature of a peak at 21GHz existed, which is attributable to mode-locked operation in the GS. In the next chapter, it will be shown how mode-locked pulses in the ES exhibit a lower characteristic pulse repetition rate of 20.5GHz (in this same laser), owing to their shorter wavelength and correspondingly increased refractive index. Second, the autocorrelator relies on the correct phase matching of the nonlinear crystal, which is strongly dependent with wavelength. In order to obtain an autocorrelation trace for ES pulses (as shown in the next chapter), the angle of the crystal had to be changed significantly, in order to satisfy phase-matching conditions. The acquired autocorrelation traces can therefore be confidently attributed to the GS transition only.

4.2.2. Characterisation of the new mode-locking regime

There are several routes to achieve simultaneous excited-state emission in a two-section laser - the easiest route is to manipulate the bias conditions. The injected current on the gain section has to be high enough in order to populate the higher energy levels

[12] No ES laser emission was observed from the Innolume modules, as these lasers were very long.

corresponding to the excited states. Simultaneously, the level of reverse bias also has to be high in order to increase the absorption level and thus the cavity losses. By increasing these losses, the threshold of laser emission in the ES moves to lower currents, as shown in Fig. 4.2.

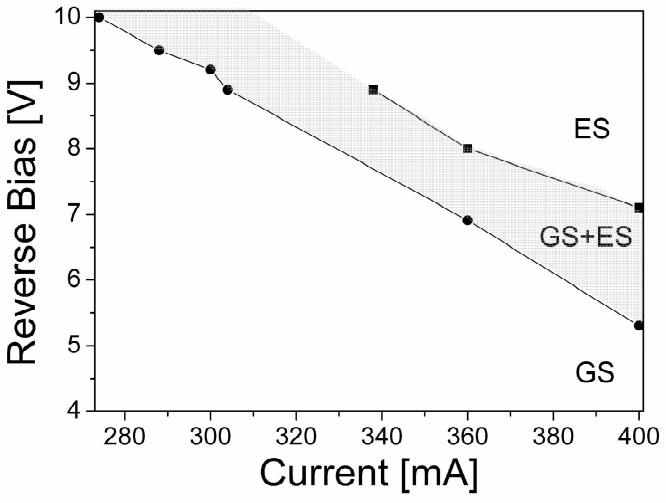

Fig. 4.2 – Bias conditions for emission on the ground (GS) and excited states (ES). The shaded region corresponds to simultaneous emission in both states (GS+ES). Below/above the delimited region, emission involves only GS/ES, respectively.

With this is mind, we have tried to separate the effects of the gain and the losses, obtaining simultaneous ES laser emission by either:

- increasing the current in the gain section, while keeping a constant reverse bias in the saturable absorber;

- increasing the reverse bias in the saturable absorber, while keeping a constant current in the gain section.

Let us consider the first scenario. A light-current characteristic is shown in Fig. 4.3 for a constant reverse bias (V_{abs}=8.86 V) applied to the absorber section. As the current in the gain section was increased beyond 300mA, simultaneous laser emission involving excited-state (ES) transitions was observed, while at the same time the GS mode-locked output power was shifted to lower power levels. As the current was further increased, the GS output power evolved with a similar differential efficiency as before, while the ES output power was nearly constant. For current values above 340mA, the GS power level dropped significantly, with the ES optical power prevailing.

Above the laser threshold, stable GS mode locking at 21GHz was observed over a wide range of injected current values (the regions where mode locking was unstable are indicated by the shaded areas in Fig. 4.3). The dependence of the measured pulse duration on the injection current is represented in the same figure. Before the onset of ES lasing, the pulse durations increase with current, for the reasons pointed out in the previous chapter. However, in the region where GS and ES co-exist, this trend reverses, with pulse durations decreasing sharply from 11ps to 6ps. This is the first time, to our knowledge, that the duration of the pulses generated by a passively mode-locked diode laser are seen to decrease with increasing current.

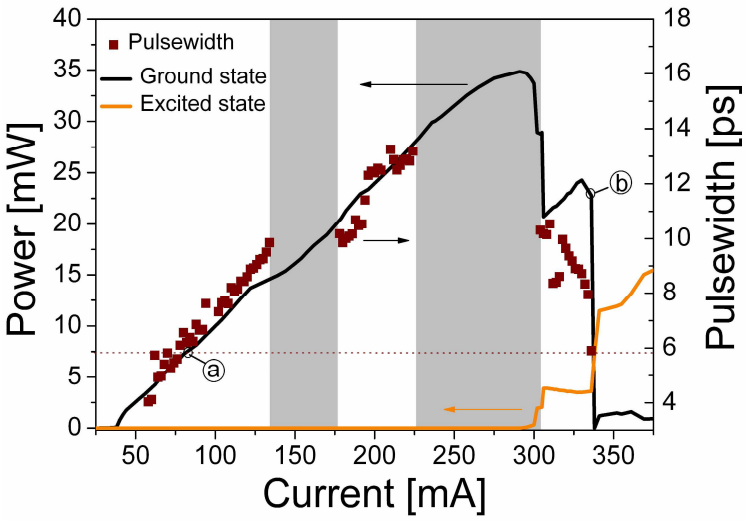

Fig. 4.3 - Light-current characteristic of the device, at constant reverse bias V_{abs}=8.9 V, and pulse duration (squares). The shaded areas correspond to unstable mode locking. The highlighted points a) and b) correspond to operating conditions resulting in a similar pulse duration of 6ps (brown dot horizontal line).

It is important to stress that the average power obtainable in this regime for a similar pulse duration of 6ps is nearly three times higher (23mW, pointed by b) in Fig. 4.3), than the obtained in the low current regime at 88mA (8mW, pointed by a) in Fig. 4.3). The autocorrelation of the shortest pulse obtained is shown in Fig. 4.4.

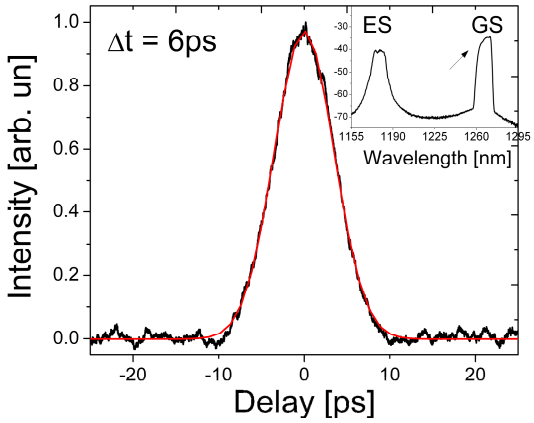

Fig. 4.4 – Autocorrelation of the shortest pulse available in the new mode-locking regime.

The combination of shorter pulses with higher average powers in this new regime enabled the generation of pulses with enhanced peak power, under higher current and reverse bias conditions – as can be observed in Fig. 4.5, the peak power increase with current is accelerated, comparing to the previous regime (GS only).

The decrease of pulse duration, together with a slight decrease in the spectral bandwidth also impacts significantly on the time-bandwidth product, which decreases with increasing current – in stark contrast with the trend of the previous mode-locking regime (Fig. 4.5).

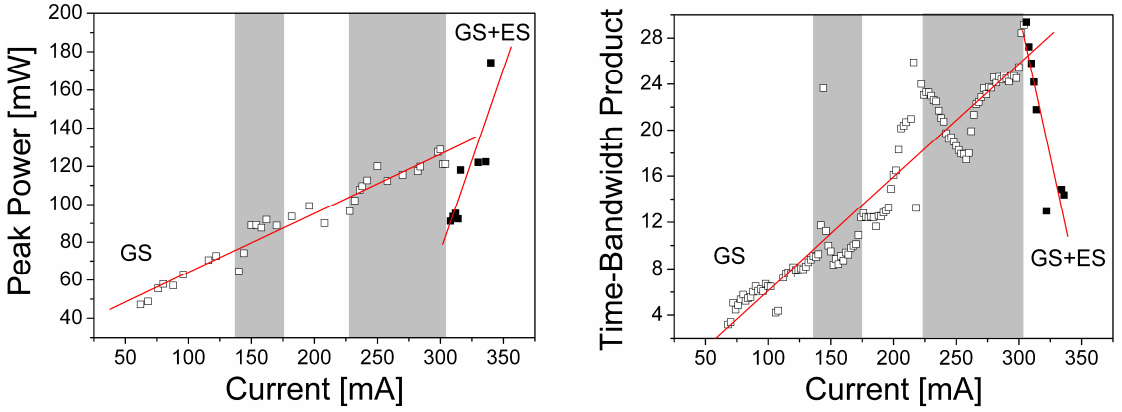

Fig. 4.5 – Variation of the peak power and time-bandwidth product with current, in both mode-locking regimes: GS only (open squares) and GS in the presence of ES lasing (solid squares).

The evolution of the optical and RF spectral characteristics as a function of current are shown in Fig. 4.6, where it can be observed how the noise associated with unstable mode locking is drastically reduced and a very sharp RF spectrum is present in the new mode-locking regime. The sideband noise becomes very low and is comparable to that observed in the stable mode-locking regime at currents just less than 218mA.

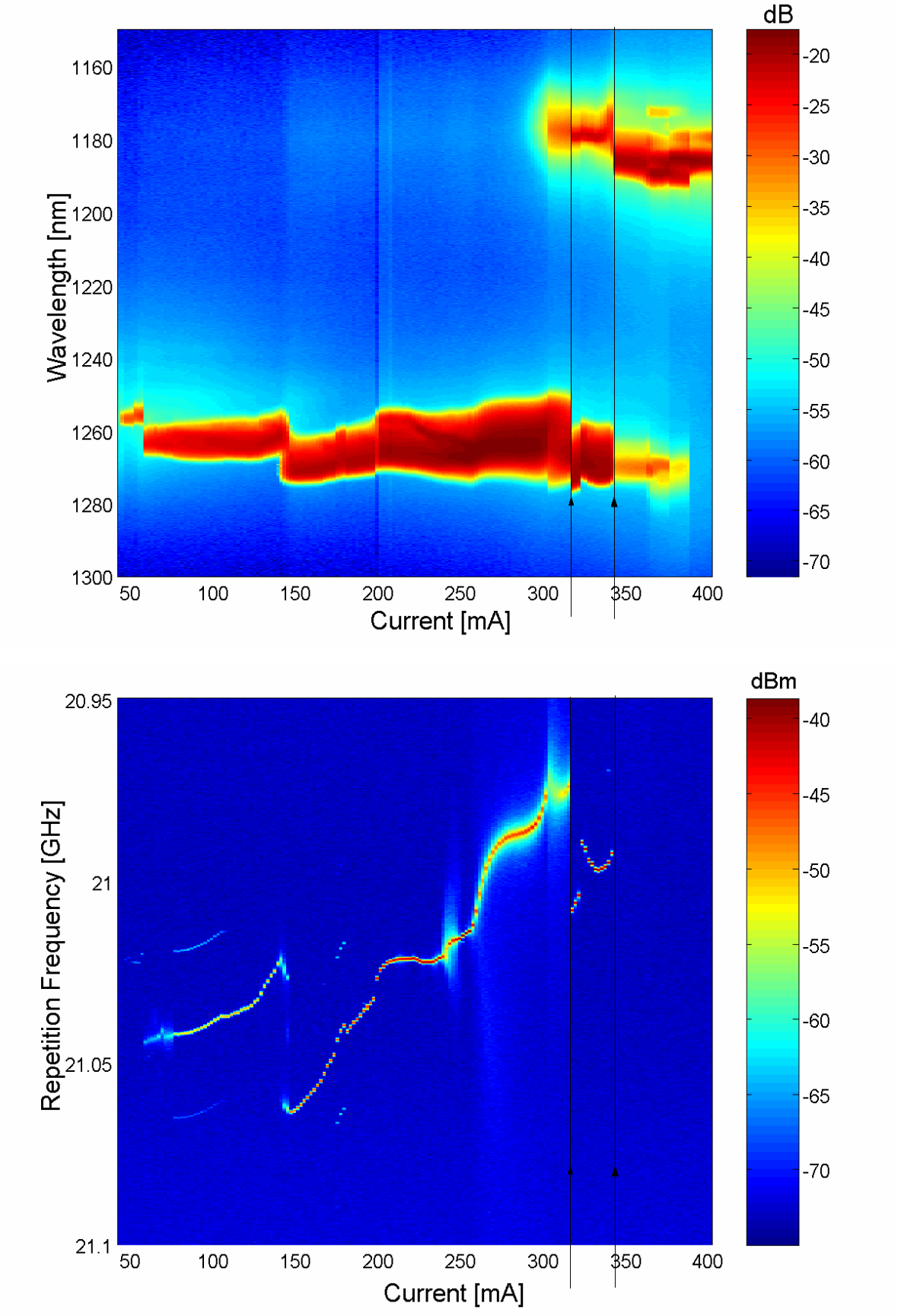

Fig. 4.6 - Performance of the Ioffe laser with increasing current up to 400mA: optical spectrum (top) and RF spectrum (bottom). The arrow lines delimit the region of stable mode-locking with GS+ES. The reverse bias level was kept constant at 8.9V.

Let us now examine the second scenario, that is, how the new mode-locking regime emerges and develops with increasing reverse bias, with a fixed injection current of 400mA. At this high level of bias current, stable GS mode locking is never observed, except when ES emission takes place, as depicted in Fig. 4.7.

After an initial region where mode locking is not very stable (patterned area), the pulse duration is seen to decrease with increasing reverse bias, as previously observed and explained in the context of the GS mode-locking regime described in the previous chapter. The decrease is not so spectacular as occurs with the gain current, but this is perhaps due to the fact that the optical power level in this scenario is nearly the double of the power level represented in Fig. 4.3. In any case, the trend of pulse duration decrease with reverse bias in the regime ES+GS is similar to what is usually observed with GS only.

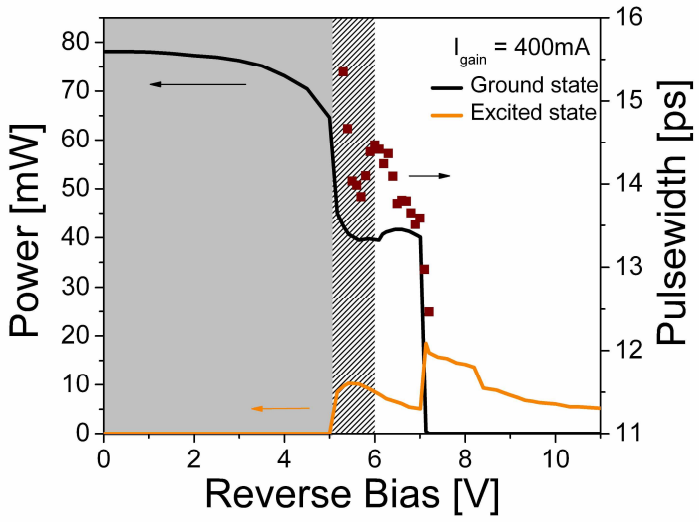

Fig. 4.7 – Output power for increasing reverse bias, at constant injection current I_{gain}=400mA, together with pulse durations (squares). The shaded areas correspond to unstable mode locking.

In terms of optical power, the same effective drop is observed as in the previous case. However, it is interesting to realise that only the optical power of the ES mode seems to decrease slightly, while at the GS, it keeps relatively constant. Measurements performed at a lower current injection (360mA) showed that the optical power of both GS and ES decreased only very slightly with increasing reverse bias. One argument is that possibly at this high level of current injection, increasing the reverse bias in such a narrow region between 6V and 7V is not significant enough to decrease the optical power effectively. The evolution of the optical and RF spectral characteristics as a function of reverse bias is shown in Fig. 4.8.

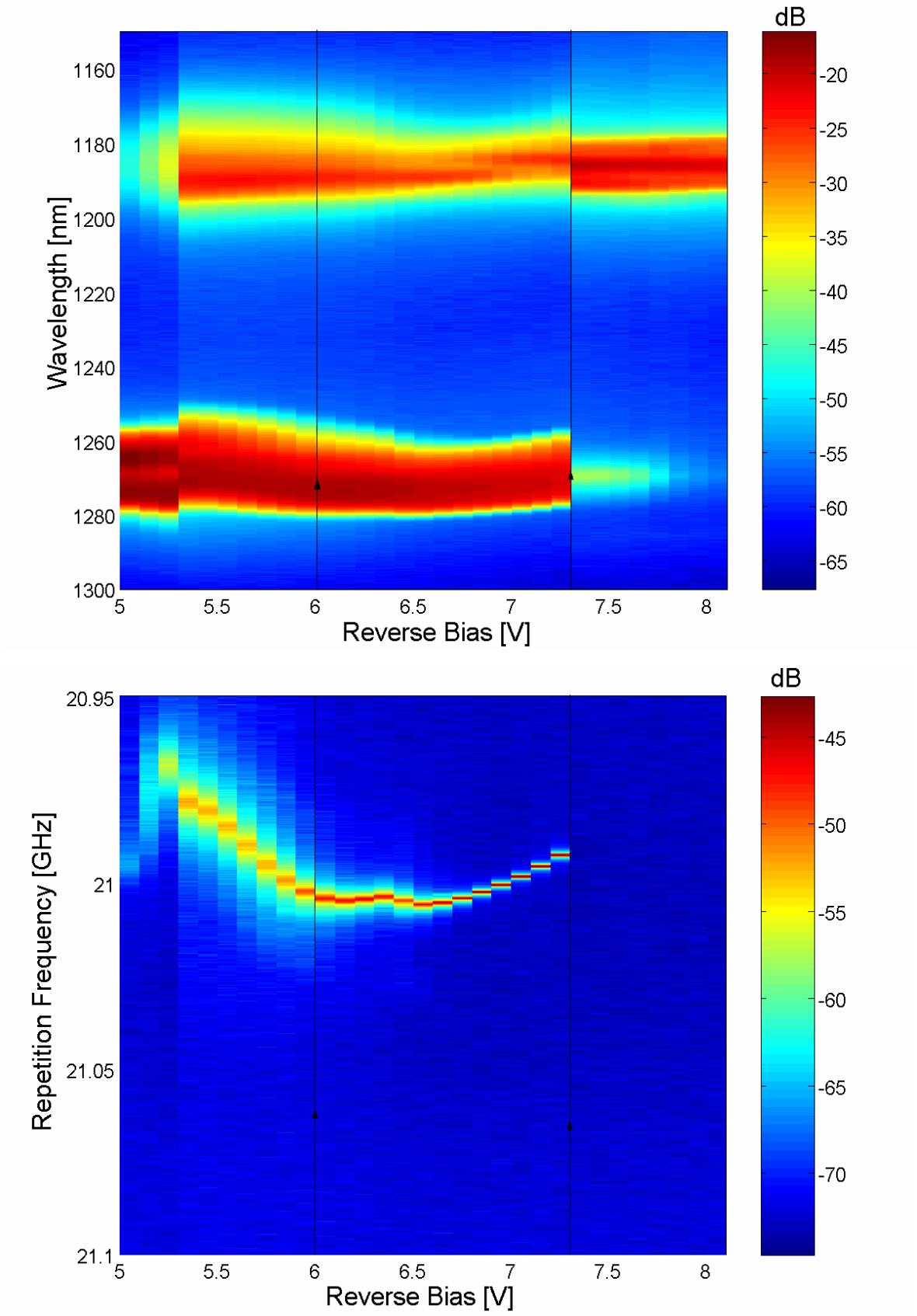

Fig. 4.8 – Performance of the Ioffe laser with increasing reverse bias: optical spectrum (top) and RF spectrum (bottom). The arrow lines delimit the region of stable mode-locking with GS+ES. The gain current was kept constant at 400mA.

4.3. Discussion of results

First and foremost, it is important to stress that the new mode-locking regime is not caused by an increasing temperature on the chip. The first argument for ruling out this effect is that although there was a drop in power with the onset of ES lasing, the differential efficiency of GS is nearly the same as in the previous mode-locking regime, where only GS existed. If the macroscopic temperature was to be increasing significantly with current and thus having the effect of shortening the pulse durations[13], the average power should decrease accordingly – and that is not observed. No thermal rollover was observed in the region where GS and ES coexist, only an abrupt drop upon the prevalence of ES emission over GS, at 340mA. The central wavelength of emission of the GS spectral band is slightly red-shifted in this new mode-locking regime, but still lies within the range of wavelengths that were previously accessed in the previous regime.

In any case, it is possible that the abrupt drop of power has further contributed to the transition from an unstable to a stable mode-locking situation in both scenarios (increasing current or reverse bias), by weakening the broadening effects caused by high intracavity power. But this effect alone can not account for the decrease of pulse duration with increasing current/power, and therefore other mechanisms must be explored to explain this phenomenon.

By studying the separate influence of reverse bias and current injection, it was possible to attempt a differentiation between the effects imposed by the saturable absorber or the gain section, and in the following sections, several possibilities that could explain this new mode-locking regime will be advanced.

4.3.1. Effects of the saturable absorber on the pulse duration

When the ES is emitting alongside the GS mode-locked pulses, there is a continuous generation of photocarriers in the absorber, at the ES level. There are two routes for these photocarriers: they can either be removed by the applied reverse bias or relax down to an available GS level.

On the other hand, the photocarriers generated by the GS are only generated every 40ps in the absorber. The situation is now different in the sense that some of the

[13] As will be later demonstrated on Chapter 6, the pulse duration decreases with increasing temperature.

absorbing QDs that used to have available empty levels for the photocarriers to occupy are already populated with the photocarriers that previously relaxed down from the ES level. With fewer unoccupied QDs available, less photons are needed to bleach the absorber and so the absorption saturates much more rapidly than in the situation where only GS exists. Comparing to the optical spectra in the mode-locking region prior to the appearance of ES, the spectrum has a stronger asymmetric edge on the side of longer wavelengths (Fig. 4.9). This suggests that the shaping mechanism became stronger for the leading edge in this new regime (assuming the sign of the chirp is the same as in the previous mode-locking regime). The spectrum is also slightly narrower and has a missing component on the blue-side, corresponding to the trailing edge. The key to further shaping in this trailing edge could be linked either to a faster absorption recovery time, or to a slower gain recovery, as explained in the next section.

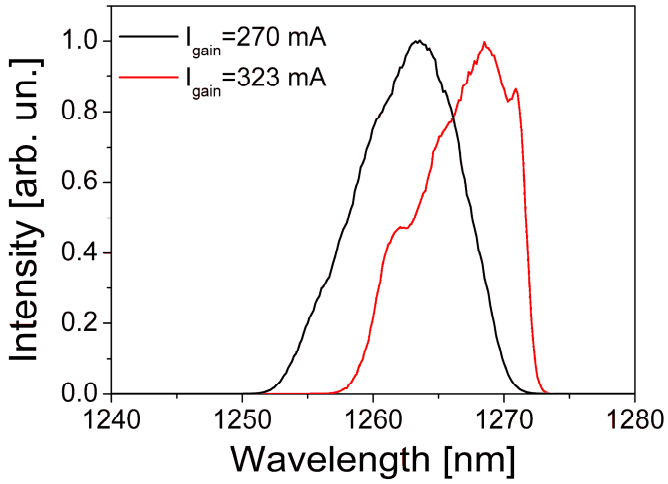

Fig. 4.9 – Exemplifying normalised optical spectra at a constant reverse bias of 8.9V, for a current of 270mA and 323mA, corresponding to unstable mode-locking before the appearance of ES and to the new mode-locking regime, where GS and ES coexist (ES was omitted, to simplify the graph representation).

Another important mechanism that may be taking place is the presence of photocarriers in the ES that could change significantly the refractive index and its dependence with the photocarriers generated in the GS. This could have an impact on the LEF of the absorber and thus on the amount of SPM imparted by this section of the laser, which could be further aiding to the compression of the pulses.

4.3.2. Effects of the gain section on the pulse duration

The trends observed with the change in current in the gain section are strikingly different from what is observed in the usual mode-locking regime, with the pulse duration decreasing significantly as both the current in the gain section and the optical power increase.

In this new regime, the carrier dynamics between ES and GS is dramatically changed, as a part of the carriers that were previously populating the GS level via relaxation from the ES level are now engaged in the stimulated emission at the ES spectral band. There are two main consequences from this new dynamics: the cooling of carriers that lie above the GS level and a slower gain recovery on the GS spectral band.

There have been several pump-probe studies that demonstrated how the gain recovery at the GS level is very fast (and complete), provided that the higher ES levels are highly populated [10,11]. When the ES population is depleted via stimulated emission, the carrier capture to the GS via ES occurs less frequently, so that the gain recovery takes longer to occur – and this effect may play a part in the shortening of the pulses. A slower gain recovery will help to shape the trailing edge – as there is no gain available, the amplification of the trailing edge is suppressed, and thus the pulse is shortened. An evidence that could support this view is that in this new mode-locking regime, the spectrum appears to be "cut" on the blue side – which would correspond to the trailing edge of an up-chirped pulse . On the other hand, a slower gain recovery for every pulse in average, would result in a lower power level in average terms, which could also support the initial down-shift in the optical power. However, this effect alone (slower gain recovery) can not explain the observed trend with increasing current - as current increases, the gain recovery should speed up with the more carriers available, and the effect should ease.

Possibly the most important effect is the cooling of the carriers that lie in the higher energy levels. With simultaneous laser emission from the ES, a strong depletion of the higher populated levels occurs. This carrier depletion should have an impact on the refractive index and gain of the laser, in such a manner that the LEF decreases significantly, because the carrier pile-up on the ES is now suppressed. It has been shown that the LEF associated with GS can even become negative with simultaneous ES emission [5], as depicted in Fig. 4.10.

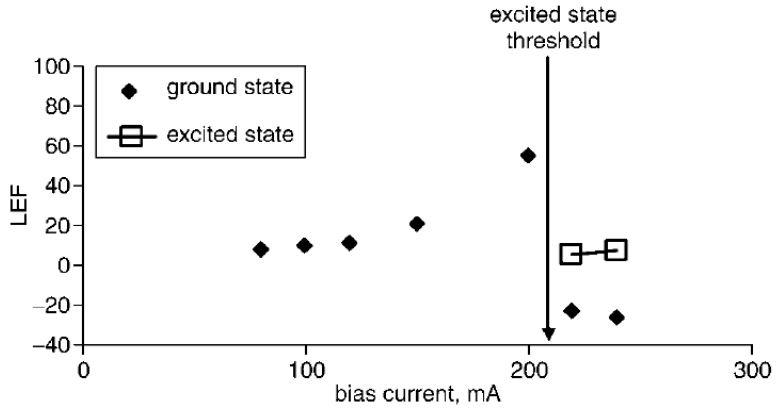

Fig. 4.10 – Ground-state and excited-state LEF as a function of current. Reprinted from [5].

A lower LEF along the overall cavity will result in a decrease of SPM and of the up-chirp imparted to the pulses, which together with the positive dispersion of the laser material will result in a decrease of the pulse duration. We believe that this effect in the gain section may hold the main key to the mode locking enhancement[14] here observed.

4.3.3. Effects on the optical power

As pointed out before, the same differential efficiency was observed for GS, after ES appeared – there is only a drop of the overall power level, that is, when summing the total optical power generated by the ES and the GS, there is a discontinuity between the optical power before and after ES lasing (Fig. 4.11).

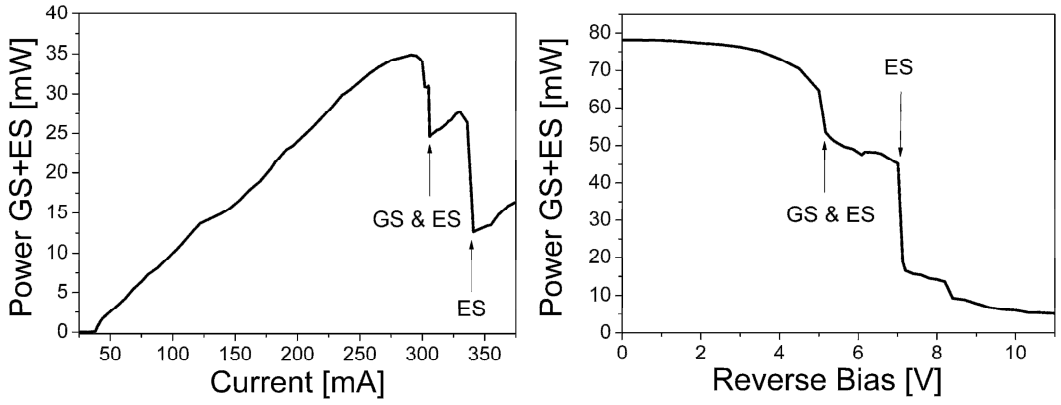

Fig. 4.11 – Total optical power, combining the contributions from GS and ES, where the power drops are evidenced for the transitions from GS to GS&ES, and to single ES laser emission.

[14] A method to determine the effect on the chirp and whether it is negative or positive would be to set up a dispersion compensation scheme so as to compress the pulses and thus determine the magnitude and sign of the chirp.

This is contrary to what has been observed in literature [9,12], where the sum of the GS and ES optical power should match the GS optical power, right before the appearance of ES. However, this effect reported in literature was observed single-section lasers operating in cw mode, and not mode-locked two-section lasers. We believe that the dynamics of gain recovery associated with the generation and propagation of a picosecond pulse in the laser cavity plays an important role in the power-drop observed. The absence of highly-populated ES levels and the resulting slower (and possibly incomplete) gain recovery contributes to a lower gain in average terms, and thus lower obtainable power. Interestingly, after the power-drop, the average power at the GS level does not cease to increase. Indeed, the carriers provided by the injection current are still being captured efficiently by the GS levels, albeit at a slower rate. This observation is in agreement with the findings recently published – that the direct capture from the wetting layer can also contribute to the refilling of ground state [10], in the absence of carrier reservoir in the ES levels.

One effect that could also inhibit the optical power associated with the ES lies in the high/anti-reflectivity coatings of the laser facets, which were optimised for GS and not for ES. A higher mirror loss for ES could also contribute to the power drop, but it was realised that this effect is relatively minor and only contributes with a difference of approximately 10%. The calculations were as follow.

Assuming a linear dependence with current I, the output power of a laser diode P_{out} is:

$$P_{out} = \frac{h\nu}{q}\frac{\eta_i \alpha_m}{\alpha_m + \alpha_i}\left(I - I_{th}\right) \tag{4.1}$$

where h is Planck's constant, ν is the optical frequency, q is the charge of the electron, η_i is the internal quantum efficiency, α_m is the loss associated with the mirrors, α_i is the internal optical loss and I_{th} is the threshold current. The differential external efficiency η_d can be defined as:

$$\eta_d = \frac{q}{h\nu}\frac{dP_{out}}{dI} = \eta_i \frac{\alpha_m}{\alpha_m + \alpha_i} \tag{4.2}$$

The spectral dependence of the reflectivity on the AR/HR coatings on the Ioffe laser is not known, but typical values found on the literature have shown to be much easier the deposition of broadband (>100nm) constant HR coatings than AR coatings. The reflectivity of an AR coating (R_{AR}) can vary by a few percent, thus having a stronger effect in the mirror losses for ES than R_{HR}. Furthermore, the expression for the mirror loss further reinforces the predominant role of the AR-coatings (L is the length of the laser cavity):

$$\alpha_m = \frac{1}{2L}\ln\left(\frac{1}{R_{AR}R_{HR}}\right) = -\frac{1}{2L}\left(\ln R_{AR} + \ln R_{HR}\right) \tag{4.3}$$

Because $R_{AR} \sim 0$ and $R_{HR} \sim 1$, the contribution from $\ln\left(R_{HR}\right)$ can be neglected, and indeed, changing R_{HR} within 0.8-0.99 has nearly no effect on the mirror loss. Thus:

$$\alpha_m \sim -\frac{1}{2L}\ln R_{AR} \tag{4.4}$$

So, if the AR coating is less optimal for the ES (meaning $R_{AR} > 0.01$), less ES photons will escape the front facet compared to those that are generated, thus decreasing the output power and differential efficiency. For illustration, $\alpha_i = 2\,cm^{-1}$ was considered in the following calculations of the variation of output power with increasing mirror loss, as shown in Table 4.1.

Table 4.1 – Variation of output power with increasing mirror loss.

	R_{AR}	$\alpha_m\left(cm^{-1}\right)$	$\frac{\alpha_m}{\alpha_m+\alpha_i}$	Power variation from ideal case
Ideal case	0.01	11	0.85	-
Probable case	0.05	7.1	0.78	7%
Worst case	0.33	2.6	0.57	33%

These calculations show that the variation in efficiency and optical power of the ES lasing mode due to the mirror losses would be only 7%; even in the unlikely scenario that corresponds to no effect at all of the AR coating, the variation would be only 33%. In conclusion, the mirror losses for the ES are higher, but play a minor role in the observed optical power drop. Indeed, other important phenomena can influence

the power drop of the ES mode, such as a higher saturable and non-saturable absorption and a stronger contribution of non-radiative mechanisms across the ES transition, phenomena which have not yet been thoroughly investigated in the literature. Furthermore, the quantification of these effects requires the theoretical simulation of the quantum-dot laser using a model for mode-locking in quantum-dot lasers across GS and ES (a development beyond the scope of this thesis). In fact, rate and field equations are necessary to account for the complex interaction of the carriers in the different levels and for the dynamic saturable and non-saturable absorption, which is influenced by both GS and ES optical power and carrier interaction/sweep-out in the absorber.

Finally, it is important to stress that due to the presence of the saturable absorber, there is not a continuous transition and build-up from threshold for the ES, but instead a sudden transition occurs at the ES threshold point. This is further accentuated by the fact that the degeneracy of the excited states is higher and thus a higher differential gain/absorption is to be expected. The sudden jump is caused by the saturation of the absorption at the ES spectral band – a hint that the saturable absorber could be used for generating pulses on the ES band, as will be shown in the next chapter.

4.3.4. Effects on the phase noise

With the onset of ES laser emission, the RF spectrum becomes better defined and the phase noise skirts around the peak frequency are almost completely eliminated, as observed in Fig. 4.6 and Fig. 4.8. We believe that this behaviour is attributable to amplified spontaneous emission (ASE), which increases steadily before ES lasing and is strongly suppressed thereafter. The discrete nature of the density of states in QDs suggested a suppressed ASE. However, with increasing current and the consequent carrier pile-up on the ES levels, increased levels of ASE on the ES spectral band would generate random fluctuations in photon density, gain and index of refraction, which contribute to variations in the round-trip time [13]. Therefore, it can be anticipated that in this new mode-locking regime, pulse timing jitter will also be reduced significantly.

We performed similar measurements for different fixed reverse bias conditions and the behaviour described above was found to hold over a wide range of injection currents.

4.4. Conclusion

We have demonstrated a new regime for mode locking in a QD-based laser where the simultaneous presence of excited-state cw lasing is seen to reduce dramatically the duration and phase noise of ground-state pulses. The method presented is simple and relies solely on the electrical pumping conditions. In this mode-locking regime, the pulse duration decreases as current is increased thereby enabling the generation of ultrashort pulses with up to a three-fold increase in power when compared to pulses of identical duration generated at lower currents. With the information available at the moment, we believe that this phenomenon is related with the depletion/creation of carriers in the ES levels in the gain/absorber sections and the corresponding influence on the overall LEF. These results, based on unique properties available to QD lasers are expected to lead to the exploitation of their full potential as compact sources of ultrashort, high-power, low-noise pulses.

4.5. References

[1] T. C. Newell, D. J. Bossert, A. Stintz, B. Fuchs, K. J. Malloy, and L. F. Lester, "Gain and linewidth enhancement factor in InAs quantum-dot laser diodes," *IEEE Photon. Technol. Lett.*, vol. 11, pp. 1527-1529, 1999.

[2] A. Martinez, A. Lemaitre, K. Merghem, L. Ferlazzo, C. Dupuis, A. Ramdane, J. G. Provost, B. Dagens, O. Le Gouezigou, and O. Gauthier-Lafaye, "Static and dynamic measurements of the alpha-factor of five-quantum-dot-layer single-mode lasers emitting at 1.3 μm on GaAs," *Appl. Phys. Lett.*, vol. 86, pp. 211115, 2005.

[3] H. Su and L. F. Lester, "Dynamic properties of quantum dot distributed feedback lasers: high speed, linewidth and chirp," *J. Phys. D*, vol. 38, pp. 2112-2118, 2005.

[4] M. T. Choi, W. Lee, J. M. Kim, and P. J. Delfyett, "Ultrashort, high-power pulse generation from a master oscillator power amplifier based on external cavity mode locking of a quantum-dot two-section diode laser," *Appl. Phys. Lett.*, vol. 87, pp. 221107-3, 2005.

[5] B. Dagens, A. Markus, J. X. Chen, J. G. Provost, D. Make, O. Le Gouezigou, J. Landreau, A. Fiore, and B. Thedrez, "Giant linewidth enhancement factor and purely frequency modulated emission from quantum dot laser," *Electron. Lett.*, vol. 41, pp. 323-324, 2005.

[6] M. G. Thompson, K. T. Tan, C. Marinelli, K. A. Williams, R. V. Penty, I. H. White, M. Kuntz, D. Ouyang, D. Bimberg, V. M. Ustinov, A. E. Zhukov, A. R. Kovsh, N. N. Ledentsov, D. J. Kang, and M. G. Blamire, "Transform-limited optical pulses from 18 GHz monolithic modelocked quantum dot lasers operating at 1.3 μm," *Electron. Lett.*, vol. 40, pp. 346-347, 2004.

[7] M. V. Maximov, L. V. Asryan, Y. M. Shernyakov, A. F. Tsatsul'nikov, I. N. Kaiander, V. V. Nikolaev, A. R. Kovsh, S. S. Mikhrin, V. M. Ustinov, A. E. Zhukov, Z. I. Alferov, N. N. Ledenstov, and D. Bimberg, "Gain and threshold characteristics of long wavelength lasers based on InAs/GaAs quantum dots formed by activated alloy phase separation," *IEEE J. Quantum Electron.*, vol. 37, pp. 676-683, 2001.

[8] V. M. Ustinov, A. E. Zhukov, A. Y. Egorov, and N. A. Maleev, *Quantum Dot Lasers*. New York: Oxford University Press, 2003.

[9] A. Markus, J. X. Chen, C. Paranthoen, A. Fiore, C. Platz, and O. Gauthier-Lafaye, "Simultaneous two-state lasing in quantum-dot lasers," *Appl. Phys. Lett.*, vol. 82, pp. 1818-1820, 2003.

[10] S. Dommers, V. V. Temnov, U. Woggon, J. Gomis, J. Martinez-Pastor, M. Laemmlin, and D. Bimberg, "Complete ground state gain recovery after ultrashort double pulses in quantum dot based semiconductor optical amplifier," *Appl. Phys. Lett.*, vol. 90, pp. 033508-3, 2007.

[11] P. Borri, S. Schneider, W. Langbein, and D. Bimberg, "Ultrafast carrier dynamics in InGaAs quantum dot materials and devices," *J. Opt. A*, vol. 8, pp. S33-S46, 2006.

[12] E. A. Viktorov, P. Mandel, Y. Tanguy, J. Houlihan, and G. Huyet, "Electron-hole asymmetry and two-state lasing in quantum dot lasers," *Appl. Phys. Lett.*, vol. 87, pp. 053113-3, 2005.

[13] P. Vasil'ev, *Ultrafast Diode Lasers: Fundamentals and Applications*. Boston: Artech House, 1995.

5. EXCITED-STATE MODE LOCKING IN QUANTUM-DOT LASERS

In this chapter, the mode-locking regime of a QD laser that operates either in the ground state (1260nm) or in the excited state (1190nm) bands is demonstrated, at repetition frequencies of 21GHz and 20.5GHz, respectively. Switching between these two operational regimes was achieved through the variation of the dc current supplied to the gain section and/or the reverse bias on the absorber section.

5.1. Potential advantages for operating in the excited-state transition

In this work, ES emission has been considered as an extra degree of freedom to improve the performance of the laser (Chapter 4), and we believe there are useful aspects for a mode-locking regime where a train of short pulses deploys only the ES transitions.

The first relevant advantage relates to the faster absorption recovery along the ES band [1]. Indeed, there are two paths for (fast) absorption recovery in a QD with carriers in the ES: these can escape from the QD to the wetting layers, or quickly relax to the GS level. On the other hand, sub-picosecond gain recovery times have been demonstrated not only for GS but also for ES transitions in electrically pumped QD amplifiers [2]. At low injection currents, the gain recovery time for the ES is slightly slower than for the GS, but at higher injection currents, the two values are very similar, as the wetting layer acts as reservoir of carriers for the ES level.

Furthermore, several different measurements have been showing that the linewidth enhancement factor (LEF) decreases significantly for wavelengths below the GS transition, even becoming negative at ES - thus suggesting the potential of chirp free operation for the spectral range involved [3].

It should also be noted that laser emission that engages the ES transitions is characterised by a higher differential gain than that for the GS counterpart, with concomitant benefits for mode-locked QD lasers. Higher differential gain also results in a higher possible modulation speed, which varies with the square root of the differential gain. The capture of carriers to the ES is also faster, as the ES levels lie closer to the wetting layer. These effects have even prompted an interesting theoretical study that indicated ES as a spectral alternative for high-speed modulation in QD lasers [4].

More recently, Dr Rafailov, Douglas McRobbie, myself and others demonstrated an optically gain-switched QD laser, where pulses were generated from both GS and ES. Interestingly, the pulses generated via ES were shorter than those generated through GS transitions alone [5].

The potential for shorter and chirp-free pulses from ES transitions motivated the investigation of a mode-locking regime that would engage the ES spectral band. Such regime was achieved in a QD laser where the mode-locked operation can involve electrically switchable GS or ES transitions that are spectrally distinct. The exploitation of these effects could enable a range of applications extending from time-domain

spectroscopy, through to optical interconnects, wavelength-division multiplexing and ultrafast optical processing.

5.2. Mode-locked operation in the ES transition

These studies were performed on the Ioffe laser, previously described in Section 3.3.1. The laser was electrically pumped by dc bias. Part of the laser output was directed to a diffraction grating to spatially separate the two distinct wavelength bands that were then monitored by two independent power meters, in a setup similar to what has been described in the previous chapter.

A light current characteristic of this laser is shown in Fig. 5.1, where a constant reverse bias (V_{abs}=8.9V) was applied to the absorber section. By increasing the current in the gain section, laser emission involving the ES transitions appears. Clear evidence of hysteresis for the onset of ES lasing can be observed that also affects lasing in the GS band. This hysteresis indicates the presence of saturable absorption for the ES mode.

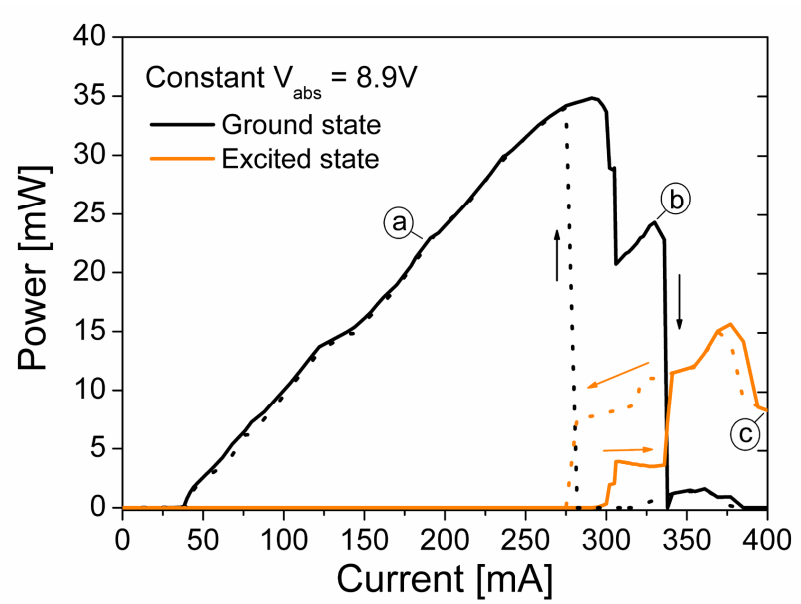

Fig. 5.1 – Light-current characteristics of the two-section device, at constant reverse bias, for increasing (solid) and decreasing (dashed) currents. The operating points a), b) correspond to stable mode-locked operation via GS, whereas point c) corresponds to unstable mode locking via ES. The optical and RF spectra for these points are shown in Fig. 5.3.

Similar behaviour was observed in the case illustrated in Fig. 5.2, when the injected current was constant at 400mA but the reverse bias was varied from 0V to 11V. In fact, as the reverse bias is increased, the accessible gain for the ground state transitions is unable to compensate the intracavity losses, thus favouring ES lasing in preference to GS lasing. By tuning the current and reverse bias, it was possible to switch the mode-locking band from the GS to the ES regime.

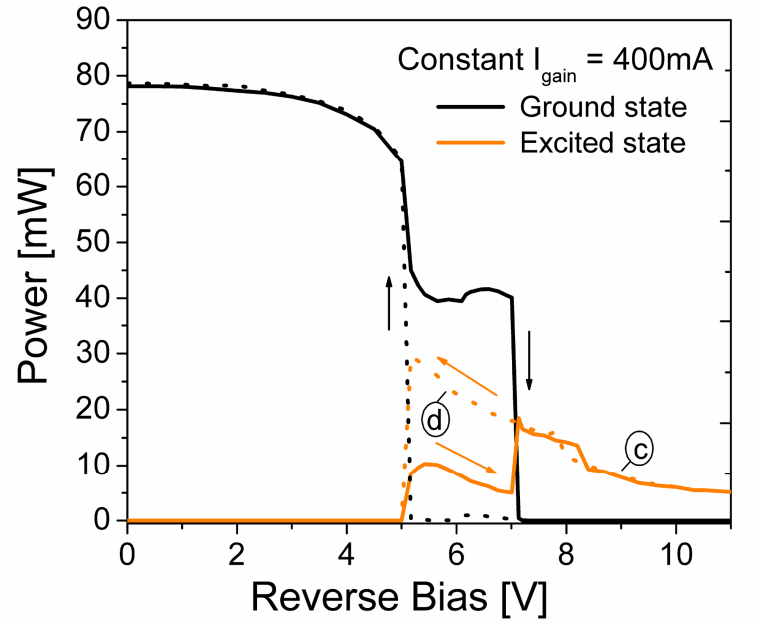

Fig. 5.2 – Output power from the two-section device at constant current, for increasing (solid) and decreasing (dashed) reverse bias. The operating points c) and d) correspond to unstable and stable mode-locked operation via ES, respectively. The optical and RF spectra for these points are shown in Fig. 5.3

Above laser threshold, stable mode locking via GS transitions was observed at 21GHz, for a wide range of injected current values, before and indeed after the ES lasing had become established, as was demonstrated in the previous chapter. The relevant optical and RF spectra are depicted in Fig. 5.3, where the curves a) and b) correspond to the operating points highlighted in Fig. 5.1, respectively before and after the onset of ES lasing. As the injection current was further increased, the ground state lasing intensity decreased significantly and eventually disappeared when the input current exceeded 340mA (Fig. 5.1). Above this current level, laser emission was confined to the excited state transitions and mode-locked operation via this spectral band was observed for a wide range of reverse bias in the range of 5-9V. The stability of mode locking via ES was significantly improved when the reverse bias was

decreased, and very stable mode locking involving ES transitions was observed between the reverse bias values of 5V and 6.5V. To illustrate this, the operating point c) depicted in Fig. 5.1 and Fig. 5.2 can be considered. For the corresponding set of bias conditions (I_{gain}=400mA and V_{abs}=8.9V), the optical and RF spectra are shown in curve c) on Fig. 5.3, and as observed, the mode locking via ES was not stable. While maintaining the same injection current, a decrease in the reverse bias led to the descending path of the hysteresis curve depicted in Fig. 5.2. It was observed that for reverse bias values between 6.5V and 5V, the mode locking stability was improved significantly as illustrated by curve d) in Fig. 5.3. As can be observed in the transition from point c) to point d), the optical power associated with the ES increases substantially from 8mW to 24mW, and more importantly, the ASE associated with the GS is strongly suppressed.

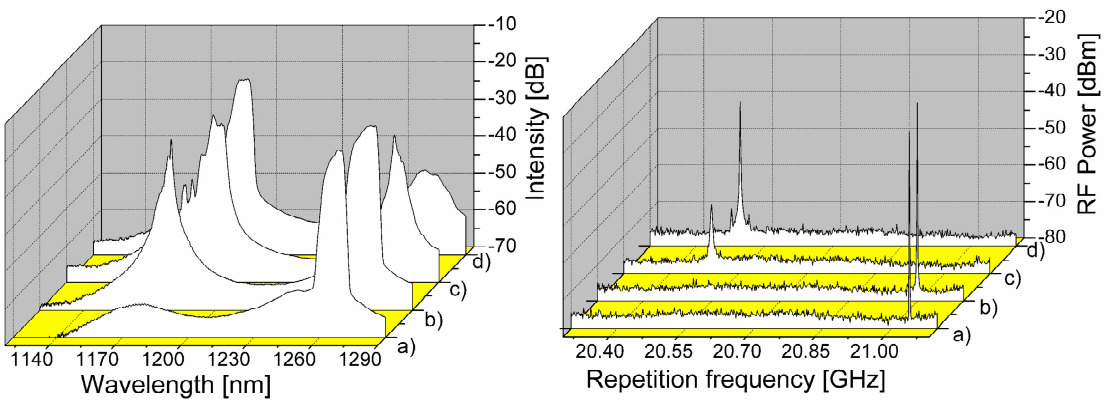

Fig. 5.3 - Optical spectra (left) and RF spectra (right) corresponding to mode-locked operation in the ground state (a, b) and excited state (c, d). The bias conditions are detailed in Fig. 5.1 and 5.2.

The repetition frequency of the mode locked pulses via ES was 20.5GHz, which is slightly lower than that for the GS regime. This is to be expected because of the higher refractive index at the shorter wavelengths. It is important to stress that the average power level of both GS and ES mode locked outputs is relatively high, at 35mW for the GS and 25mW for the ES operations.

In the range of bias conditions explored in this study, the shortest pulse duration measured for ES transitions was ~7ps, where the spectral bandwidth was 5.5nm, at an output power of 23mW (Fig. 5.4).

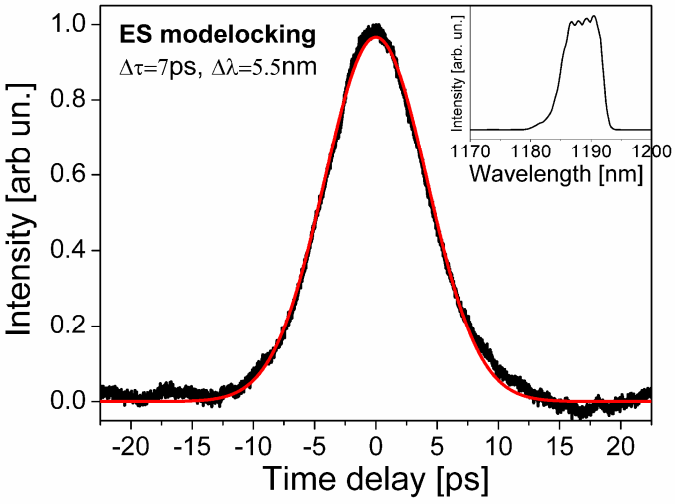

Fig. 5.4 - Background-free autocorrelation of the mode-locked output via excited-state operation, corresponding to operating point d) shown in Fig. 5.2 and Fig. 5.3 (inset is the corresponding spectral profile). The autocorrelation trace was best fitted to a Gaussian function.

The pulse durations obtained via ES are slightly longer than those generated by GS mode locking at the same power level, in the new ML regime enhanced by ES. Pulses generated from ES mode locking are also far from the transform limit (time-bandwidth product exceeded 7). Finally, it is important to bear in mind that this laser was not designed for ES operation, so mode locking in this band was only achieved at the expense of injecting high drive currents, which has the well known effect of significantly broadening the pulses.

5.3. Further investigations based on these results

After our first demonstration of ES mode locking [6,7], further work was developed on this area by Prof. Delfyett's group at CREOL, Florida. Instead of using a monolithic device, this group exploited the added flexibility of external cavity configurations to develop a laser where the generation at the GS and ES bands could be achieved using intracavity optical elements [8], instead of relying solely on the increase of the bias conditions as in this work. This configuration allowed an easier feedback and lower operation current, thus preventing the possibilities of overheating the laser device and more importantly, avoiding the temporal broadening of pulses due to high values of bias current. Using an external compression setup, it was verified that both pulses generated by GS and ES were up-chirped. Before compression, the pulse durations achieved were in the order of 11ps for ES (1193 nm) and 14ps for GS (1275 nm). After

compression, pulse durations of 1.2ps and 970fs were achieved for ES and GS, respectively.

A similar setup was used by the same group to tune the wavelength from GS into the ES, with an according decrease of chirp/LEF as the wavelength was blue-shifted [9].

5.4. Discussion of the results

Throughout our work and the work of other groups on this new regime of mode locking, it has been realised that GS and ES mode locking were not observed simultaneously. Effectively, it seems that they may be competing for the same saturable absorption, owing to the unique inter-level carrier dynamics present in QD lasers. This is further supported by the fact that multi-mode mode locking has been observed in some occasions throughout this work for different modes limited to the GS spectral band. Spectrally, these modes are closely spaced (few nm), and so they generate interleaved trains of pulses with very similar repetition frequencies. This does not seem to pose any problem of mode competition, suggesting that these modes, because they belong to different populations of QDs (with different sizes), would require independent saturable absorption. This is not the case for GS and ES modes, that would be competing for the same quantum dots. The absorber recovery time, which is one of the most important parameters to be considered in pulse shaping, may be significantly inhibited across the ES spectral band if GS photocarriers are present in the levels below (caused by GS lasing/ spontaneous emission). This would suppress the relaxation path from ES to GS in the absorber, as the ES carriers have less void states to decay to – which could significantly increase the absorption recovery time, and thus inhibit mode locking. It is therefore a non-reciprocal situation: GS mode locking can be enhanced by the simultaneous presence of ES cw laser emission, whereas ES mode locking can only occur on its own. This is supported as well by the observation that the ES mode locking was more stable for lower values of reverse bias. Indeed, as the reverse bias was decreased, the optical power associated with the ES increased significantly, while suppressing the ASE in the GS spectral band - therefore causing less interference in the absorption recovery dynamics. The suppression of ASE also decreased the phase noise in the RF spectrum associated with ES mode locking.

Moreover, this study provides some useful indications on the feasibility of engaging simultaneously GS and ES in a truly dual-wavelength mode locking. A key requirement would have to be the synchronicity of the pulses, so that there would not exist any detrimental effects in the absorber carrier dynamics, from one mode to another (and assuming that GS and ES photocarriers generated in the absorber could be efficiently extracted at the same time). The synchronicity of pulses with such a spectral separation will be difficult to achieve, owing to the high dispersion level across the semiconductor gain medium. In the laser studied, the difference in pulse repetition frequencies between the GS and ES pulses was 500MHz. This effect can be minimised by using a longer diode laser (Fig. 5.5), and an even better option would be to use an external cavity configuration. In any case, it would be necessary to include adjustable[15] intra-cavity dispersion compensation to synchronise the two modes. From the point of view of the carrier dynamics in the gain section, if both modes oscillate simultaneously, that also poses the problem of significant carrier depletion from the carrier reservoirs. It would take probably longer for the gain to recover, and/or it could not recover completely. Choosing a configuration that enables a lower repetition rate would be necessary to compensate for a slower gain recovery.

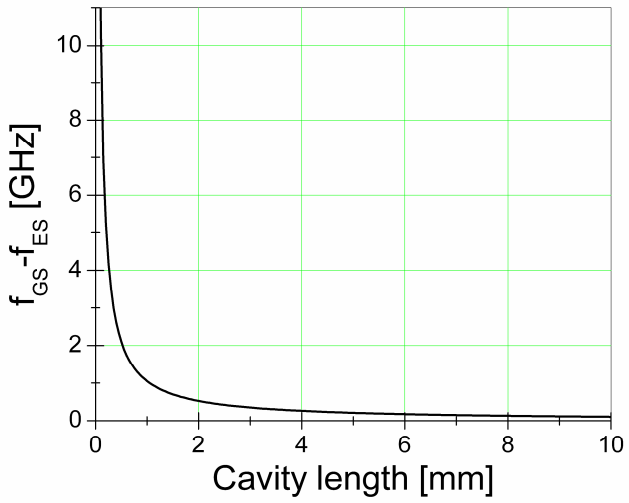

Fig. 5.5 – Calculation of the difference between the pulse repetition frequencies *f* for GS (1260nm) and ES (1190nm), with increasing cavity length (with an all-active semiconductor gain material).

[15] The requirement for an *adjustable* dispersion compensator is linked to the variations in refractive index of the semiconductor gain medium, with bias conditions and temperature – which in turn can also affect the emission wavelength.

A further step down this research line would be to exploit the high inhomogeneous broadening that can be engineered to overlap GS and ES modes in laser emission [10], and coherently engage all the spectrum in the generation of shorter pulses. However, this can only be possible if the points mentioned above are first accounted for.

5.5. Conclusion

In summary, mode-locked operation that can involve ground-state and excited-state transitions was demonstrated in a QD laser. Switching between these two states in the mode-locking regime was readily controlled by manipulating the electrical biasing conditions.

Ground-state and excited-state mode locking occurred at 1260nm and 1190nm, respectively, and exhibited average powers in excess of 35mW for ground state and 25mW for excited state operations. Although pulse durations from ES spectral band have been below expectations so far, the exploitation of the ES transitions - a unique feature of QD lasers - could lead to a new generation of high-speed sources, where mode locking involves electrically switchable GS or ES transitions that are spectrally distinct.

5.6. References

[1] P. Borri, W. Langbein, J. M. Hvam, F. Heinrichsdorff, M. H. Mao, and D. Bimberg, "Spectral hole-burning and carrier-heating dynamics in InGaAs quantum-dot amplifiers," *IEEE J. Sel. Topics Quantum Electron.*, vol. 6, pp. 544-551, 2000.

[2] S. Schneider, P. Borri, W. Langbein, U. Woggon, R. L. Sellin, D. Ouyang, and D. Bimberg, "Excited-state gain dynamics in InGaAs quantum-dot amplifiers," *IEEE Photon. Technol. Lett.*, vol. 17, pp. 2014-2016, 2005.

[3] S. Schneider, U. K. Woggon, P. Borri, W. Langbein, D. Ouyang, R. Sellin, and D. Bimberg, "Ultrafast Gain Recovery Dynamics of the Excited State in InGaAs Quantum Dot Amplifiers," *Conference on Lasers and Electro-Optics/Quantum Electronics and Laser Science and Photonic Applications Systems Technologies*, paper CThH6, 2005.

[4] O. Qasaimeh and H. Khanfar, "High-speed characteristics of tunnelling injection and excited-state emitting InAs/GaAs quantum dot lasers," *IEE Proc. Optoel.*, vol. 151, pp. 143-150, 2004.

[5] E. U. Rafailov, A. D. McRobbie, M. A. Cataluna, L. O'Faolain, W. Sibbett, and D. A. Livshits, "Investigation of transition dynamics in a quantum-dot laser optically pumped by femtosecond pulses," *Appl. Phys. Lett.*, vol. 88, pp. 41101-3, 2006.

[6] M. A. Cataluna, E. U. Rafailov, A. D. McRobbie, W. Sibbett, D. A. Livshits, and A. R. Kovsh, "Ground and excited-state modelocking in a two-section quantum-dot laser," *18th Annual Meeting of the IEEE Lasers and Electro-Optics Society*, *Technical Digest*, ThS2, 870-871, Sydney, Australia, 2005.

[7] M. A. Cataluna, E. A. Viktorov, P. Mandel, W. Sibbett, D. A. Livshits, J. Weimert, A. R. Kovsh, and E. U. Rafailov, "Temperature dependence of pulse duration in a mode-locked quantum-dot laser," *Appl. Phys. Lett.*, vol. 90, pp. 101102-3, 2007.

[8] J. Kim, M.-T. Choi, and P. J. Delfyett, "Pulse generation and compression via ground and excited states from a grating coupled passively mode-locked quantum dot two-section diode laser," *Appl. Phys. Lett.*, vol. 89, pp. 261106-3, 2006.

[9] J. Kim, M. T. Choi, W. Lee, and P. J. Delfyett, "Wavelength tunable mode-locked quantum-dot laser," *Enabling Photonics Technologies for Defense, Security, and Aerospace Applications II*, *Proc. SPIE*, 62430M, M2430-M2430, Kissimmee, FL, 2006.

[10] A. Kovsh, I. Krestnikov, D. Livshits, S. Mikhrin, J. Weimert, and A. Zhukov, "Quantum dot laser with 75 nm broad spectrum of emission," *Opt. Lett.*, vol. 32, pp. 793-795, 2007.

6. TEMPERATURE EFFECTS ON MODE-LOCKED QUANTUM-DOT LASERS

In this chapter, stable passive mode locking of a quantum-dot laser over an extended temperature range (from 20^{o}C to 80^{o}C) is demonstrated. It was observed that the pulse duration and the spectral width decreased significantly as the temperature was increased up to 70^{o}C. The process of carrier escape in the absorber was identified as the main contributing factor that led to a decrease in the absorber recovery time with increasing temperature, thus facilitating a decrease in the pulse durations.

6.1. Introduction

Due to their density of states, QDs offer great potential for designing temperature-resilient devices. If their high-speed performance is also proven to be resilient to temperature, QD lasers can become the next generation of sources for ultrafast optical telecoms and datacoms, because the constraint of using thermo-electric coolers can be avoided, thus decreasing cost and complexity. In order to meet the requirements for high-speed applications, it is also important to investigate the temperature dependence of the pulse duration. For instance, in communication systems with transmission rates of 40Gb/s or more, the temporal interval between pulses is less than 25ps – therefore, the duration of the optical pulses should be well below this value, at any operating temperature.

Despite the technological impact that a temperature-resilient ultrafast QD laser can offer, until 2005 there had not been any studies regarding if and how the temperature affected the stability of mode locking in QD lasers. In this context, we have demonstrated for the first time that passive mode locking of QD lasers remains stable in a broad temperature range. We have also shown that, perhaps counterintuitively, the pulse duration and the spectral width decrease significantly as temperature is increased up to 70^{o}C. These experimental results have been successfully modelled by Dr. E. V. Viktorov and Prof. P. Mandel, from the *Université Libre de Bruxelles*, with whom I have initiated a very successful collaboration in mid-2006. The simulations were the result of intense and fruitful discussions between me and Dr. Viktorov about the temperature-dependent phenomena occurring in the QD laser, and therefore, although I did not perform the simulations, I extensively contributed for the character of the final model. The simulations were able to reproduce the results by taking into account the temperature dependence of carrier capture and escape from the quantum dots. These results are not only important from a technological point of view, but they also further the understanding of the physical mechanisms that are behind the generation of short pulses in QD lasers.

6.2. Threshold current variations with temperature

In the following sections, the results refer to the Ioffe laser. The device was mounted p-side up on a copper heatsink, and a Peltier cooler was used to control the operating temperature. The gain section of the laser was electrically pumped by continuous-wave bias, in order to study the performance of the device under real-life working conditions. The absorber section was reverse biased so as to achieve mode-locked operation.

Typical cw light-current characteristics for various heatsink temperatures are illustrated in Fig. 6.1, when the bias applied to the absorber section was 0 V. Under these conditions, a significant thermal rollover behaviour appeared only when the temperature was increased to 80°C.

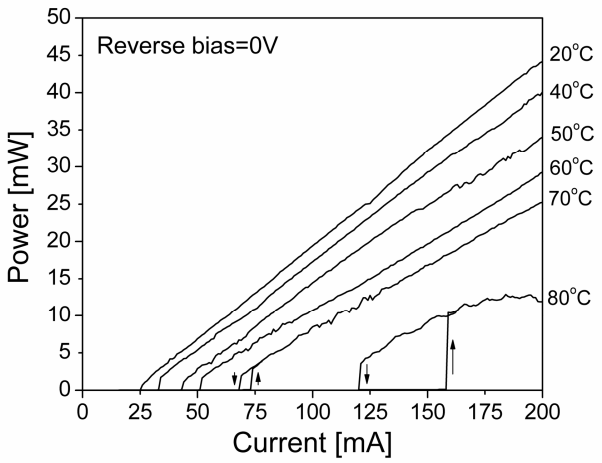

Fig. 6.1 - Typical cw light-current characteristics of the two-section QD laser as a function of temperature, for a bias of 0V in the absorber section.

For each temperature, the reverse bias was varied between 0V and 10V, and the corresponding threshold current was measured, as depicted in Fig. 6.2. It was also observed that the modulation of losses by the reverse bias in the saturable absorber was more important for higher temperatures – and indeed, pronounced hysteresis was observed when temperatures exceeded 60°C.

In Fig. 6.2, only two threshold current values are featured for a temperature of 80°C. The reason for this is that at this temperature, the laser emission shifted to ES as the reverse bias was increased beyond 1V. The switch to ES at higher temperatures can be explained by the higher level of losses in the laser and also by the thermal excitation of carriers from the GS to the ES levels with increasing temperature [1].

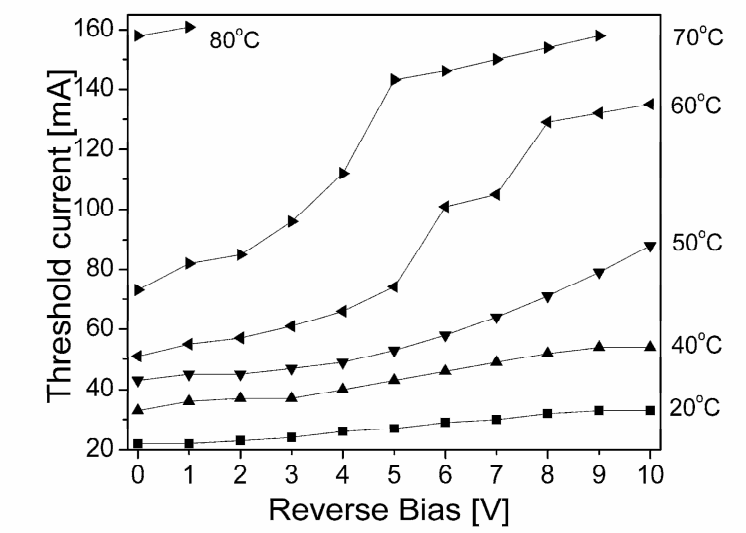

Fig. 6.2 - Dependence of the threshold current on reverse bias and temperature.

Taking into account the phenomenological relationship $I_{th} = I_{th0} \exp(T/T_0)$, it is possible to calculate the characteristic temperature T_o, which is a measure of the stability of threshold current I_{th} with temperature T (and where I_{th0} is a constant) [2]. For example, an infinite characteristic temperature will imply that the threshold current is invariant with temperature.

In order to define a realistic T_o for these two-section lasers, it was taken into account that the absorber section is never forward biased while in mode-locked operation, and that current is pumped solely into the gain section. Therefore, T_o was calculated using the threshold current values measured while the absorber was reverse biased in the range of 0V – 10V. For temperatures equal and above 60°C, the lower threshold current of the hysteresis loop was considered. A characteristic temperature T_o of 41K was obtained for the range of operating temperature 20°C - 80°C. T_o was relatively constant across the whole range of reverse bias values, confirming that it is essentially dependent on the properties of the gain section, as already demonstrated for two-section quantum-well lasers, in a previous work [3]. This value of T_o is thus valid across the whole mode-locked operating range.

At this point, several important comments are due here, as T_o is a finite and actually quite small value. An infinite T_o had been predicted for QD lasers [4], where the three-dimensional confinement in an infinite potential would lead to a δ-like density of states, and therefore no thermal spreading of carriers would occur, even with increasing temperature, provided that higher sub-bands would not become populated – thus meaning that the carriers would always be confined to a single state. However, the

confinement potential is not infinite in a real QD. With increasing temperature, carriers are thermally excited to higher sub-bands [1] and/or to the wetting layers [5], which leads to significant gain saturation.

In line with these investigations, it has been demonstrated that techniques tackling gain saturation can greatly improve T_o. One of such techniques is p-doping [6,7], used extensively in recent years to decrease temperature sensitivity of the threshold current, resulting in values of T_o up to 650K [8]. Through p-doping, a surplus of holes is made available within the material, in order to reduce the effect of thermionic hole emission [9]. Indeed, because the hole levels are energetically more closely spaced than electron levels, the excitation of holes into higher subbands may lead to a significant reduction in the population inversion with increasing temperature. The characteristic temperature T_o can also be improved by engineering the shape of the QD and increasing the energy separation between the GS and ES levels in the dot [10]. Additionally, gain saturation can also be minimised by increasing the number of QD layers in the laser material, which can also be combined with p-doping techniques [7]. It is important to refer that the Ioffe laser was not designed for temperature resilience in particular, and therefore did not include any of the aforementioned engineering optimisations.

Finally, it is important to add that Auger recombination could ultimately prevent a totally temperature-insensitive behaviour of QD lasers, in particular around room temperature [11]. It has been demonstrated recently that Auger recombination accounts for a very significant proportion of the overall recombination current in QD lasers emitting at 1.3μm or more[16] [11,12]. The rate of Auger recombination increases with temperature, and being a nonradiative process, it also has the effect of increasing the threshold current (although the radiative recombination current does remain constant with temperature in QD lasers).

Auger recombination may also be the main responsible for an increase in the homogeneous broadening with temperature [13], which could also have an impact on the spectral characteristics.

[16] Auger processes become more important for lower bandgaps, as the carrier scattering becomes more probable.

6.3. Stability of mode locking over a broad temperature range

Stable mode-locked operation was observed from 20°C to 70°C, with extinction ratios well over 20dB and a -3 dB-linewidth smaller than 80kHz. The mode-locking regime became less stable only at 80°C, where the -3dB-linewidth was 700kHz and the extinction ratio was 15dB. No self-pulsations were observed in the whole temperature range considered. Fig. 6.3 shows typical light-current characteristics under various heatsink temperatures and reverse bias conditions, corresponding to stable mode-locked operation over a wide range of current injection. In order to better compare the performance at different temperatures, the optical and RF spectra were acquired at a constant optical output power of 7mW, as depicted in Fig. 6.4, which shows very stable mode locking at temperatures up to 70°C, and only becoming less stable at 80°C.

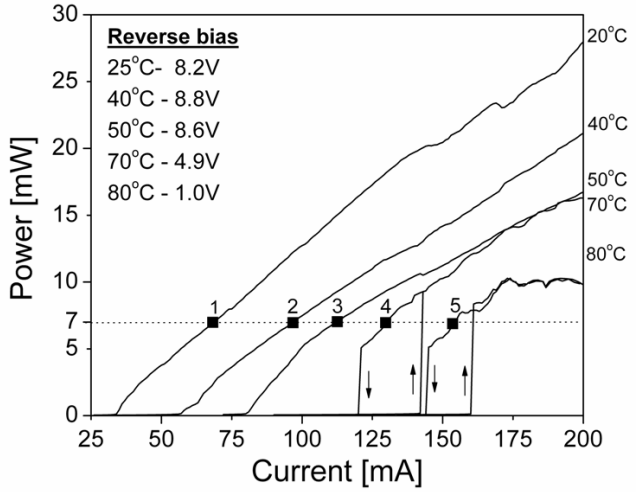

Fig. 6.3 - Typical light-current characteristics of the two-section QD laser as a function of temperature, while in mode-locked operation.

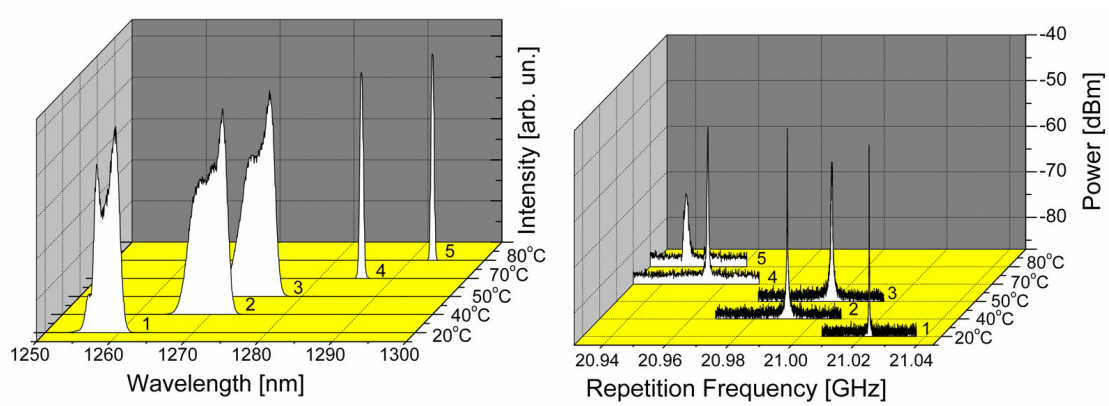

Fig. 6.4 – Optical (left) and RF (right) spectra. The operating points 1, 2, 3, 4 and 5 correspond to mode-locked operation at a constant power of 7mW, as shown in Fig. 6.3.

The repetition rate does not change dramatically with temperature, mostly due to the interplay between the thermal expansion of the laser and the change of refractive index with both temperature and wavelength. In fact, the pulse repetition frequency is dictated by the round-trip cavity time, which is influenced by the refractive index and the length of the cavity. As the temperature is increased, the consequent thermal expansion of the cavity length will lead to a decrease in repetition frequency. On the other hand, the refractive index of a semiconductor for a given wavelength decreases with temperature, thus having the effect of increasing the repetition rate. This effect is accentuated by the thermal red-shift of wavelengths with temperature, meaning that the circulating pulses inside the cavity will experience an even lower refractive index. The balance between these two effects leads to a relatively unchanged repetition frequency, which is a desirable feature for some applications. The large thermal red-shift in wavelength is an obvious disadvantage; however, it should be noted that this structure was not optimised for high-temperature operation. The results presented here suggest that by carefully tailoring the semiconductor structure [14], it would be possible to obtain a mode locked QD laser with an extremely low shift of emission wavelength with temperature.

6.3.1. Reverse bias range

The reverse bias conditions for stable mode-locked operation between 20^{o}C and 80^{o}C were also investigated, while keeping a constant current injection of 190mA. Fig. 6.5 illustrates the reduction of the level of reverse bias in order to maintain stable mode-locked operation with increasing operation temperature. The same trend was observed for other constant current injections.

The upper limit of the reverse bias tuning range only decreases significantly at 50^{o}C and beyond due to the fast saturation of ground-state gain that shifts laser emission to excited-state transitions (emission wavelength around 1190nm). The tuning range can thus be improved by preventing early ground-state gain saturation, using a p-type doped laser structure [6], and/or with more QD layers [15].

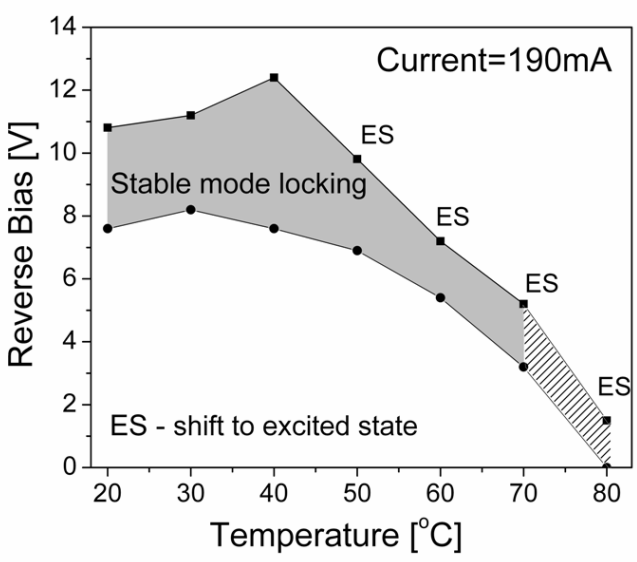

Fig. 6.5 - Dependence of the tuning range of reverse bias with increasing temperature, for stable mode-locked operation (shaded area). The gain current injection was kept constant at 190mA. For temperatures at and above 50°C, the upper limit of the mode locking region was limited by a shift of the laser emission to excited-state (ES) transitions.

6.4. The influence of temperature on pulse duration and spectrum

Using a background-free autocorrelator based on second-harmonic generation, the pulse duration was measured up to 70°C. Fig. 6.6 depicts the decreasing pulse duration with temperature, while keeping a constant injection current of 190mA, and adjusting the reverse bias so as to achieve the minimum pulse duration at each temperature. It was also observed that the spectrum became narrower and red-shifted with increasing temperature. The combination of all these effects resulted in a 7-fold decrease of the time-bandwidth product, as also shown in Fig. 6.6. Nevertheless, the pulses are still strongly frequency chirped due to the high dispersion in the semiconductor material. This observed decrease in bandwidth as a function of temperature has been investigated extensively elsewhere and several possible reasons have been suggested. One implies an increase in the homogeneous linewidth [16] but another is that a decrease in population inversion over the entire gain spectrum due to thermal coupling to the wetting layer would reduce the number of modes that reach threshold [17,18].

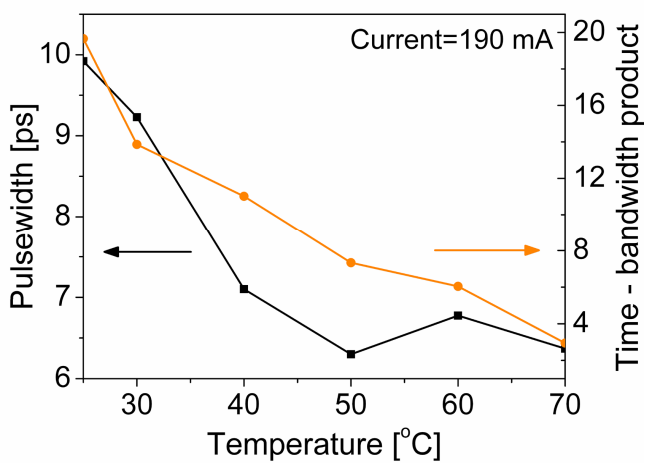

Fig. 6.6 – Dependence of the minimum pulse duration and duration-bandwidth product with temperature, at a constant injection current (with optimised reverse bias for each temperature).

The experimental dependence of pulse duration with increasing reverse bias for several fixed values of temperatures is presented in Fig. 6.7. The possibility of obtaining even shorter pulses at higher temperatures was limited by the shift from ground-state to excited-state emission, as the reverse bias was increased and the ground-state gain saturated.

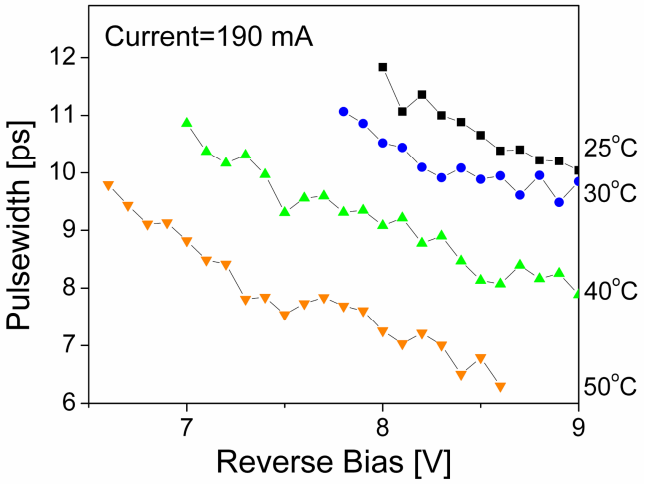

Fig. 6.7 - Dependence of the pulse duration on reverse bias for the Ioffe laser, at a constant injection current, for several temperatures.

As the temperature increases, the threshold current increases and the differential efficiency decreases, and thus for a given fixed bias current (Fig. 6.7), the optical power is lower at higher temperatures. This also implies that with increasing temperature, the effect of self-phase modulation is weaker, which could account for the

decrease in pulse duration. In order to isolate the effect of the self-phase modulation, the pulsewidth was also measured at constant optical output power. The results depicted in Fig. 6.8 show that for a constant output power, the pulsewidth decreases with increasing temperature, and therefore the pulsewidth decrease can not be solely attributed to an optical power decrease. As will be demonstrated in the following section, a reduction in the absorber recovery time plays a crucial role in the decrease of the pulse duration with increasing temperature.

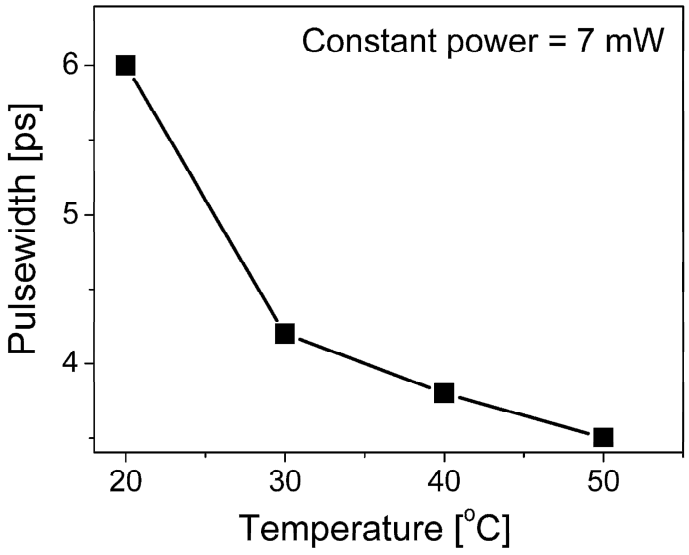

Fig. 6.8 - Dependence of the pulse duration with temperature for the Ioffe laser, at a constant optical average power.

6.5. Modelling the temperature effects on mode locking

6.5.1. Capture and escape processes in the quantum dots

The gain and absorption recovery processes are crucial in the generation of pulses in a mode-locked laser. One of the keys to understand the influence of temperature in these two processes can be considered by taking into account the capture and the escape times to/from the quantum dots, and their dependence on temperature.

The carrier capture and escape times depend on the availability of phonons. It is assumed that their temperature dependence can be described by the Bose-Einstein distribution, such that:

$$\tau_{g,q}, \tau_{g,q}^{esc} \sim e^{\left(E_{wl}-E_{gs}\right)/kT} - 1 \tag{6.1}$$

where E_{wl} and E_{gs} are the energy levels corresponding to the quantum well and to the ground state of the quantum dot. The choice of a Bose-Einstein distribution is consistent with the property that capture and escape are instantaneous processes $\left(\tau_{g,q} = \tau_{g,q}^{esc} = 0\right)$ if $E_{wl} = E_{gs}$. It was found that this ansatz leads to predictions that match well the experimental results. A similar distribution was discussed in references [19] and [20]. The increased capture rate at high temperature has been measured experimentally [19,21]. In the numerical simulations, a carrier capture time of $\tau_g = 10\,ps$ was assumed for the gain section and $\tau_q = 50\,ps$ for the absorber section, at 20 ^{o}C and $E_{wl} - E_{gs} = 230\,meV$.

The modelling of the escape processes is more tentative, less investigated and related to the impact of the first excited state. The model developed in collaboration with Dr. Viktorov does not take the first excited state into account as it lead to significant additional complexity due to the electron-hole energy exchange asymmetry between the ground and excited states at elevated temperatures [22]. Instead, just a general trend was examined and the following two main situations were considered: the capture is either much faster than the escape $\left(\tau_g << \tau_g^{esc}\right)$ in the gain section or it is much slower than the escape $\left(\tau_q >> \tau_q^{esc}\right)$ in the absorber section. In the gain section, the ratio τ_g / τ_g^{esc} can be estimated from the quasi-equilibrium condition

$\tau_g^{esc} \sim \tau_g \times e^{\left(E_{gs}-E_{wl}\right)/kT}$ [23,24]. For these small values of escape rate $\left(\tau_g / \tau_g^{esc} < 0.1\right)$, the escape process in the gain section can be considered negligible in the model. In the absorber section, quasi-equilibrium conditions cannot be applied, and the thermal escape time at room temperature was arbitrarily considered to be 5ps, which satisfies $\tau_q >> \tau_q^{esc}$ and is close to the estimate in reference [25].

6.5.2. Equations

To account for the decrease in pulse duration with increasing operating temperatures, the model for mode-locking in QD lasers was used, as described in more detail in reference [26]. Thus:

$$\gamma^{-1}\partial_t A(t) + A(t) = \sqrt{\kappa} e^{\left(1-i\alpha_g\right)G(t-T)/2-\left(1-i\alpha_q\right)Q(t-T)/2} A(t-T), \tag{6.2}$$

$$\partial_t \rho_g = -\gamma_g \rho_g + F_g\left(\rho_g, N_g\right) - e^{-Q}\left(e^{G}-1\right)|A|^2, \tag{6.3}$$

$$\partial_t \rho_q = -\gamma_q \rho_q + F_q\left(\rho_q, N_q\right) - s\left(1-e^{-Q}\right)|A|^2, \tag{6.4}$$

$$\partial_t N_g = N_{g0} - \Gamma_g N_g - 2F_g\left(\rho_g, N_g\right), \tag{6.5}$$

$$\partial_t N_q = N_{q0} - \Gamma_q N_q - 2F_q\left(\rho_q, N_q\right). \tag{6.6}$$

where $A(t)$ is the normalized complex amplitude of the electric field, the variables $\rho_g(t)$ and $\rho_q(t)$ describe the occupation probabilities in a dot located either in the amplifier or in the absorber section, respectively, the variables $N_{g,q}(t)$ describe the carrier densities in the wetting layers, scaled to the QD carrier density. The variables $G(t) = 2g_g L_g\left[2\rho_g(t)-1\right]$ and $Q(t) = 2g_q L_q\left[2\rho_q(t)-1\right]$ are the dimensionless saturable gain and absorption. The parameters $g_{g,q}$, $\Gamma_{g,q}$, and $\gamma_{g,q}$ are, respectively, the differential gains, the damping rate in the wetting layers and the carrier relaxation rates in the dots, γ is the dimensionless bandwidth of the spectral filtering section, α_g $\left(\alpha_q\right)$ the linewidth enhancement factors in the gain (absorber) section. The time delay T is equal to the cold cavity round trip time. The attenuation factor $\kappa < 1$ describes total non-resonant linear intensity losses per cavity round trip. The dimensionless

parameters N_{g0} and N_{q0} describe pumping processes in the amplifier and the absorber sections. The parameter s is the ratio of the saturation intensities in the gain and absorber sections. The functions $F_{g,q}\left(\rho_{g,q}, N_{g,q}\right) = B_{g,q} N_{g,q}\left(1-\rho_{g,q}\right) - R^{esc}_{g,q}\rho_{g,q}$ describe the carrier exchange rate between the wetting layers and the dots. $B_{g,q} = \tau^{-1}_{g,q}$ and $R^{esc}_{g,q} = \left(\tau^{esc}_{g,q}\right)^{-1}$ are temperature-dependent coefficients defining carrier capture and escape from the dots to the wetting layer.

6.5.3. Simulation results

In the numerical simulation, plotted in Fig. 6.9, the objective was to match qualitatively the pulsewidth dependence. The trends observed experimentally are well described by the model and it can be observed that the pulse durations decreases smoothly by about a factor of two for temperature increases over the 25-50°C latitude . This temperature range is arbitrary and has been used solely to demonstrate the trends. Indeed, the actual temperature of the carriers is, of course, higher than the temperature of the lattice, which was measured experimentally. The difference between the carrier temperature and the temperature of the lattice is due to the carrier heating caused by carrier injection and short energy pulses circulating in the cavity. It is however rather difficult to estimate this difference.

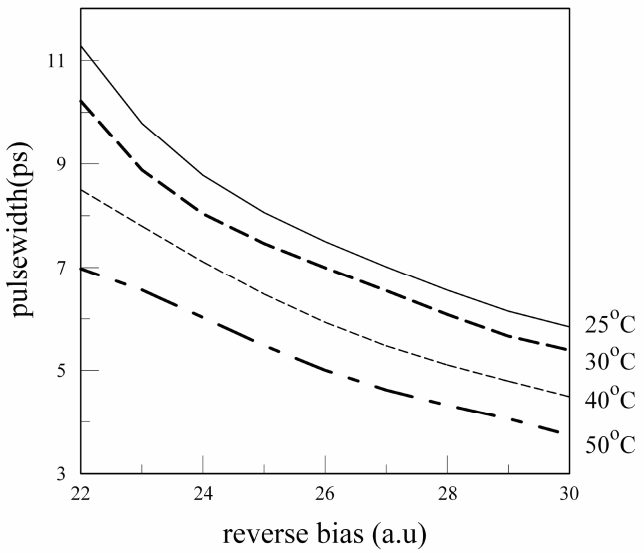

Fig. 6.9 - Numerical simulations. Dependence of the pulse duration with reverse bias at a constant injection current, for several temperatures. The parameters for the numerical simulation are: $\kappa = 0.2;\ T = 5;\ \gamma = 10;\ \gamma_g = \gamma_q = \Gamma_g = 0.01;\ \Gamma_q = 1;\ \alpha_g = \alpha_q = 2;\ 2g_g L_g = 2.4;$ $2g_q L_q = 13.5;\ s = 30;\ N_{g0} = 10.$

Experimental results demonstrate an even faster decrease of the pulse durations with temperature than that implied by the results of Fig. 6.9. This can be attributed to the higher temperature of the carriers together with the complexity of multiple-phonon scattering [19] that is not accounted for in the simple assumptions made for the capture and escape rates in equation (6.1).

It followed from the modelling that the role of the temperature-dependent capture and escape processes in the gain section was relatively minor. Indeed, it was observed that the duration of the mode-locked pulses was determined primarily by the increasing escape rate in the absorber section of the laser device, with increasing temperature.

6.5.4. Further confirmation of the role of escape processes

After these results were published, experiments performed in St Andrews by David Malins and co-workers, and in collaboration with our group, demonstrated that the absorption recovery time decreased significantly with increasing temperature [27], as evidenced in Fig. 6.10. The temporal absorption dynamics was investigated using ultrafast pump-probe spectroscopy in *p-i-n* 5 layer InAs QD modulator, to which a fixed reverse bias was applied.

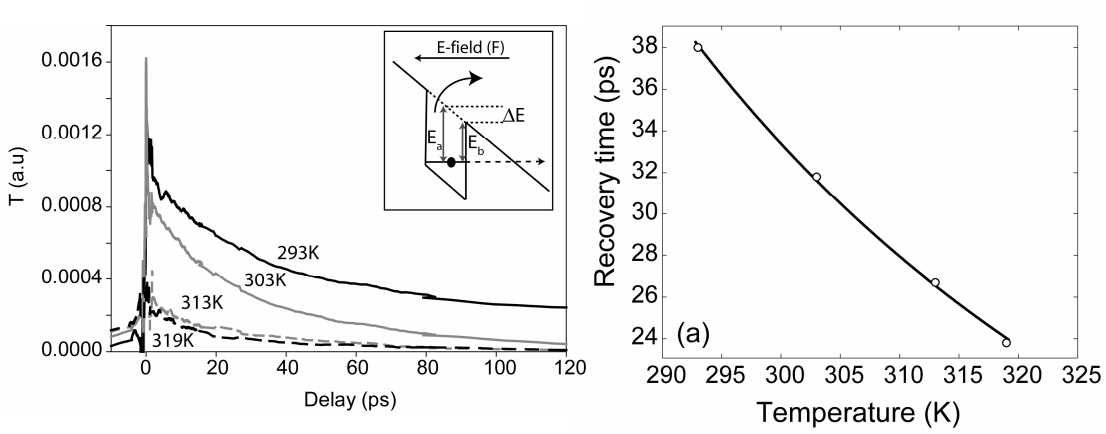

Fig. 6.10 - Change in probe transmission as a function of probe delay for a range of temperatures. Inset (in the left) illustrates thermionic emission and tunnelling processes. [27]

In a different paper where the absorption dynamics is analysed, there are also remarks about the role of temperature on the absorption recovery time, particularly how the thermal excitation of the carriers to the wetting layer facilitates their sweep out from the waveguide [28]. This also shows the role of the wetting layer as a stepping stone for removal of carriers.

6.6. Conclusion

Stable mode locking was demonstrated at a 21 GHz pulse repetition rate from a two-section QD laser, at temperatures ranging from 20°C to 80°C, with relatively high output average power. Between 20°C and 70°C, the RF spectra exhibit typical extinction ratios well over 20dB and a -3dB-linewidth smaller than 80kHz. Between 70°C and 80°C, the mode locking is less stable, with extinction ratios around 15dB and a -3dBm-linewidth of 700kHz. The repetition rate is not significantly altered with increasing temperature. It was also observed that to provide stable mode-locking operation with increasing operating temperature, the reverse bias on the absorber section must be reduced accordingly.

The results presented here suggest that by combining the optimal properties of a p-type doped QD material in a two-section laser configuration, it would be possible to fabricate a mode-locked device with even more resilience to temperature, paving the way for ultra-stable, uncooled mode locked diode lasers with a view to applications in ultrafast communications.

The influence of temperature on the mode-locking performance of a two-section QD laser was also investigated. It has been shown experimentally that both the pulse duration and the spectral width decrease as temperature was increased, resulting in an overall decrease of the time-bandwidth product. A model has been developed in collaboration with the group at *Université Libre de Bruxelles* to simulate this behaviour, where the temperature dependence is linked to the capture and escape rates into the quantum dots. The simulations indicated that the escape process in the absorber is the most important mechanism in the shortening of the pulse durations with increasing current. This observation provides an important insight into the specific carrier mechanisms that have an impact on the mode-locking performance of quantum-dot lasers.

6.7. References

[1] G. Park, O. B. Shchekin, and D. G. Deppe, "Temperature dependence of gain saturation in multilevel quantum dot lasers," *IEEE J. Quantum Electron.*, vol. 36, pp. 1065-1071, 2000.

[2] G. P. Agrawal and N. K. Dutta, *Long-wavelength semiconductor lasers*. New York: Van Nostrand Reinhold, 1986.

[3] J. O'Gorman, A. F. J. Levi, T. Tanbun-Ek, and R. A. Logan, "Saturable absorption in intracavity loss modulated quantum well lasers," *Appl. Phys. Lett.*, vol. 59, pp. 16-18, 1991.

[4] Y. Arakawa and H. Sakaki, "Multidimensional quantum well laser and temperature dependence of its threshold current," *Appl. Phys. Lett.*, vol. 40, pp. 939-941, 1982.

[5] D. R. Matthews, H. D. Summers, P. M. Smowton, and M. Hopkinson, "Experimental investigation of the effect of wetting-layer states on the gain-current characteristic of quantum-dot lasers," *Appl. Phys. Lett.*, vol. 81, pp. 4904-4906, 2002.

[6] O. B. Shchekin and D. G. Deppe, "1.3 μm InAs quantum dot laser with T_o = 161 K from 0 to 80 ^oC," *Appl. Phys. Lett.*, vol. 80, pp. 3277-3279, 2002.

[7] O. B. Shchekin and D. G. Deppe, "Low-threshold high-T_o 1.3-μm InAs quantum-dot lasers due to p-type modulation doping of the active region," *IEEE Photon. Technol. Lett.*, vol. 14, pp. 1231-1233, 2002.

[8] S. S. Mikhrin, A. R. Kovsh, I. L. Krestnikov, A. V. Kozhukhov, D. A. Livshits, N. N. Ledentsov, Y. M. Shernyakov, I. I. Novikov, M. V. Maximov, V. M. Ustinov, and Z. I. Alferov, "High power temperature-insensitive 1.3 μm InAs/InGaAs/GaAs quantum dot lasers," *Semiconductor Sci. Tech.*, vol. 20, pp. 340-342, 2005.

[9] O. B. Shchekin and D. G. Deppe, "The role of p-type doping and the density of states on the modulation response of quantum dot lasers," *Appl. Phys. Lett.*, vol. 80, pp. 2758-2760, 2002.

[10] O. B. Shchekin, G. Park, D. L. Huffaker, and D. G. Deppe, "Discrete energy level separation and the threshold temperature dependence of quantum dot lasers," *Appl. Phys. Lett.*, vol. 77, pp. 466-468, 2000.

[11] I. P. Marko, A. D. Andreev, A. R. Adams, R. Krebs, J. P. Reithmaier, and A. Forchel, "The role of Auger recombination in InAs 1.3 μm quantum-dot lasers investigated using high hydrostatic pressure," *IEEE J. Sel. Topics Quantum Electron.*, vol. 9, pp. 1300-1307, 2003.

[12] I. P. Marko, A. R. Adams, S. J. Sweeney, D. J. Mowbray, M. S. Skolnick, H. Y. Y. Liu, and K. M. Groom, "Recombination and loss mechanisms in low-threshold InAs-GaAs 1.3 μm quantum-dot lasers," *IEEE J. Sel. Topics Quantum Electron.*, vol. 11, pp. 1041-1047, 2005.

[13] H. H. Nilsson, J. Z. Zhang, and I. Galbraith, "Homogeneous broadening in quantum dots due to Auger scattering with wetting layer carriers," *Phys. Rev. B*, vol. 72, 2005.

[14] F. Klopf, S. Deubert, J. P. Reithmaier, and A. Forchel, "Correlation between the gain profile and the temperature-induced shift in wavelength of quantum-dot lasers," *Appl. Phys. Lett.*, vol. 81, pp. 217-219, 2002.

[15] A. E. Zhukov, A. R. Kovsh, N. A. Maleev, S. S. Mikhrin, V. M. Ustinov, A. F. Tsatsul'nikov, M. V. Maximov, B. V. Volovik, D. A. Bedarev, Y. M. Shernyakov, P. S. Kop'ev, Z. I. Alferov, N. N. Ledentsov, and D. Bimberg, "Long-wavelength lasing from multiply stacked InAs/InGaAs quantum dots on GaAs substrates," *Appl. Phys. Lett.*, vol. 75, pp. 1926-1928, 1999.

[16] A. Sakamoto and M. Sugawara, "Theoretical calculation of lasing spectra of quantum-dot lasers: effect of homogeneous broadening of optical gain," *IEEE Photon. Technol. Lett.*, vol. 12, pp. 107-109, 2000.

[17] A. Patane, A. Polimeni, M. Henini, L. Eaves, P. C. Main, and G. Hill, "Thermal effects in quantum dot lasers," *J. Appl. Phys.*, vol. 85, pp. 625-627, 1999.

[18] H. Huang and D. G. Deppe, "Rate equation model for nonequilibrium operating conditions in a self-organized quantum-dot laser," *IEEE J. Quantum Electron.*, vol. 37, pp. 691-698, 2001.

[19] J. Feldmann, S. T. Cundiff, M. Arzberger, G. Bohm, and G. Abstreiter, "Carrier capture into InAs/GaAs quantum dots via multiple optical phonon emission," *J. Appl. Phys.*, vol. 89, pp. 1180-1183, 2001.

[20] D. Bimberg, M. Grundmann, and N. N. Ledentsov, *Quantum Dot Heterostructures*. Chichester: John Wiley & Sons Ltd., 1999.

[21] J. Urayama, T. B. Norris, H. Jiang, J. Singh, and P. Bhattacharya, "Temperature-dependent carrier dynamics in self-assembled InGaAs quantum dots," *Appl. Phys. Lett.*, vol. 80, pp. 2162-2164, 2002.

[22] E. A. Viktorov, P. Mandel, Y. Tanguy, J. Houlihan, and G. Huyet, "Electron-hole asymmetry and two-state lasing in quantum dot lasers," *Appl. Phys. Lett.*, vol. 87, pp. 053113-3, 2005.

[23] H. Jiang and J. Singh, "Nonequilibrium distribution in quantum dots lasers and influence on laser spectral output," *J. Appl. Phys.*, vol. 85, pp. 7438-7442, 1999.

[24] A. Markus and A. Fiore, "Modeling carrier dynamics in quantum-dot lasers," *Physica Status Solidi A-Applied Research*, vol. 201, pp. 338-344, 2004.

[25] P. Borri, W. Langbein, J. M. Hvam, F. Heinrichsdorff, M. H. Mao, and D. Bimberg, "Spectral hole-burning and carrier-heating dynamics in InGaAs quantum-dot amplifiers," *IEEE J. Sel. Topics Quantum Electron.*, vol. 6, pp. 544-551, 2000.

[26] E. A. Viktorov, P. Mandel, A. G. Vladimirov, and U. Bandelow, "Model for mode locking in quantum dot lasers," *Appl. Phys. Lett.*, vol. 88, pp. 201102-3, 2006.

[27] D. B. Malins, A. Gomez-Iglesias, M. A. Cataluna, E. U. Rafailov, W. Sibbett, and A. Miller, "Temperature dependence of electroabsorption dynamics in an InAs quantum dot saturable absorber at 1.3μm.," *European Conference on Lasers and Electro-Optics*, *Technical Digest*, CF-6, Munich, Germany, 2007.

[28] D. R. Matthews, G. T. Edwards, H. D. Summers, and P. M. Smowton, "Saturable absorber characteristics in quantum dot lasers," *Novel in-Plane Semiconductor Lasers III*, *Proc. SPIE*, 96-106, 2004.

7. SUMMARY AND OUTLOOK

7.1. Summary

In this work, three novel functionalities of mode-locked QD lasers have been described. These are (i) a new mode-locking regime where the simultaneous excited-state emission enabled the generation of ultrashort and low-noise pulses under the conditions of higher levels of current injection and at higher powers; (ii) the first demonstration of mode locking involving the excited-state spectral band and (iii) the resilience of mode-locking performance at temperatures as high as 80°C.

In Table 7.1, some of the key results presented in the thesis are summarised for the different mode-locking regimes studied.

Table 7.1 – Summary of the mode-locking (ML) performance, under several regimes (Ioffe laser). τ_p: pulse duration. λ_0: central wavelength. $\Delta\lambda$: spectral bandwidth. P_{av} /P_{peak}: average/peak power.

ML Regime	τ_p [ps]	λ_0 [nm]	$\Delta\lambda$ [nm]	P_{av} [mW]	P_{peak} [mW]	Added level of functionality
Mode locking via GS	10.5	1266	7	23	100	-
Mode locking via GS, enhanced by ES emission	6	1268	8.5	23	175	Shorter pulses at higher current/output power
Mode locking via ES	7	1190	5.5	23	147	New spectral band accessible
Mode locking at 50°C	6.2	1277	5.3	15	106	Resilience to temperature

The results presented in the literature show that monolithic passively mode-locked quantum-dot lasers can at present surpass the performance of similar quantum-well lasers in terms of pulse duration [1,2]. There are other particular features where QD lasers have already been shown to have a superior performance, notably in the case of pulse timing jitter where record low-values have been reported [3,4]. In this thesis, it is shown that the appeal of QD lasers also resides in the novel functionalities that are distinctive of QDs. These are: the exploitation of an excited-state level as a means to achieve novel mode-locking regimes; the temperature resilience offered by the quantised density of states; lower threshold and higher output power levels and access to the enlarged spectral bandwidths associated with the inhomogeneously broadened

gain features. These characteristics are not only useful from an operational point of view, but also provide some insights into a more comprehensive understanding of the underlying physical mechanisms of mode locking in QD lasers.

One of the main conclusions from the systematic characterisation presented in Chapter 3 is that the value of the inhomogeneous broadened gain in mode-locked operation is more limited than expected. Indeed, inhomogeneous broadening seems be contributing to the higher values of frequency chirp and time-bandwidth product, instead of facilitating the generation of shorter pulses. Such behaviour raises the hypothesis that the laser cavity modes that are distributed across different parts of the inhomogeneously broadened optical spectrum fail to lock coherently. It is possible that phase locking is easier to achieve within the same population of similar quantum dots as would be expected in a part of the spectrum that is homogeneously broadened. Nevertheless, the presence of a broadband gain can still be a very useful feature, as for spectral tunability, for example.

The pulse duration results from the balance between several broadening and compression effects. Self-phase modulation is the effect that contributes most to pulse broadening, while the fast recovery of the absorption in the saturable absorber is the prime shaping mechanism of the trailing edge of the pulse, resulting in a shorter pulse duration with decreasing absorber recovery time. Self-phase modulation results from the interaction of the pulse with the gain and the resulting large changes in the nonlinear refractive index. This leads to a phase change across the pulse, owing to the coupling between gain and index, which is regulated via the linewidth enhancement factor. The resultant up-chirp combined with the positive dispersion of the gain material, leads to substantial pulse broadening, which increases with optical power. The effect of self-phase modulation remains one of the main hurdles to the generation of shorter pulses from QD lasers, as the linewidth enhancement factor in these lasers can be very significant. The pulse duration increases linearly with optical power, due to the increasing contribution of self-phase modulation, with a slope that depends on the value of reverse bias applied to the saturable absorber – the highest the reverse bias, the lower is the rate of pulse duration increase with power. Taking into account the results from Chapter 3, the rate of increase of pulse duration with optical power is 1.4ps/mW for a reverse bias of 2V and 0.9ps/mW for a reverse bias of 4.5V. However, the rate of decrease of the pulse duration with increasing reverse bias is of the form of a decreasing exponential function, and therefore tends to become practically stagnant

with high values of reverse bias, at constant optical power. From the data of Chapter 3, a decrease rate of the order of -2ps/V is possible up to a certain value of reverse bias, while this rate becomes significantly lower for higher values of reverse bias (-0.2ps/V and lower). This same effect happens with increasing temperature, where the rate of pulse decrease is also of the form of a decreasing exponential function. Indeed, in Chapter 6 the experimental data show that a decrease in the absorber recovery time with temperature is still not enough to generate transform-limited pulses and this reinforces the idea that self-phase modulation effects are highly detrimental. This is supported by the results in Chapter 4, where the carrier cooling associated with the excited-state emission, and the possible decrease of linewidth enhancement factor, has a direct impact on the decrease of the pulse duration at a rate of -1.7ps/mW. Another major conclusion from this work is that the role of the excited state can not be neglected in the generation of ultrashort pulses. The population of carriers at the levels above the ground state lead to an increase of the linewidth enhancement factor [5] with a consequent negative effect on the duration of the generated pulses (via ground state). In this thesis, an effective technique to mitigate this effect was demonstrated by using simultaneous laser emission involving the excited state, resulting in a strong suppression of the carrier pile-up on the higher populated levels, and consequent decrease of the linewidth enhancement factor across the ground state [5]. An alternative technique to minimize the effect of the carrier population on the higher levels is to consider tunnel-injection structures, as described in the next section.

7.2. Future investigations

Although there have been many advances in the control of the growth of QD laser having ultra-low threshold current and temperature resilience, it is not yet understood what is the most advantageous QD structure layout to be used in the regime of mode locking. In particular, it is not clear what is the optimum level of inhomogeneous broadening that results in shorter and higher peak power pulses. Therefore, it is relevant to investigate if and how the inhomogeneously broadened spectral modes are engaged coherently in the generation of ultrashort pulses and how that effect could be used to improve the performance of the lasers towards sub-picosecond pulse durations.

Exploiting novel QD materials based on p-doped and tunnel injection structures could also bring advantages in minimising the effect of any deleterious self phase modulation effects in mode-locked lasers. A theoretical and experimental comparison of undoped and p-doped lasers has shown how this technique can improve the linewidth enhancement factor [6]. By tuning the level of doping, lasers can exhibit zero and even negative linewidth enhancement factor at low current densities [7]. Tunnel injection QD structures can also be of great interest for use in mode-locked lasers, as the injection of cold carriers may bring many benefits to the operation of mode-locked lasers [8]. The linewidth enhancement factor has been recently calculated and has been demonstrated to be much less than that reported for other lasers [9]. Selective excitation of population in these lasers has been demonstrated, which could lead to a mitigation of the inhomogeneous broadening effects and contribute to a narrower spectrum and the production of transform-limited pulses [10].

The excited-state spectral band can also be exploited in tunable lasers using QD materials where the inhomogeneous broadening is controlled so as to maximise the overlap between ground and excited states. While in cw operation, QD lasers have been demonstrated with tunability ranges up to 200nm [11], by exploiting the gain available from the ground state and excited states. A tunable mode-locked QD laser would unlock the potential to generate ultrashort pulses from a very compact and efficient laser system having tunability over a significant spectral region.

7.3. References

[1] E. U. Rafailov, M. A. Cataluna, W. Sibbett, N. D. Il'inskaya, Y. M. Zadiranov, A. E. Zhukov, V. M. Ustinov, D. A. Livshits, A. R. Kovsh, and N. N. Ledentsov, "High-power picosecond and femtosecond pulse generation from a two-section mode-locked quantum-dot laser," *Appl. Phys. Lett.*, vol. 87, pp. 81107-3, 2005.

[2] M. G. Thompson, A. Rae, R. L. Sellin, C. Marinelli, R. V. Penty, I. H. White, A. R. Kovsh, S. S. Mikhrin, D. A. Livshits, and I. L. Krestnikov, "Subpicosecond high-power mode locking using flared waveguide monolithic quantum-dot lasers," *Appl. Phys. Lett.*, vol. 88, pp. 133119-3, 2006.

[3] M.-T. Choi, J.-M. Kim, W. Lee, and P. J. Delfyett, "Ultralow noise optical pulse generation in an actively mode-locked quantum-dot semiconductor laser," *Appl. Phys. Lett.*, vol. 88, pp. 131106-3, 2006.

[4] M. G. Thompson, D. Larson, A. Rae, K. Yvind, R. Penty, I. H. White, J. Hvam, A. Kovsh, S. Mikhrin, D. A. Livshits, and I. Krestnikov, "Monolithic hybrid and passive mode-locked 40GHz quantum dot laser diodes," *32nd European Conference on Optical Communication*, *Technical Digest*, We4.6.3, Nice, France, 2006.

[5] B. Dagens, A. Markus, J. X. Chen, J. G. Provost, D. Make, O. Le Gouezigou, J. Landreau, A. Fiore, and B. Thedrez, "Giant linewidth enhancement factor and purely frequency modulated emission from quantum dot laser," *Electron. Lett.*, vol. 41, pp. 323-324, 2005.

[6] J. Kim and S. L. Chuang, "Theoretical and experimental study of optical gain, refractive index change, and linewidth enhancement factor of p-doped quantum-dot lasers," *IEEE J. Quantum Electron.*, vol. 42, pp. 942-952, 2006.

[7] R. R. Alexander, D. Childs, H. Agarwal, K. M. Groom, H. Y. Liu, M. Hopkinson, and R. A. Hogg, "Zero and controllable linewidth enhancement factor in p-doped 1.3 μm quantum dot lasers," *Japanese Journal of Applied Physics*, vol. 46, pp. 2421-2423, 2007.

[8] P. J. Delfyett: Personal communication, 2006.

[9] Z. Mi and P. Bhattacharya, "Analysis of the linewidth-enhancement factor of long-wavelength tunnel-injection quantum-dot lasers," *IEEE J. Quantum Electron.*, vol. 43, pp. 363-369, 2007.

[10] A. A. George, P. M. Smowton, Z. Mi, and P. Bhattacharya, "Long wavelength quantum-dot lasers selectively populated using tunnel injection," *Semiconductor Sci. Tech.*, vol. 22, pp. 557-560, 2007.

[11] P. M. Varangis, H. Li, G. T. Liu, T. C. Newell, A. Stintz, B. Fuchs, K. J. Malloy, and L. F. Lester, "Low-threshold quantum dot lasers with 201 nm tuning range," *Electron. Lett.*, vol. 36, pp. 1544-1545, 2000.